THE OCCURRENCE AND EXTENT OF COLLAPSE SETTLEMENT IN RESIDUAL GRANITE IN THE STELLENBOSCH AREA

BY

NANINE GILDENHUYS

Thesis submitted in partial fulfillment of the requirements for the degree of Masters in Engineering (MSc Eng) at the University of Stellenbosch

Supervisor: Dr. M De Wet

December 2010

DECLARATION

I, the undersigned, hereby declare that the work contained in this thesis is my own original work and that I have not previously in its entirety or in part, submitted it at any University for a degree.

Signature: ……

N. Gildenhuys

Date: ……

ABSTRACT

Large areas of the earth's surface are covered by soils that are susceptible to large decreases in bulk volume when they become saturated. These soils are termed *collapsing soils* and are very common in parts of the USA, Asia, South America and Southern Africa. This study is concerned with the occurrence of these collapsible soils in the residual granites of the Stellenbosch area. The study was undertaken as relatively little is known about the collapse phenomenon in the problematic weathered granites of the Western Cape. The majority of research thus far has been carried out on the deep residual soils formed on basement-granite in the Transvaal areas, whereas little attention has been paid to the Cape granites.

The aim of the study was achieved through the experimental work which included double oedometer testing, indicator analyses and shear strength testing. Double oedometer tests were performed to quantify the potential collapse settlement of the soils from the demarcated study area. To provide a better understanding of the collapse behaviour of the soils, indicator analyses, which included Atterberg limits and particle size distributions, were performed. Direct shear tests were further carried out on saturated and natural moisture content specimens to establish the effect of collapsibility on shear strength and whether substantial additional settlement of the saturated soils would occur during shear.

It was found that collapsible soils are prevalent in the demarcated study area as the majority of soils showed a potential collapse settlement of 1% or more. Collapse exceeding 5% were calculated in a few instances proving some soils to be highly collapsible. The double oedometer and indicator analyses results were used in an attempt to obtain a relationship between collapse settlement and a combination of easily determined properties such as dry density (void ratio), moisture content and grading, but no meaningful conclusions have emerged. The shear strength tests indicated that a clear correlation does not exist between collapsibility and shear strength. It was further established that a relationship between collapse settlement determined during the double oedometer testing and the volume change during shear

strength testing cannot be assumed. It can thus be concluded that soils can be very unpredictable and further research on the collapse phenomenon is indicated.

OPSOMMING

Groot dele van die aarde se oppervlakte is bedek deur grondtipes wat geneig is tot ‘n afname in volume as dit deurweek word. Hierdie gronde word *swigversakkende gronde* genoem en dit word algemeen teëgekom in dele van die VSA, Asië, Suid-Amerika en Suider-Afrika. In hierdie studie word die voorkoms van swigversakkende gronde in die residuele graniet in die Stellenbosch area ondersoek. Die studie is onderneem aangesien relatief min i.v.m. die swigversakking-verskynsel in die problematiese verweerde graniet van die Weskaap bekend is. Die meeste van die navorsing sover is onderneem op die diep residuele gronde wat gevorm is op die Argaïese graniet in die Transvaal gebied, en betreklik min aandag is geskenk aan die Kaapse graniet.

Tydens die studie is eksperimente wat dubbele oedometer toetse, indikator analises, en skuifsterkte toetse insluit, uitgevoer. Dubbele oedometer toetse is uitgevoer om die potensiële swigversakking van die grond in die afgebakende studiegebied te kwantifiseer. In ‘n poging om die swigversakking-verskynsel van die grond beter te verstaan, is indikator analises wat Atterberg grense en partikel grootte verspreiding insluit, uitgevoer. Direkte skuiftoetse is ook uitgevoer op deurweekte grondmonsters en op monsters wat natuurlike vog bevat, om sodoende die effek van swigversakking op skuifsterkte vas te stel en om uit te vind of aansienlike addisionele sakking van die deurweekte gronde tydens skuif plaasvind.

Daar is gevind dat swigversakkende gronde die oorheersende grondtipe in die afgebakende studiegebied is waar meeste van die gronde ‘n potensiële swigversakking van meer as 1% toon. ‘n Swigversakking van meer as 5% is in ‘n paar gevalle bereken, wat bewys dat sommige grondtipes hoogs versakkend is. Die resultate van die dubbele oedometer en indikator analises is gebruik in ‘n poging om te bewys dat daar ‘n verhouding bestaan tussen swigversakking en ‘n kombinasie van kenmerke wat maklik vasgestel kan word soos droë digdheid (ruimte verhouding), voginhoud en gradering, maar daar kon nie tot ‘n sinvolle slotsom gekom word nie. Die skuifsterkte toetse toon dat daar nie ‘n duidelike korrelasie bestaan tussen swigversakking en skuifsterkte nie. Daar is verder vasgestel dat dit nie moontlik is om te aanvaar dat daar

‘n verhouding bestaan tussen swigversakking soos vasgestel tydens die dubbele oedometer toetsing, en die verandering in volume tydens skuifsterkte toetsing nie. Daar is dus tot die slotsom gekom dat grond baie onvoorspelbaar kan wees en dat verdere navorsing na die swigversakking-verskynsel nodig is.

ACKNOWLEGDEMENTS

I would like to express my sincere gratitude and appreciation to the following persons, without whom I would not have been able to successfully complete this study:

- Dr Marius De Wet for his professional guidance and assistance
- My mother Marianne Gildenhuys for her patience, support and invaluable assistance
- My father Petrus Gildenhuys for his financial support throughout my studies
- Fritz Marais for his encouragement and selfless support
- Mr Ben Marais, Collin Isaacs and Gavin Williams who assisted with the field and laboratory work
- Prof Kim Jenkins, Mr Leon Croukamp and Mr J.C. Engelbrecht for their guidance and valuable inputs
- Mr Frank Du Plessis and personnel of Kantey and Templer for their assistance and professional typing of the soil profiles
- The owners of the farms Audacia, Eikendal and Ernie Els Wines and Stellenbosch Municipality, who gave permission to perform the field work on their premises
- Melanie Bailey and Fran Ritchie for their editing of the thesis
- My Creator, God the Father, for blessing me abundantly and whose Grace and Guidance has allowed me to complete my studies.

TABLE OF CONTENTS

LIST OF TABLES

LIST OF FIGURES

CHAPTER 1: INTRODUCTION

1.1 BACKGROUND AND MOTIVATION FOR STUDY

During July 1953 a 125 000 litre reinforced concrete water tower consisting of a circular tank supported on four columns 15,25m high was erected in White River, Eastern Transvaal. It was constructed on residual granite soil which was dry and stiff and appeared to be sound material. The foundation bases of each of the columns were founded at a depth of about 1,5m below ground level. In August 1957, four years later, a tenant of a nearby house observed a marked tilt of the tower in an easterly direction. The settlement of the western bases of 57 mm and 75 mm can probably be ascribed to normal consolidation settlement during and after construction, whereas the additional settlement of 75 to 100 mm of the eastern bases had resulted from a phenomenon which has become known as that of 'collapsing soils' (Brink, 1996).

A soil with a collapsible fabric can endure relatively large imposed stresses with small settlements at a low in-situ moisture content. If wetting up occurs, it will show a decrease in volume and associated settlement with no increase in the applied stress. A change in the soil structure (collapse of soil structure) is responsible for the change in volume of the soil (Schwartz, 1985).

Collapse was initially thought to occur only in altered Aeolian sands, but in 1957 the investigation into the differential settlement of the water tower near White River discussed above, resulted in the first reported case of collapse settlement of a residual granite soil (Brink, 1985). Residual granites cause foundation problems due to their collapsible grain structure. Colloidal coatings adhere to individual quartz grains which impart an apparently high strength to the soil when dry. Therefore, an unsuspecting engineer would not waver in applying moderately high foundation pressures after investigating the soil profile. If the soil becomes saturated under load, the colloidal bridges between the quartz particles become lubricated and lose strength at once. The denser state of packing into which the quartz particles fall may result in sudden foundation settlements of some extent (Brink, 1978).

Although granites and granite-gneisses and their associated residual soils are bare over extensive parts of Southern Africa, the majority of research concerning collapsible soils previously focused on the residual granite soils of the basement complex (Brink, 1978). The less problematic weathered granites of the Cape granite suite have received much less attention. Although fewer problems have been associated with the residual granitic soils of the Western Cape, serious problems have nevertheless occurred in areas where these soils occur (Brink, 1981).

In this study the endeavour is to further our knowledge regarding collapse behaviour in residual granites of the Western Cape.

1.2 THE AIM OF THE RESEARCH STUDY

The aim of the research study is to determine the occurrence of collapsible soils as well as the extent of the collapse problem in the residual granites of the Stellenbosch area.

Further objectives include the following:

- Providing possible explanations concerning the collapse behaviour of the soils as well as attempting to define the mechanisms of collapse through Atterberg limits and particle size distributions;
- Determining the influence of collapsibility on the shear strength of the soils;
- Studying the vertical deformation of the soil samples during shear in an attempt to reinforce the collapse results from the double oedometer tests;
- Determining the effect of topography and drainage on the collapsibility of the soils.

1.3 DEMARCATION OF FIELD OF RESEARCH

Demarcation of the field of research is necessary in order to ensure the feasibility of the study. An area between Stellenbosch and Somerset West in the Western Cape was selected as the study area. The study area is situated on the eastern side of the R44 between Stellenbosch and Somerset West and was selected as it is located close to the University of Stellenbosch and thus accessible to the researcher. It was further chosen as difficulties related to collapsible soils have been encountered here.

1.4 RESEARCH METHODOLOGY

The research methodology entailed a literature study, field work and experimental work. This research report is divided into the following five chapters:

- **Chapter 1: Introduction.** In this chapter an outline of the motivation for the study, the aims of the study, the demarcation of the field of research and the methodology of research undertaken, are provided.
- **Chapter 2: Literature study.** The purpose of the literature study is to provide a basis or background for the research study. Literature from various sources was examined to provide a thorough background on the collapse phenomenon in Southern Africa. The main focus of the chapter is the evaluation, prediction, and identification of collapsible soils, as well as the distribution of these soils in South Africa and the problems associated with construction thereon. A short description of other problematic characteristics associated with residual granite soils is also given. Special attention is paid to the decomposition of granite and its weathering products. Construction remedies for building sites where collapsible soils are encountered are also addressed.
- **Chapter 3: Demarcated study area and field work.** Field work forms the basis of the experimental work of the research study. In this chapter the focus is on the procedures followed in the execution of the field work and a background concerning the geology of the study area is provided. The field work includes soil sampling and soil profiling. An excavator was used to dig a total of fourteen pits on three farms and in a cemetery. Fourteen undisturbed soil samples were collected for laboratory testing.

- **Chapter 4: Experimental work.** In chapter 4 the focus is on the experimental work carried out to achieve the aims of the study. The results and interpretations of the results are included in this chapter. The experimental work entails double oedometer testing, shear strength testing and indicator analyses. Double oedometer tests were performed to predict the amount of settlement of the soils from the study area and subsequently the occurrence of the collapse problem. To better understand the collapse behaviour of the soils, indicator analyses were carried out. Direct shear tests were further performed to determine the influence of collapsibility on shear strength and to study the vertical deformation of the soils during shear.
- **Chapter 5: Conclusions and recommendations.** In the last chapter the conclusions and recommendations resulting from the research study can be found.

CHAPTER 2: LITERATURE STUDY

2.1 INTRODUCTION

Granite is one of the most well known rocks. It is an easily identifiable rock of widespread occurrence. Granite is formed from lavas rich in silica (usually 68-70%), potash, alumina, and soda, but normally poor in lime, iron, and magnesia. It is usually an intrusive massive rock. Granites are coarse-grained rocks and the chief minerals making up granite include quartz, plagioclase feldspar, orthoclase feldspar, biotite mica and muscovite mica. Lesser constituents include iron ores (Army Code No 71044, 1976). These rocks differ extensively in type by the addition and substitution of other minerals (Chamberlin et al., 1914).

Residual granite is formed by the in-situ decomposition (chemical weathering), or the disintegration (physical weathering) of rock, to a level of softness which gives an unconfined compressive strength of the unbroken material of less than 700kPa.
Residual soils derived from granite will contain primary quartz grains, mica flakes and secondary kaolinite derived from the decomposition of feldspars (Jennings et al., 1973).

The main structure of these soils usually consists of bulky-sized quartz particles, with silts, fine sands and colloidal matter in between. The individual grains are coated with the colloidal material. Intense leaching of the soluble and colloidal matter creates a structure resembling a honeycomb. When this soil becomes saturated with water it collapses and so creates problems in buildings, roads, airfields, railways, and earth dams and reservoirs (Schwartz, 1985).

These collapsible soils, including the evaluation, prediction, and identification thereof, will be the main focus of the chapter, as well as the distribution of the soils in South Africa and the problems associated with construction thereon. A short description of other problematic characteristics related to residual granite soils will also be given. In the study special attention will be paid to Cape granite and therefore the distribution of granites throughout the South-Western Cape will be given so that the possible widespread occurrence of the collapse problem in the area can be understood.

Understanding the development of residual soils and being familiar with its products, is critical in comprehending the collapse phenomenon, therefore the decomposition of rock and its weathering products will be discussed in detail. The conclusion of the chapter will comprise of a discussion on construction remedies for building sites where collapsible soils are encountered.

2.2 CAPE GRANITE SUITE

The Cape granites, intrusive into the Malmesbury Group, are high-level diapiric plutons which crystallized from magmas formed by anatexis at increasingly higher levels in the crust (Schoch et al., 1977). Radiometric dating indicates an age range of 632 ±10 Ma for the earliest phase to 530 ±15Ma for the youngest phase (Leygonie, 1977).

With the exception of isolated occurrences in Namaqualand and in the Southern Cape, near George, exposures of Cape Granite are restricted to the South Western Cape. Figure 2.1 below shows the localities of plutons of the Cape Granite suite, which includes Swellendam, Robertson, Greyton, Onrus, Wellington, Paarl, Paardeberg, Saldanha-Langebaan, Stellenbosch, Kuils River-Helderberg, Darling, Avoca, Dassen Island, Haelkraal and the Cape Peninsula.

Although broadly termed ‘granites’, the lithology of the suite is actually quite complex, with the rocks ranging in composition from coarse-grained porphyritic biotite granites, to finer grained quartz porphyries, and even including some syenites and some quartz diorites (Brink, 1981).

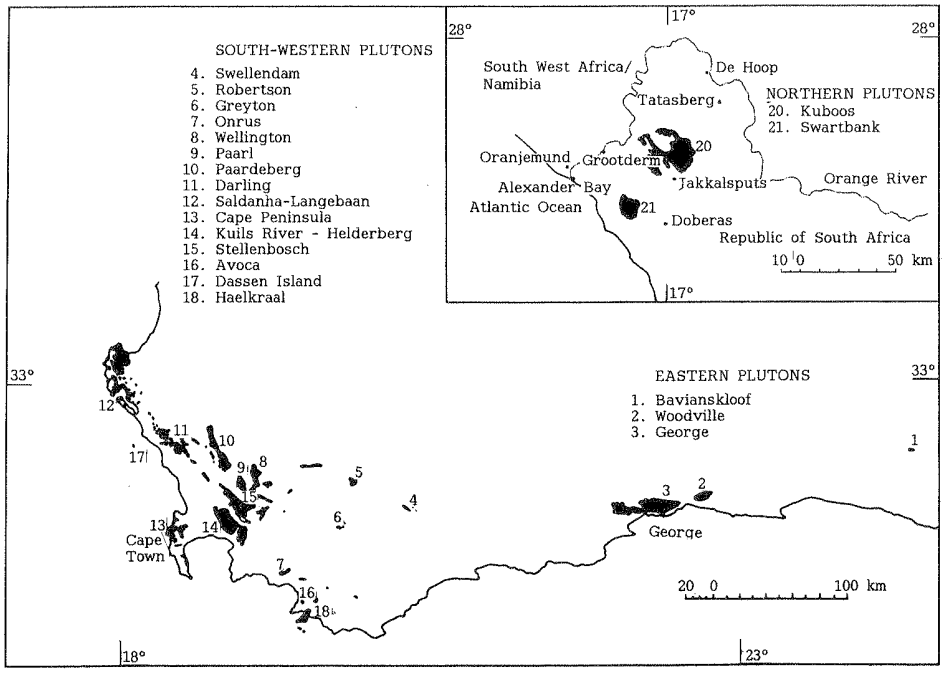

Figure 2.1: Localities of plutons of the Cape Granite Suite (Brink, 1981)

The widespread occurrence of Cape granite gives an indication of the possible extent of the collapse problem in the South Western Cape.

2.3 DEVELOPMENT OF RESIDUAL SOIL

A residual soil is formed from the in-situ decomposition of rock. Decomposition can result from chemical weathering or mechanical disintegration. In the relatively humid areas of the eastern part of South Africa as well as the southwestern coastal areas, chemical decomposition is the prevailing mode of rock weathering, producing generally deep residual soils with medium to high compressibility and low shear strengths. In the fairly arid western part of South Africa, where mechanical disintegration is the leading mode of weathering, the material will be more stable and the thickness of the soil profile smaller (Zeevaert, 1983).

The following aspects concerning the development of residual soils will forthwith be discussed, namely:

- The physical and chemical weathering of rock and its weathering products;
- The effects of climate, topography and drainage on the weathering of rock;
- The decomposition of granite and its products;

- Factors influencing the weathering of granite.

To complete this section, a short discussion on the geology of residual soils and the strength of residual soils will be given.

2.3.1 Physical weathering

As indicated by Mitchell (1993) generally five processes of physical weathering are important:

1. **Unloading.** When the effective confining pressure is reduced, cracks and joints may form to depths of hundreds of meters below the ground surface. Reduction in confining pressure may be a consequence of uplift, erosion, or changes in fluid pressure. Exfoliation, which is the peeling off of surface layers of rock, may occur during rock excavation and tunnelling.
2. **Thermal expansion and contraction.** The outcomes of thermal expansion and contraction range from the creation of planes of weakness from strains already present in the rock to complete fracture.
3. **Crystal growth, including frost action.** Significant disintegration may be caused by the crystallization pressures of salts, especially the pressure related to the freezing of water in saturated rocks.
4. **Colloid plucking.** The shrinking of colloidal material on drying, can apply a tensile stress on surfaces with which they are in contact.
5. **Organic activity.** An important weathering process is the growth of plant roots in existing fractures in rocks. Additionally, the activities of worms, rodents, and man may cause considerable mixing in the weathering zone.

2.3.2 Chemical weathering

Chemical decomposition and leaching play a critical role in the formation of residual soils (Schwartz, 1985). According to Mitchell (1993) physical weathering processes are normally the forerunners of chemical weathering. Their primary contributions are to loosen rock masses, reduce particle size, and increase the available surface area for chemical attack.

Some important chemical processes as indicated by Mitchell (1993) are listed below:

1. **Hydrolysis**, almost certainly the most important chemical process, is the reaction between the mineral and the H^+ and $(OH)^-$ of water. The tiny size of the H^+ ion allows it to enter the lattice of minerals and replace existing cations. For example:

   Orthoclase feldspar:

   $$\text{K-silicate} + H^+ OH^- \leftrightarrow \text{H-silicate} + K^+ OH^- \text{ (alkaline)}$$

   Anorthite:

   $$\text{Ca-silicate} + 2H^+OH^- \leftrightarrow \text{H-silicate} + Ca(OH)_2 \text{ (basic)}$$

According to Reiche, 1945 (Mitchell, 1993) a general expression for hydrolysis of a silicate mineral is:

$$MSiAlO_{11} + H^+OH^- \leftrightarrow Al(OH)_3 + (M,H)AlSiAl^tO_n$$

where n refers to unspecified atomic ratios, and o and t refer to octahedral and tetrahedral coordinations. M points out metal cations.

Next the hydrogenated surface layers become unstable, and tetrahedra and octahedra peel off (Jenny, 1941). The formation of ordered but variable chains and networks of $Si(OH)_4$, $AL(OH)_3$, KOH and water follows. The continued driving of the reaction to the right requires the removal of soluble materials by complexing, leaching, adsorpsion, and precipitation, in addition to the continued introduction of H^+ ions. The pH of the system influences the amount of available H^+, the solubility of $SiO_2 + Al_2O_3$ and the type of clay mineral that forms (Mitchell, 1993). The solubility of silica and alumina as a function of pH is shown in figure 2.2 below.

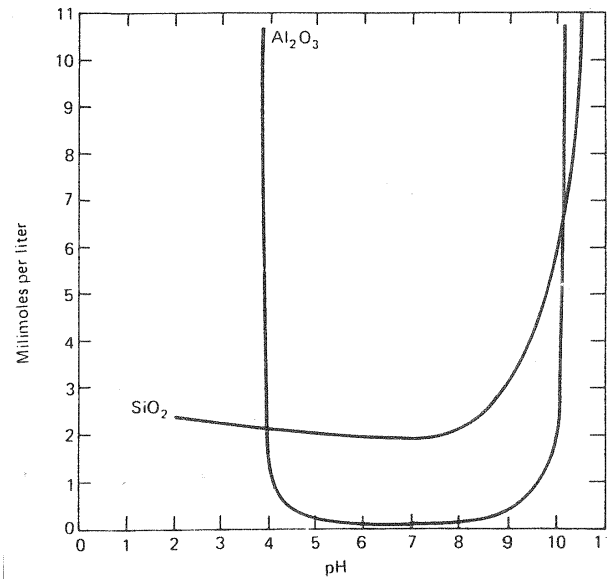

Figure 2.2: Solubility of alumina and amorphous silica in water (Keller, 1964 from Mitchell, 1993)

2. **Chelation** involves the complexing and exclusion of metal ions. It assists in driving hydrolysis reactions (Mitchell, 1993).

3. **Cation exchange** is critical in chemical weathering in at least three ways:

- It may result in the replacement of hydrogen on hydrogen bearing colloids. This lessens the ability of the colloids to bring H^+ to unweathered surfaces;
- The types of clay minerals that form are influenced by the ions held by Al_2O_3 and SiO_2 colloids;
- Physical properties of the system such as the permeability may rely on the absorbed ion concentrations and types (Mitchell, 1993).

4. According to Keller (1957) **oxidation** is the loss of electrons by cations, and **reduction** is the gain of electrons. Both reactions are important in chemical weathering. The oxidation of pyrite is characteristic of many oxidation reactions during weathering:

$2FeS_2 + 2H_2O + 7O_2 \rightarrow 2FeSO_4 + 2H_2SO_4$

$FeSO_4 + 2H_2O \rightarrow Fe(OH)_2 + H_2SO_4$
(hydrolysis)

Oxidation of $Fe(OH)_2$ gives

$4Fe(OH)_2 + O_2 + 2H_2O \rightarrow 4Fe(OH)_3$

$2Fe(OH)_3 \rightarrow Fe_2O_3 \cdot nH_2O$ (limonite)

Reduction reactions, which are of great importance relative to the influences of bacterial action and plants on weathering, store energy that can be utilized in later stages of weathering (Mitchell, 1993).

5. **Carbonation** is the amalgamation of carbonate or bicarbonate ions with earth materials. The source of the ions is atmospheric CO_2. The carbonation of dolomite limestone continues as follows (Mitchell, 1993):

$Ca\ Mg(CO_3)_2 + 2CO_2 + 2H_2O \leftrightarrow Ca(HCO_3)_2 + Mg(HCO_{3)2}$

In South Africa the most important physical processes that comminute the rock and expose fresh mineral surfaces to the effects of weathering include stress release by erosion, salt crystallization pressures and differential thermal strain. The principal chemical processes include hydrolysis, carbonation, chelation, cation exchange and oxidation and reduction. The biological processes consist of physical action (e.g. root-wedging) and chemical action (e.g. bacteriological oxidation and reduction of iron and sulphur compounds) (Engelbrecht, 2008).

2.3.3 Weathering products

The general products of weathering of which quite a few will generally coexist at the same time, include:

1. Unaltered minerals that can either be highly resistant or recently exposed;
2. Freshly formed, more stable minerals having the same structure as the original mineral;
3. Newly formed minerals that have a form comparable to the original, but a changed internal structure;
4. Products of disturbed minerals, which may be found at the site or transported from the site. Such minerals may include:
    a) Colloidal gels of Al_2O_3 and SiO_2,
    b) Zeolites,
    c) Clay minerals,
    d) Cations and anions in solution,
    e) Mineral precipitates.
5. Guest reactants which are unused (Mitchell, 1993).

The relationship between minerals and different weathering phases is given in table form below.

Table 2.1: Representative Minerals and Soils Associated with Weathering Stages (Jackson and Sherman, 1953)

Weathering Stage	Representative Minerals	Typical Soil Groups
	Early weathering stages	
1	Gypsum (also halite, sodium nitrate)	Soils dominated by these minerals in the fine silt and clay fractions are the youthful soils all over the world, but mainly soils of the desert regions where limited water keeps chemical weathering to a minimum.
2	Calcite (also dolomite apatite)	
3	Olivine-hornblende (also pyroxenes)	
4	Biotite (also glauconite, nontronite)	
5	Albite (also anorthite microcline, orthoclase)	
	Intermediate weathering states	
6	Quartz	Soils dominated by these minerals in the fine silt and clay fractions are mainly those of temperate regions developed under grass or trees. Includes the major soils of the wheat and corn belts of the world.
7	Muscovite (also illite)	
8	2:1 layer silicates (including vermiculite, expanded hydrous mica)	
	Montmorillonite	
	Advanced weathering stages	
10	Kaolinite	Many intensely weathered soils of the warm and humid equatorial regions have clay fractions dominated by these minerals. They are frequently characterized by their infertility.
11	Gibbsite	
12	Hematite (also geothite, limonite)	
13	Anatase (also rutile, zircon)	

2.3.4 Effects of climate, topography and drainage on the weathering of rock.

Climate has a dominating influence on the rate of formation of weathering products, on the main weathering processes and on the erosion rate of weathered material (Engelbrecht, 2008). Climate determines the quantity of water present, the temperature, and the nature of the vegetative cover, which in turn have an affect on the biologic cover. The broad influences of climate are the following:

- For a certain quantity of rainfall, chemical weathering advances more rapidly in warm climates than in cooler climates;
- At a stable temperature, weathering advances much more quickly in a wet climate than in a dry climate. This can be assumed if sufficient drainage is available;
- Weathering is influenced by the depth to the water table. This is the depth to which air is available as a gas or in solution;
- The type of rainfall is significant: light intensity, long duration rains soak in and aid in leaching; while short, intense rains erode and run off (Mitchell, 1993).

Throughout the early stages of weathering and soil formation, the parent material is a lot more important than it is after intense weathering for long periods of time. Ultimately, parent material becomes a less dominant factor than climate in residual soil formation. Of the igneous rock forming minerals, only quartz, and less importantly, feldspar, have adequate chemical durability to persist over long periods of weathering. Quartz is the most abundant in coarse-grained granular rock such as granite, gneiss, and granodiorite. The quartz particles typically occur in the millimetre size range. As a result, granitic rocks are the major source of sand.

Apart from its influence on climate, topography will determine primarily the rate of erosion, and therefore control the depth of soil accumulation and also the time available for weathering prior to the exclusion of material from the site. In areas where the topography is steep, rapid mechanical weathering will take place followed by swift down slope movement of the debris. This will result in the formation of talus

slopes. Talus slopes are heaps of fairly unweathered coarse rock fragments (Mitchell, 1993).

Topography and drainage are major factors in determining what clay minerals form. Reddish kaolinitic soils form in well drained conditions over a norite gabbro parent rock, whereas blackish montmorillonitic clays form from identical parent rock in weakly drained circumstances (Engelbrecht, 2008).

2.3.5 Decomposition of granite

Selective and progressive decomposition of unstable minerals in granite bedrock are the cause of breakdown of the rock by spheroidal weathering, disintegration, and disaggregation. Granitic rock can be weathered to depths of 30m or more and may consist of a mixture of solid rock and residual debris throughout most of the profile. From the base upward, the proportion of solid rock generally decreases gradually.
Granitic rock weathers broadly in accordance with Bowen's reaction series (Mitchell, 1993). See figure 2.3 below.

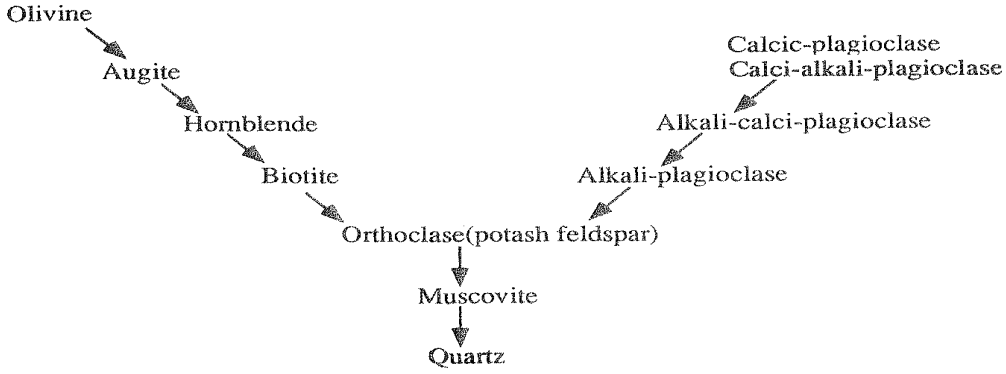

Figure 2.3: Bowen's reaction series of mineral stability. Each mineral is more stable than the one above it (Mitchell, 1993)

Firstly, biotite decomposes followed by plagioclase feldspar. When a fraction of the plagioclase has decomposed and breakdown of the orthoclase begins, the rock breaks into pieces of decomposed granite called gruss. Once most of the orthoclase has weathered to kaolinite, the gruss crumbles to silty sand. This silty sand typically

contains mica flakes. Aside from some mechanical breakdown, the quartz fragments remain unchanged (Mitchell, 1993).

A decomposed granite profile typically consists of four zones as shown in the figure below.

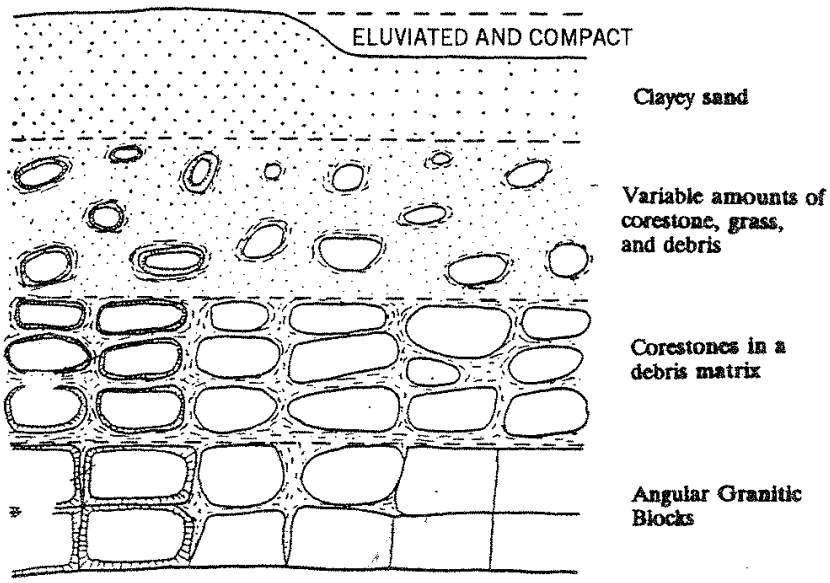

Figure 2.4: Zones of a mature profile of decomposed granite (Mitchell, 1993)

The deepest zone contains angular granitic blocks. Even though the rock may be relatively highly altered, the amount of residual debris is small. The zone above the deepest zone contains abundant angular to subangular core stones in a matrix of gruss and residual debris. The upper middle zone is the most inconsistent part of the weathering profile and generally contains more or less equal amounts of rounded core stone, gruss, and residual debris. The topmost zone typically consists of a structureless mass of clayey sand with highly variable grain size distribution (Mitchell, 1993).

The weathering products of granite include: primary quartz grains, mica flakes and secondary kaolinite derived from the decomposition of feldspars (Jennings et al., 1973).

2.3.6 Factors influencing the weathering of granite

(a) **Climate**

Since most chemical reactions take place faster at high temperatures than they do at low temperatures, the majority of the deep weathering so far recorded from granite terrains derives from the humid tropics. In arid conditions granite is much more resistant to weathering due to the absence of water (Twidale, 1982).

(b) **Rock composition**

Rock composition is an important aspect determining the nature and the rate of rock disintegration and decomposition (Twidale, 1982). Goldich (1938) indicates that the susceptibility of the general rock-forming minerals to chemical weathering is the reverse of the order in which they crystallize from an igneous melt (see figure 2.3). This is because the high temperature minerals are in greater disequilibrium than those that crystallize in cooler conditions.

Granite is one of the more resistant common rock types. But they differ in composition and this plays an important part in determining the relative toughness of the specific types of granitic rock (Twidale, 1982).

(c) **Texture**

Another variable affecting the advancement of weathering is rock texture. Provided that there is access to crystal faces in pores and intergranular spaces, fine-grained rocks should be vulnerable to chemical (moisture) attack as, compared with coarse-textured materials, they have large areas of crystal surface per unit volume. These surfaces contain high free energy and are prone to reaction with circulating liquids. Conversely, coarse-grained rocks such as granite, are supposed to be relatively resistant by virtue of their lesser areas of crystal face per unit volume (Twidale, 1982).

(d) **Partings**

Any parting or fracture in a rock is a potential path for water infiltration, and is therefore a source of weakness. Crystal cleavage, intracrystal dislocations, and crystal boundaries are paths penetrable by water, but the regular patterns of joints and faults are more important since they are frequently open, widely developed, and they tend to form continuous networks. However fractures, of any origin, are planes of weakness that have been exploited by molten materials from deep within the earth's crust, and by external agencies, particularly meteoric waters (Twidale, 1982).

2.3.7 Geology of residual soils

Although this thesis revolves around granitic residual soils, it is important that one is familiar with residual soils from other rocks as well, to ensure a thorough study. Soils residual from igneous rock, metamorphic rock, limestone, sandstone and shale will therefore be discussed.

2.3.7.1 Residual soils from igneous and metamorphic rock

Numerous parts of the world, especially the roots of mountains, are formed of granites, gneisses, schists, and other similar rocks that were formerly heated to a plastic condition. These rocks vary significantly in their resistance to weathering: Granites tend to be very durable whereas schists that are high in mica and feldspar weather rapidly. Residual soils formed from these rocks vary from relatively coarse sands to very fine-grained accumulations of mica and clay minerals, depending on the original rock composition. The deposits are very erratic in composition and in extent. In metamorphic rocks, the minerals tend to be arranged in narrow bands resembling strata, and those bands are frequently twisted and distorted from faulting and plastic flow. Residual soils from such rocks can retain the same distorted and folded bands as differences in composition and texture (Sowers et al., 1953).

2.3.7.2 Residual soils from limestone

Limestones (and dolomites) are sedimentary rocks consisting largely of calcium and magnesium carbonates. These minerals are dissolved by water containing small amounts of carbon dioxide, and the insoluble impurities remain behind as residual soil. These impurities mainly include chert (gravel and sand sizes), clay, and iron oxide; and they normally comprise from 2 to 10 per cent of the original rock.
The soils originating from limestone and dolomite are clays and sandy, gravelly clays that are usually a deep red color due to the iron (Sowers et al., 1953).

2.3.7.3 Residual soils from sandstones and shales

Sandstones and shales are formed from the consolidation or cementing of sands and clays. When sandstones are subjected to weathering, they break down physically or by the decomposition of the cementing material into the original sands. Shales slake under the action of water and air into clays. The deposits of these soils are generally thin and there is rarely a definite dividing line between soil and rock (Sowers et al., 1953).

The strength of residual soils is the key to understanding the collapse phenomenon. A short discussion on this issue follows.

2.3.8 Strength of residual soils

Since residual soils derive from the decomposition of a parent rock, they usually contain relict joints and often have fissures resulting from seasonal movement superimposed over the original fabric of the rock. Consequently, all of the points relevant to the strength of layered or jointed soils apply to residual soils. While weathering of the rock advances, the void ratio of the resultant soft rock or soil increases while its strength decreases. This applies to soils residual from sedimentary rocks and those from igneous rocks. In the case of igneous rocks, the increase in void ratio results primarily from chemical causes i.e. the change of rock forming minerals to clay minerals with a resulting expansion, leaching of soluble products of weathering, and suffusion or removal by internal erosion of weathering products.

It is found that the strength of residual soils is normally related to their density and void ratio (Engelbrecht, 2008).

2.4 COLLAPSIBLE GRAIN STRUCTURE OF RESIDUAL GRANITE

As previously mentioned, weathering of granite produces primary quartz grains, mica flakes and secondary kaolinite derived from the decomposition of feldspars (Jennings et al., 1973). It is these weathering products that form residual granitic soils.

The main structure of these soils consists of bulky-sized quartz particles. Silts, fine sands and colloids make up the remaining part of the soil. The individual grains are coated with the colloidal material. Through intense leaching of the clays, silts and colloidal matter, a structure similar to a honeycomb develops. This structure becomes very unstable when saturated and is as a result susceptible to collapse and large bulk volume decrease (Koerner, 1984).

A soil with a collapsible fabric can withstand moderately large imposed stresses with small settlements at a low in-situ moisture content. When wetting up occurs, a decrease in volume and associated settlement will take place with no increase in the applied stress. The change in volume is associated with collapse of the soil structure (Schwartz, 1985). According to Brink et al. (1982) collapse may occur in any open textured silty or sandy soil with a high void ratio which yet has a moderately high shear strength at a low moisture content owing to colloidal or other coatings around the individual grains.

When collapsing soils are saturated, the colloids and salts soften and lose strength and stiffness. As a result the fabric collapses, leading to large volume change and surface settlement. The shearing action of earthquakes or the vibrations caused by aircrafts or heavy trucks can also be the cause of the loss in strength. The rate of collapse depends on the rate at which the soil mass can be saturated by water from its environment (Schwartz, 1985).

The basic concept of collapse settlement is illustrated in the figure below.

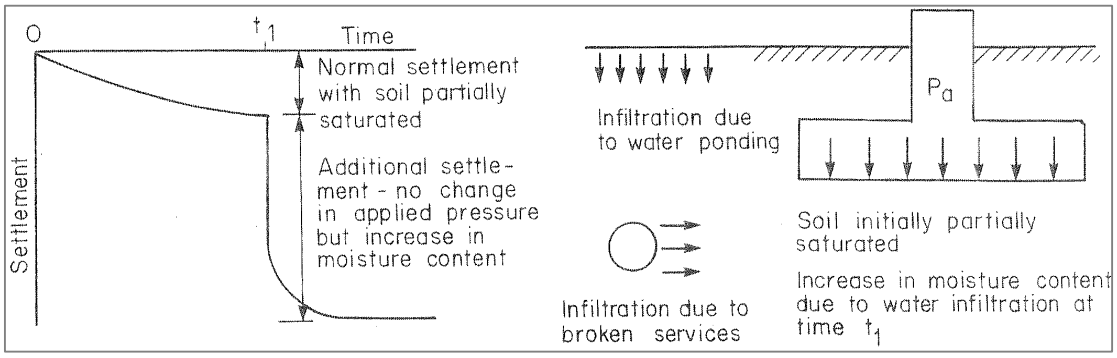

Figure 2.5: The basic concept of additional settlement due to collapse of the soil fabric (Schwartz, 1985)

According to Dudley (1970), collapse is very different from traditional consolidation as no water is being expelled and in actual fact the soil will be absorbing water and progressively losing strength. Jennings and Knight (1975) indicated that the problem is associated with a change in the compression characteristics of the soil effectuated by capilliary forces resulting from partial saturation.

From the discussion above it is clear that the following conditions must be satisfied before collapse settlement can occur:

1. A collapse fabric must be present in the soil. In South Africa this is common in many transported soils as well as in areas where quartz rich rocks such as granite or felspathic sandstone have undergone chemical weathering to create intensely leached residual soils;
2. Partial saturation is essential. When soils are below the water table, collapse settlement will not occur;
3. An increase in moisture content is essential. When the moisture content increases the bridging colloidal materials experience a loss of strength and the soil grains are forced into a denser state of packing associated with a reduction in void ratio;
4. Most of the soils with a collapse fabric in South Africa must be subjected to an imposed pressure which is greater than their overburden pressure before collapse will take place. In this hypothesis it is assumed that the natural

ground surface is stable in spite of the moisture content of the subsoil (Schwartz, 1985).

2.5 OTHER PROBLEMATIC CHARACTERISTICS ASSOCIATED WITH RESIDUAL GRANITE SOILS

Other problems identified in residual granite soils include:

- Expansiveness
- Dispersiveness
- Selective mechanical suffusion
- Compressibility/differential consolidation

2.5.1 Expansiveness

Expansive clays are almost certainly one of the most widespread of the problem soils in South Africa. The difficulties occur, not as a result of a lack of sufficient engineering solutions, but largely owing to a failure to recognise the potential problem or the extent of the movement that can be expected (Williams et al, 1985).

Expansiveness, which is the reverse of consolidation, may be defined as the gradual increase in volume of a soil under negative excess pore water pressure (Craig, 2004). Although residual granitic soils, by virtue of their low to moderate plasticity, are usually considered to be non-expansive, in certain areas slightly expansive soils has been identified (Brink, 1981).

2.5.2 Dispersiveness

Certain fine-grained soils are structurally unstable, easily dispersed, and, as a result, highly erodible. A dispersive clay can be defined as a soil in which the clay particles will detach spontaneously from one another and from the soil structure and go into suspension in quiet water (Mitchell, 1993).

These soils generally have a higher exchangeable sodium percentage (ESP) than non-dispersive soils and the phenomenon has been identified in a wide variety of soils including residual granitic soils. Recent studies on residual granite soils in the

Western Cape show that chemical dispersion of the clay particles may contribute to the collapse of a soil structure (Brink, 1981).

When a clayey soil mass with a high exchangeable sodium percentage comes in contact with flowing water, the dispersed clay particles will be carried away. The result is visible signs of piping and jugging (formation of internal cavities or 'jugs' in the mass), which will make the soil vulnerable to collapse (Brink, 1981).

2.5.3 Selective mechanical suffusion

Selective mechanical suffusion, which is the selective washing out of deflocculated kaolinite, is a phenomenon which has been identified to occur in residual soils. The washing out of the clay particles creates sink holes in the soil and can therefore make the soil susceptible to collapse (Brink, 1981).

2.5.4 Compressibility/differential consolidation

Consolidation is the gradual reduction in volume of a fully saturated soil of low permeability owing to drainage of some of the pore water, the process continuing until the excess pore water pressure set up by an increase in total stress has completely dissipated. Consolidation settlement will result, for instance, if a structure is built over a layer of saturated clay or if the water table is lowered permanently in a layer overlying clay. Differential consolidation has been identified in residual granite soils and this phenomenon may be the result of dispersion or selective mechanical suffusion (Craig, 2004).

Although collapse is clearly not the only problematic characteristic associated with residual granite soils, it is the only characteristic this study will focus on.

2.6 THE PROBLEMS ASSOCIATED WITH CONSTRUCTION ON SOILS WITH A COLLAPSIBLE FABRIC

There are numerous recorded (and almost certainly even more unrecorded) instances of problems associated with construction on soils with a collapsible fabric.

Taking into consideration the modern knowledge with regard to these soils however, it appears reasonable to conclude that problems with construction take place under one or more of the following circumstances:

1. No geotechnical investigation was done;
2. Construction was carried out prior to the identification of the collapse phenomenon. This is mainly the case with settlement and distortion occurring within many older structures;
3. During the investigation potentially collapsible soils within the profile were not correctly evaluated or identified (Schwartz, 1985). Jennings and Knight (1975) indicate that errors in the assessment of compressibility or bearing capacity have been made, given that a partially saturated condition will frequently give a potentially collapsible soil a dense or stiff consistency;
4. The client, designer or contractor ignored the recommendations made by the geotechnical engineer (Schwartz, 1985).

Typical problems with buildings, roads and earth dams/reservoirs will now be discussed.

2.6.1 Buildings

During 1955 the sudden large settlement of portions of a steel framed building near Witbank drew attention to the phenomenon of soils with a collapsible fabric. Since then investigations have revealed that numerous cases of settlement and structural damage can be accredited to structures being founded on a soil with a collapsible fabric.

The following frequent factors appear to be present in most recorded cases of collapse settlement beneath foundations:

1. Structures founded on collapsible soils may perform well for many years and then sudden collapse can take place on increase of moisture;
2. Large settlements can take place beneath even lightly loaded structures. Settlement may be as much as 10% of the thickness of the collapsible soil horizon;

3. Collapse settlement is frequently localized (for example beneath foundations neighbouring leaking pipes or adjacent to poorly drained areas where ponding of rainfall occurs) and as a result differential settlement occurs (Schwartz, 1985).

2.6.2 Pavements, airfields and railways

The failure of sections of road between Witbank and Springs constructed on a soil with a collapsible fabric, drew attention to the problem of roads and runways on collapsing soils. The road was investigated and subjected to an increased traffic load due to coal haulage. Settlement of up to 150mm of the road surface was detected. This settlement was due to densification or collapse in the in situ subgrade.

Under certain circumstances an increase in moisture content may not be necessary for collapse to take place. Traffic vibration caused by dynamic loads may be adequate to cause shear failure of bridging colloidal material and induce collapse. For roads, airfields and railways this is of particular importance as the subgrade is continuously subjected to dynamic forces (Schwartz, 1985).

2.6.3 Earth dams/ reservoirs

The general problems associated with the construction of earth dams/ reservoirs on collapsible soils may be summarized as follows:

1. Typical reservoir construction includes the excavation of material from the planned storage area to form the reservoir embankments. In a soil profile which includes potentially collapsible soils, shortage of material may be experienced caused by compaction volume reductions (Schwartz, 1985);
2. Collapse of the foundation may damage the embankment, or the embankment itself may collapse if it is not appropriately compacted to destroy the fabric;
3. The relatively open fabric of collapsible soils may lead to excessive seepage losses through foundation soils. Severe leakage could also occur through the wall, due to collapse settlement which causes cracking of the wall;

4. Overtopping of the embankment may occur with severe conditions of collapse settlement (Das, 2004).

2.7 DISTRIBUTION OF SOILS WITH A COLLAPSIBLE FABRIC IN SOUTH AFRICA

Collapse was originally thought to occur only in loose Aeolian deposits such as loessial sands. The differential settlement of a water tower near White River in 1957 is the first reported case of collapse settlement of a residual granite soil of the basement complex. Since then collapse settlement has been identified in a wide range of transported soils and also in a number of residual soils other than residual granitic soils of the Basement Complex (Schwartz, 1985).

2.7.1 Transported soils

Transported soils are soils which have been moved by a natural agency (water, wind, gravity or ice) in fairly recent geological times (Schwartz, 1985). Table 2.2 gives the origins of transported soils and an indication of possible engineering problems associated with each soil type.

Table 2.2: Transported soils and possible engineering problems (Jennings and Brink, 1978 from Schwartz, 1985)

Transported Soil Type	*Agency of Transportation*	*Source*	*Soil Type*	*Problems to Anticipate*
Talus (coarse colluvium)	Gravity	Any rock out-cropping directly above talus deposit	Unsorted angular gravel and boulders	Slope insta-bility
Hillwash (fine colluvium)	Sheetwash	Acid crystalline rock	Clayey sand	Collapsible grain structure
		Basic crystalline Arenaceous sedi-mentary	Clay Sand	Heave Collapsible grain structure
		Argillaceous sedi-mentary	Clay or silt	Heave or high compressibility Dispersive soils
Gulleywash	Gulleywash	Local catchment	Gravels, sands silts or clays	All possible problems
Lacustrine deposit	Stream depositing in pan, lake or subterranean pool in cavern-ous rock	Usually mixed source	Sand Silt Clay	Compressi-bility Heave or high compressibility
Estuarine deposit	Rivers and tides	Mixed	Sand Silt Clay	Quicksand High sensitivity compressibility
Aeolian deposit	Wind	Usually mixed source	Sand	Collapsible grain structure Compressibility
Littoral deposit	Waves	Mixed	Beach sand	Collapsible grain structure
Biotic soils	Termites	The underlying soil	Often a clayey or silty sand	Collapsible grain structure
Alluvium	Streams	All materials with-in the catchment	Gravel, sands, silts or clays	Clays commonly heaving
Slide debris	Mass wasting	Upslope rock and soil	Mixture of poorly sorted debris	Slope instabi-lity. High permeability

From the above table it is clear that the problems associated with a collapsible grain structure can be encountered in the majority of transported soils (gulley wash, hillwash, aeolian and littoral deposits, biotic soils). It is noticeable that these types of transported deposits, with their associated problems due to collapse, can be found anywhere in South Africa (Schwartz, 1985).

2.7.2 Residual soils

In South Africa any mention of soils with a collapsible fabric instantly brings to mind the problems related to residual granite soils of the Basement complex. Although this thesis will not revolve around residual granite soils of the Basement complex, it will be discussed briefly below.

The reason for this immediate association with residual granite soils of the basement complex, is probably mainly due to the severe foundation problems that have been identified with these soils in the Johannesburg-Pretoria granite inlier. The collapsible character of the residual soils derived from these ancient granites is associated with the deeply weathered soil profiles found in the humid regions in the eastern part of South Africa (Schwartz, 1985). In these humid regions chemical decomposition is the prevailing mode of rock weathering, producing soils with medium to high compressibility and low shear strengths (Zeevaert, 1983).

In the eastern regions of South Africa where rainfall is relatively high and conditions conducive to leaching prevail, the colloidal kaolinite is mostly removed in suspension by circulating ground waters, leaving behind a soil with a collapsible fabric (Schwartz, 1985).

These residual granite soils of the Basement complex have been researched extensively in the past, whereas the residual granite of the Cape Granite Suite, which this thesis revolves around, has received much less attention.

2.7.3 Other residual soils

Table 2.3 lists the reported occurrences of collapsing grain structure of residual soils, other than residual granite soils of the Basement Complex.

Table 2.3: Reported occurrences of collapsible fabric of residual soils (except granite soils of the Basement Complex) in South Africa (Schwartz, 1985)

Stratigraphic unit	*Location*	*Soil description/Properties*	*Reference*	*Remarks*
Magaliesburg Quartzite Formation of the Pretoria Group of the Transvaal Sequence	Boschdal — south of Rustenburg	Moist reddish brown very loose intact micaceous silty medium and fine sand. Residual Magaliesburg Quartzite. Dry density 1585 kg/m^3	Brink[11]	Collapse properties confirmed by oedometer tests. Decomposition in favourable topographic situation produced highly leached residual soils. No indication of how widespread phenomenon may be. Possible stratigraphic control confining collapsible material to stratum of highly felspathic quartzite.
Rooiberg Group of the Bushveld Complex	Witbank	Thin layer (1,0 m) of residual felsite of low dry density (1430 kg/m^3).	Brink[11]	No specific tests carried out to evaluate collapse. Soil assumed to have collapse properties in the dry state because of low dry density.
Sibasa and Nzhelele Formations of the Soutpansberg Group	No specific location given	Deeply weathered residual basalt (clayey silt). Low dry density (1200 kg/m^3)	Brink[17]	No specific tests given to evaluate collapse. Indicated that soil has a moderate collapse potential
Cape Granite Suite	Near Stellenbosch and near Constantia	Slightly moist grey mottled reddish brown stiff intact clayey silt. Residual Cape granite. Dry density 1440 kg/m^3	Brink[17] and Errera[6]	Oedometer tests carried out on both sites to prove collapse properties.
Clarens and Elliot. Fromations and Ecca Group of the Karoo Sequence	Mainly central Transvaal	Residual felspathic sandstones.	Weston[18] and Brink[19]	Tests carried out to prove collapse properties of Ecca Group and the Clarens Sandstone Formation.
Diabase sill intrusive into shales of the Pretoria Group	West Rand	Dry orange loose clayey and sandy silt. Low dry density (1000 to 1300 kg/m^3).	Wagener[9]	Double oedometer tests showed residual diabase to have a heave/collapse behaviour. See Fig 4.
Berea Red Sands residual from Quaternary calcarenites	Durban area	Red or orange silty sand.	Walsh Sparks[20] and Errera[6]	Laboratory tests carried out to prove collapse properties.

It is important to note that nearly all of these cases fall within or close to the areas of annual water surplus (Schulze, 1958). This again points out the important role of chemical decomposition and leaching in the formation of collapsing residual soils (Schwartz, 1985).

2.8 EVALUATION AND PREDICTION OF COLLAPSE IN SOILS

The identification and quantification of collapse settlement of soil fabric needs comprehensive field identification in addition to laboratory or in-situ testing to measure the magnitude of collapse settlement (Byrne et al., 1995). A number of test procedures for the evaluation of soils believed to be collapsible have evolved. Most of these tests are more research tools than day-to-day routine methods to be used for identification and design purposes (Das, 2004).

2.8.1 Field identification

The first step in identifying a potentially collapsible soil in the field is the accurate recording of the soil profile. Dry or slightly moist soils indicate partial saturation and even though the in situ consistency will depend on the moisture content, a loose or open fabric will typically be apparent while recording the soil profile. With a hand lens, colloidal coatings and clay bridges are also visible. The accurate identification of the origin of the soils within the profile will also give an indication of whether problems with collapse could occur (Schwartz, 1985).

Jennings and Knight (1975) explain a simple field test (the ‘sausage’ test) to identify a collapsible soil. The method is to carve two cylindrical samples of undisturbed soil of relatively equal diameter and length, to wet and knead one sample and reshape it into a cylinder of the original diameter. When compared with the undisturbed twin sample an obvious decrease in length will confirm a collapsible grain structure. A comparable reduction in volume may be observed by backfilling a pit or trial hole. A more complicated type of test involves the loading of a plate at the bottom of a test pit, or horizontally against the side walls. The deflection upon flooding of the pit is then measured (Schwartz, 1985). Using pressure meters or penetration testing is not viable because saturation of the soil is a problem (De Wet, 2009).

In regions where some development has already taken place, the most important field evidence is the presence of cracking and distortion of existing buildings. Rigid concrete structures will lean towards the area of maximum collapse, whereas flexible steel buildings will show distortion of the less rigid parts. In association with knowledge of the soil profile, an assessment of the cracking pattern must be

undertaken. Similar cracking patterns are frequently associated with both collapse and heave phenomena (Schwartz, 1985).

2.8.2 Laboratory tests

Laboratory tests quantitatively study the collapse on wetting. Still, for tests to be accurate enough for design purposes, laboratory experiments need to follow stress paths and other in situ conditions very accurately. This raises questions about the design value of some tests (De Wet, 2009).

Silty or sandy soils of low clay content are generally associated with collapse problems. Particle size distribution and Atterberg Limits will help to identify these soil types. It is vital to take into consideration that a low clay content does not necessarily imply that collapse will occur. Soils with a collapsible fabric frequently have a low dry density. It is also important not to assume that all soils with a low dry density will have a tendency to collapse and that all soils with a high dry density will not collapse.

In view of the wide range of soils which exhibit collapse properties it is obvious that the following tests should be considered only as index type tests which might be helpful in the identification of potentially collapsible soils and possibly the depth to which these soils occur in the soil profile (Schwartz, 1985).

2.8.2.1 Tests carried out using the consolidometer

(a) **The double-oedometer test**

The double oedometer test can be considered as the standard approach used for the quantification of potential collapse settlement. The test involves subjecting two identical undisturbed samples to the consolidation process, the one sample being saturated and the other at natural moisture content (Das, 2004). The procedures to allow for different initial void ratios of the two undisturbed samples are of particular importance, as is adopting the correct interpretation for normally consolidated and

over-consolidated soils (Schwartz, 1985). Jennings and Knight (1975) propose the following steps for interpretation of the double oedometer test:

1. Plot the e-log p graphs for both specimens.
2. Calculate the in situ effective pressure, p_o. Draw a vertical line corresponding to the pressure p_o.
3. From the e-log p curve of the soaked specimen, determine the preconsolidation pressure, p_c.
4. Determine e_o, corresponding to p_o from the e-log p curve of the soaked specimen.
5. Through point (p_o, e_o) draw a curve that is comparable to the e-log p curve obtained from the specimen tested at natural moisture content.
6. Determine the incremental pressure, Δp, on the soil caused by the construction of the foundation. Draw a vertical line corresponding to the pressure of $p_o + \Delta p$ in the e-log p curve.
7. Now, determine Δe_1 and Δe_2. The settlement of soil without change in the natural moisture content is

$$S_1 = \Delta e_1 / (1 + e_o) \times H$$

Also, the settlement caused by the collapse of the soil structure is

$$S_1 = \Delta e_2 / (1 + e_o) \times H$$

where H = the thickness of soil vulnerable to collapse

The suggested procedure for the interpretation of the double oedometer test, of normally- and over-consolidated soils, is illustrated in figures 2.6(a) and 2.6(b) below.

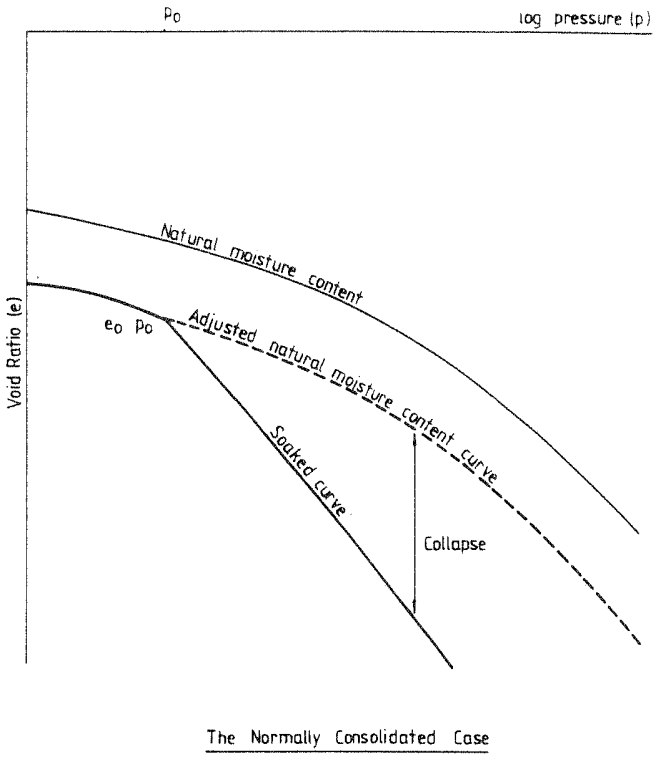

Figure 2.6(a): Interpretation of the double oedometer test of normally consolidated soils (Schwartz, 1985)

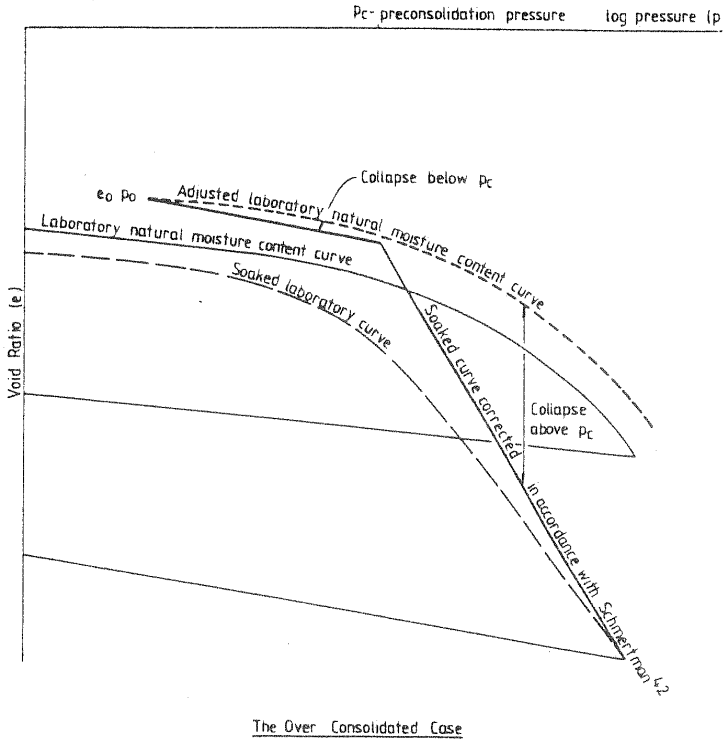

Figure 2.6(b): Interpretation of the double oedometer test of over-consolidated soils (Schwartz, 1985)

Once the correct interpretation has been applied to the double oedometer test curves, prediction of consolidation at natural moisture content and collapse settlement may be carried out using normal consolidation theory (Schwartz, 1985).

Aitchison (1973) emphasizes three sources of error in the prediction of collapse settlement using the double oedometer test:

1. Collapse may depend on the initial state of suction of the soil (particularly in clay soils)
2. The collapse procedure may be stress path dependent
3. The collapse mechanism may be controlled by a factor other than sheer saturation with water.

However, if necessary, the first two sources of error can be allowed for by modifying the double oedometer test. The third source of error is only likely to occur in unusual cases of collapse. In such a case a suitable testing program would have to be developed (Aitchison, 1973).

(b) **The single consolidometer test**

Considering the difficulties associated with the interpretation of the double oedometer test, it would appear fitting to consider using a method which would require the testing of only one undisturbed sample. The sample is loaded at natural moisture content to the expected stress from the structure and then soaked. The consolidation at natural moisture content and the additional settlement due to collapse could then be calculated (Byrne et al., 1995).

An advantage of the test is that an attempt is being made to trail the loading and moisture content paths to which the soil will be subjected in the field. However, an over-prediction of settlement will result from this method seeing that no correction can be made for the regeneration of lateral stresses in the consolidometer while the soil is saturated (Schwartz, 1985).

(c) **The Collapse Potential Test**

The collapse potential test is a special case of the single consolidometer test in which the sample is saturated at a load of 200 kPa (Schwartz, 1985). According to Jennings and Knight (1975) the Collapse Potential is not a design parameter, but is an index figure providing the engineer with a guide to the collapse situation and whether there is good reason for further investigation.

A typical test result from the Collapse Potential Test is illustrated in figure 2.7 below.

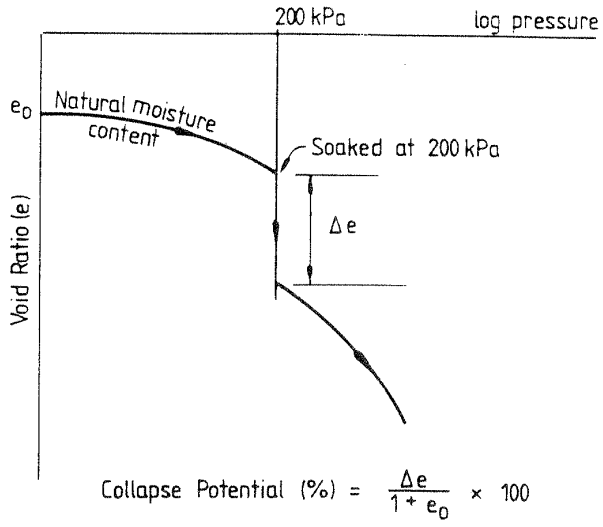

Figure 2.7: Typical collapse potential test result (Schwartz, 1985)

As indicated by Schwartz (1985) the collapse potential, C_p may be calculated as:

$C_p = \Delta\varepsilon = (e_1 - e_2) / (1 + e_0)$

where e_0 = natural void ratio of the soil

$\Delta\varepsilon$ = vertical strain

Guiding values of Collapse Potential are presented in the table below.

Table 2.4: Collapse potential (Byrne et al., 1995)

Collapse Potential	Severity of Problem
0% - 1%	No problem
1% - 5%	Moderate problem
5% - 10%	Problem
10% - 20%	Severe problem
> 20%	Very severe problem

2.8.2.2 Triaxial testing

As previously mentioned, laboratory experiments need to follow stress paths and other in situ conditions very precisely for test results to be accurate enough for design purposes. Triaxial stress path testing may be the only suitable way of accomplishing this. Although no fault can be found with the principle behind the test procedure, it is impractical for routine testing (Schwartz, 1985).

2.8.3 Sampling procedures in soils with a collapsible fabric

The consistency of the test procedures discussed above is clearly dependent on the tests being carried out on representative undisturbed samples (Schwartz, 1985). According to Jennings and Knight (1975) one should use block samples cut by hand from a test pit or trial hole or take samples in the field directly into consolidometer rings.

The sampling procedures proposed by Jennings and Knight were not practicable for this research project. The sampling method used to collect soil samples for this thesis, will be discussed in chapter 3.

2.9 OTHER METHODS OF IDENTIFICATION OF COLLAPSIBLE SOILS

Numerous investigators have proposed various methods for evaluating the physical parameters of collapsing soils for identification (Das, 2004). A few of these methods are discussed briefly in the table below.

Table 2.5: Reported criteria for identification of collapsing soil (Das, 2004 - Modified from Lutenegger and Saber, 1988)

Investigator	Year	Criteria
Denisov	1951	Coefficient of subsidence: $K = \frac{\text{void ratio at liquid limit}}{\text{natural void ratio}}$ K = 0.5–0.75: highly collapsible K = 1.0: noncollapsible loam K = 1.5–2.0: noncollapsible soils
Clevenger	1958	If dry unit weight is less than 12.6 kN/m^3(≈80 lb/ft^3), settlement will be large; if dry unit weight is greater than 14 kN/m^3(≈90 lb/ft^3) settlement will be small.
Priklonski	1952	$K_D = \frac{\text{natural moisture content} - \text{plastic limit}}{\text{plasticity index}}$ $K_D < 0$: highly collapsible soils $K_D > 0.5$: noncollapsible soils $K_D > 1.0$: swelling soils
Gibbs	1961	Collapse ratio, $R = \frac{\text{saturation moisture content}}{\text{liquid limit}}$ This was put into graph form.
Soviet Building Code	1962	$L = \frac{e_o - e_L}{1 + e_o}$ where e_o = natural void ratio and e_L = void ratio at liquid limit. For natural degree of saturation less than 60%, if $L > -0.1$, the soil is a collapsing soil.
Feda	1964	$K_L = \frac{w_o}{S_r} - \frac{\text{PL}}{\text{PI}}$ where w_o = natural water content, S_r = natural degree of saturation, PL = plastic limit, and PI = plasticity index. For $S_r < 100\%$, if $K_L > 0.85$, the soil is a subsident soil.
Benites	1968	A dispersion test in which 2 g of soil are dropped into 12 ml of distilled water and specimen is timed until dispersed; dispersion times of 20 to 30 s were obtained for collapsing Arizona soils.
Handy	1973	Iowa loess with clay (<0.002 mm) contents: <16%: high probability of collapse 16–24%: probability of collapse 24–32%: less than 50% probability of collapse >32%: usually safe from collapse

From the table it is evident that various criteria for the identification of collapsing soils were developed between 1951 and 1973. Since then, however, insufficient research on the subject has been carried out.

2.10 ENGINEERING SOLUTIONS TO THE COLLAPSE PROBLEM

Various solutions have been applied, both successfully and unsuccessfully, to overcome difficulties related to the collapse phenomenon in the construction of engineering structures (Schwartz, 1985). A variety of solutions is presented below.

1. **Precluding the triggering mechanism**

To apply this solution effectively it will be necessary to adopt procedures to ensure that the water does not enter the collapsing soil horizons. However, in practice this is very difficult to achieve (De Wet, 2009).

2. **Chemical stabilization**

A stabilizing agent may be used to strengthen the structural bonds or to fill voids. This is a logical solution, but whether it can be implemented productively in all cases is still uncertain. This could be an area for future research (De Wet, 2009).

3. **Piled and pier foundations**

Structural loads may be transferred through the collapsible soils by means of piled or pier foundations. This method may be used especially when the soils are of transported origin since the collapsible horizon may then be relatively shallow and underlain by stable soils or even rock. In the evaluation of pile capacity no dependence should be placed on skin friction in the collapsible material. Under certain circumstances negative skin friction must be allowed for in the design.

Granites of the Basement complex often have deeper collapsible soil profiles, and in such cases transferring the structural load through the collapsible horizons may not be an economical solution. Under these circumstances it may be feasible to use displacement piles to a restricted depth (Schwartz, 1985).

4. **Design for the collapse as quantified**

The engineering structure can be designed to withstand the predicted collapse settlement by increasing structural flexibility by the provision of joints or reducing the bearing pressures to restrict collapse settlement. Raft foundations have so far been used successfully for structures built on these soils. The nature of the collapse phenomenon however is such that structures may perform well for many years provided there is no increase in the moisture content of the underlying soil. Without any well documented case histories which would have to include observations regarding moisture conditions below the raft foundations, it is impossible to comment on the aptness of this design procedure (Schwartz, 1985).

5. **Densification**

Densification by a variety of methods has been tried with various degrees of success. Also, the depth to which densification is required and the degree of densification are factors which should be looked at individually for each project (Schwartz, 1985).

The various densification methods that could be used are discussed below.

5.1. **Excavation and recompaction**

This method entails the removal of material to a pre-determined depth and then using the excavated material to form a stable compacted layer. With fine grained soils difficulties could be experienced in achieving compaction densities greater than 93 % Mod AASHTO. It is important to note that compaction should always be carried out at a moisture content above the optimum (Schwartz, 1985).

5.2. **Vibroflotation**

Vibroflotation has been used effectively in collapsible soils to provide safe bearing pressures of up to 400kPa. A combination of vibration and inundation are used to compact the soil. The increase in load bearing pressure can be ascribed to soil densification and the installation of gravel columns (De Wet, 2009).

5.3. **Dynamic deep compaction**

There are only a small number of reported cases where this method has been used. This can be ascribed to the high cost and time consumption of the method (Schwartz, 1985).

5.4. **In situ densification by surface rolling**

This method uses impact or vibratory rollers for in situ densification of collapsible soils. Initially, astonishingly good results were obtained, but unfortunately these results could not be maintained. The impact roller may be a useful tool for in situ densification, but careful evaluation of site conditions is critical before deciding whether satisfactory in situ densification will be achieved (Schwartz, 1985).

2.11 CONCLUSIONS

During the literature study it has become clear that insufficient research on the evaluation and prediction of collapsible soils has been carried out since the publication of Ken Schwartz's paper on collapsible soils published in the Civil Engineer magazine in 1985. However, these old fashioned methods of evaluation and prediction of the collapse phenomenon are still being used with confidence by engineers today. This is a reflection on the quality of the original research work (Schwartz, 1985).

The aim in this thesis will be to further our knowledge of the collapse phenomenon and specifically the evaluation and prediction of these soils. Field and experimental work will be carried out to evaluate the soils under question and also to predict and quantify collapse settlement in the demarcated research area.

CHAPTER 3: DEMARCATED STUDY AREA AND FIELD WORK

3.1 INTRODUCTION

Byrne et al. (1995) state the importance of thorough field work in addition to laboratory testing for identification and quantification of collapse settlement of soil fabric. Accordingly the research of this thesis was based on field work as well as laboratory testing. In this chapter the focus will be on the procedures followed in the execution of the field work, namely:

- Soil sampling
- Soil profiling

The area of research was demarcated to ensure the feasibility of the study. The study area, general geology of the study and surrounding areas and geology of the individual areas from which samples were collected are dealt with in this chapter.

3.2 DEMARCATED STUDY AREA

An area between Stellenbosch and Somerset West in the Western Cape was demarcated as the study area. The study area forms part of the Kuils River-Helderberg pluton. Four locations east of the R44 were selected for sample collection, including three wine farms namely Audacia, Eikendal, Ernie Els Wines and Jamestown cemetery. Illustrated in figure 3.1: 1 = Jamestown cemetery, 2 = Audacia, 3 = Ernie Els Wines and 4 = Eikendal.

This area was selected as it is a manageable size but still large enough to ensure the feasibility of the study. The area was further chosen as it is close to the University of Stellenbosch, which makes it accessible to the researcher, as well as for the fact that difficulties related to collapsible soils have been encountered here.

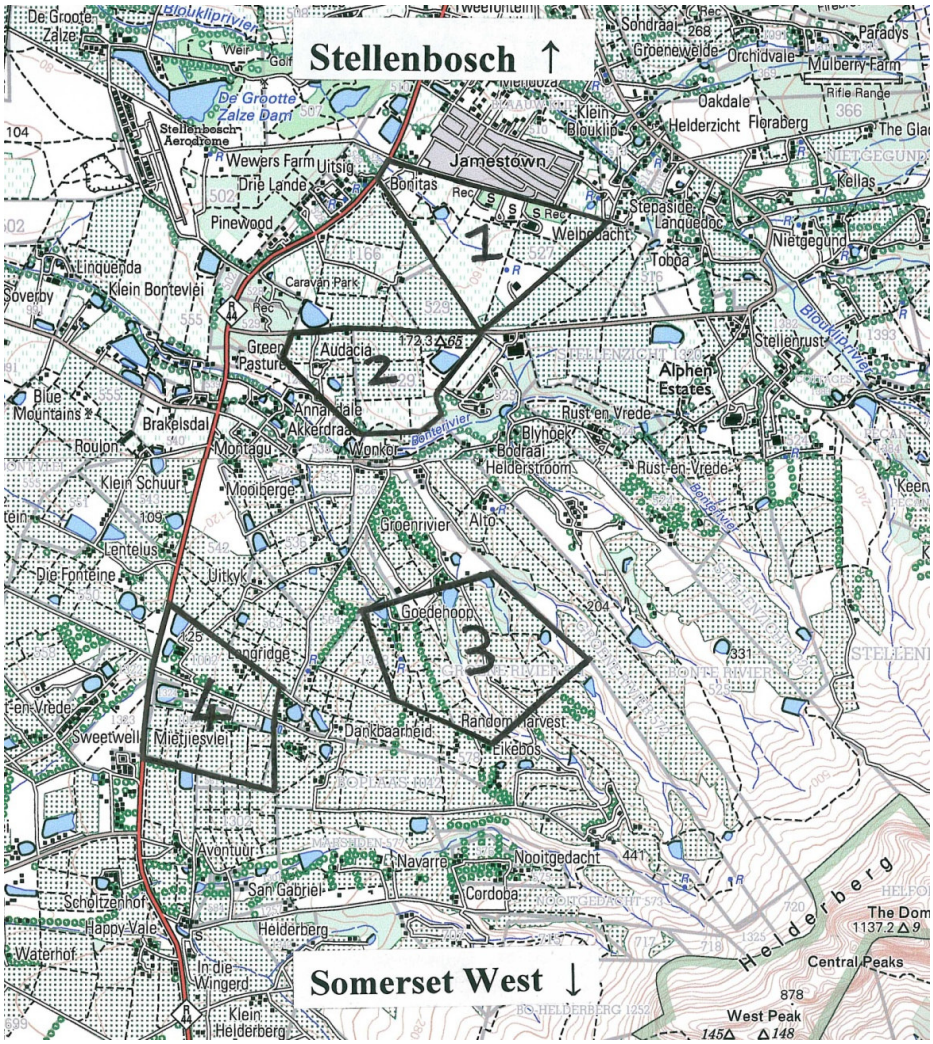

Figure 3.1: Topographic map illustrating sampling locations

Once the study area was selected, an indirect site investigation was carried out by studying geological and topographic maps. The general geology of the study and surrounding areas will be discussed now, followed by the geology of the three farms and cemetery.

3.2.1 General geology of the Kuils River-Helderberg pluton which includes the study area

The geology of the abovementioned pluton is illustrated in figure 3.2 below, where the area in red represents the study area.

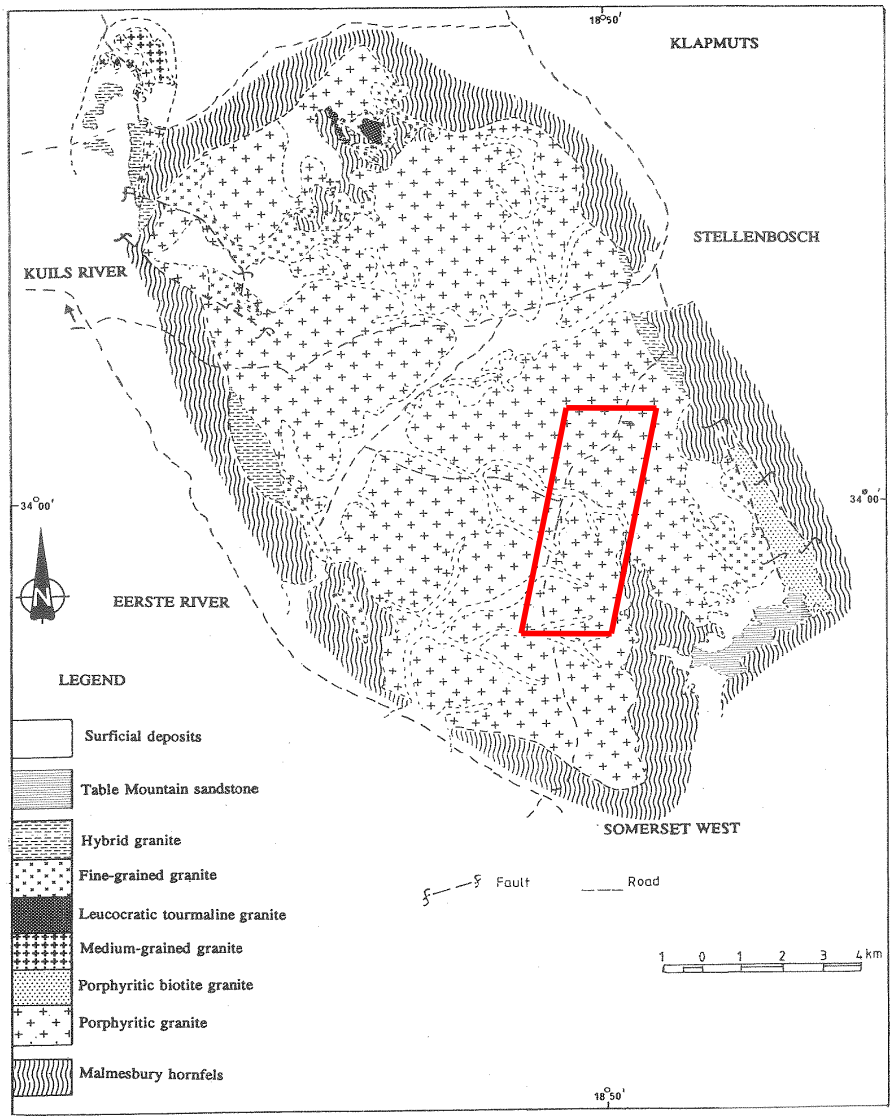

Figure 3.2: Geology of the Kuils River-Helderberg pluton (Theron et al., 1992)

The granite pluton is elongated to the northwest with estimated dimensions of 25 by 11 km. It is surrounded by the towns of Kuils River, Stellenbosch, Eerste River and Somerset West.

The major portion of the pluton, including the study area, constitutes coarse-grained porphyritic granite. It is a leucocratic rock consisting of 42,5 per cent K-feldspar, 12,5 per cent plagioclase, 26,25 per cent quartz, 11,25 per cent biotite and 7,5 per cent muscovite. This coarse-grained variety has a smaller percentage of plagioclase and muscovite compared to the finer-grained granites, but a higher percentage of biotite. The coarse porphyritic granite is surrounded by Malmesbury sediments. The contact between the porphyritic granite and Malmesbury hornfels is only rarely exposed.

Biotite-rich xenoliths of Malmesbury derivation occur erratically throughout the coarse porphyritic granite. Patches of medium-grained granite occur sporadically in the coarse-grained porphyritic variety throughout the pluton. Fine-grained granite, porphyritic biotite granite and hybrid granite occur mostly as patches along the outer border of the coarse porphyritic granite. Table Mountain sandstone crop up only in the southeastern corner of the pluton, whereas surficial deposits occur sporadically throughout the entire pluton and specifically in the study area (Theron et al., 1992).

The northwestern and southeastern borders of the pluton are fragmented by two faults respectively. These faults have a northwesterly strike and are more or less 5km in length (Theron et al., 1992).

3.2.2 Geology of areas where samples were collected

As mentioned previously three farms and a cemetery, spread evenly over the research area, were chosen for the collection of soil samples. The selection of each location was subjected to permission being granted by the respective owners and the Stellenbosch Municipality.

The geology of Audacia, Eikendal, Ernie Els Wines and Jamestown cemetery are illustrated in figure 3.3 below and will be briefly discussed.

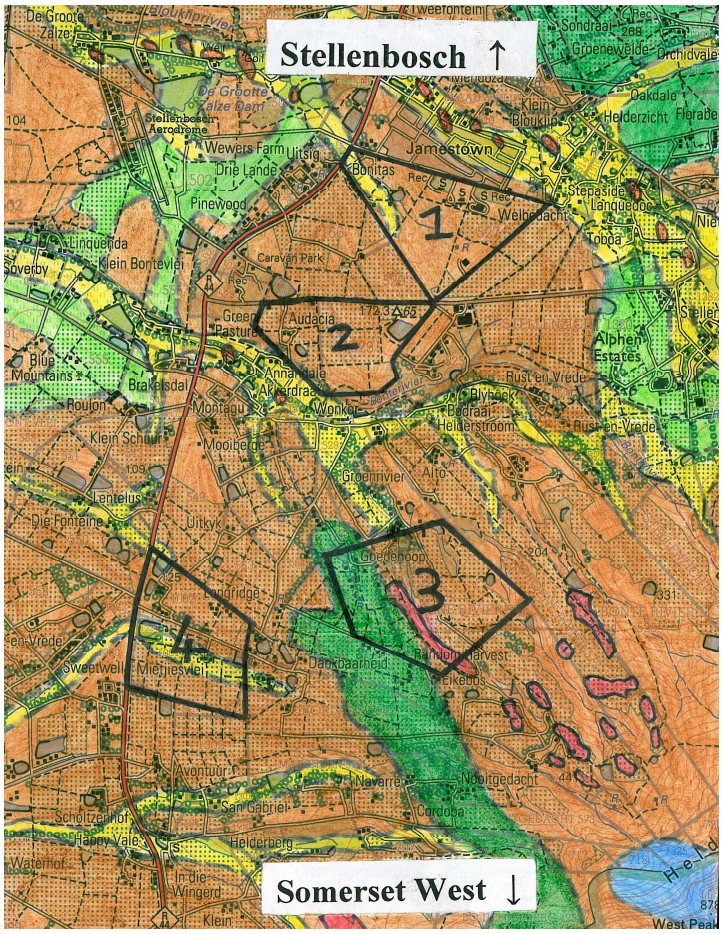

Figure 3.3: Geological map of study area (copyright, Council for Geoscience)

Illustrated in the figure: brown = residual granite; dark green = residual Malmesbury shale; light green = colluvium; yellow = alluvium; red = outcrop or near surface granite; blue = outcrop or near surface sandstone.

1. Jamestown Cemetery

The entire cemetery is situated on coarse-grained porphyritic granite, apart from a thin band of alluvium found in the northwestern corner of the cemetery.

2. Audacia

The farm Audacia consists entirely out of coarse-grained porphyritic granite.

3. Ernie Els Wines

The western part of Ernie Els consists out of Malmesbury shale and the rest of the farm out of coarse-grained porphyritic granite. A granite outcrop is visible alongside the western border of the residual granite.

4. Eikendal

A band of alluvium divides Eikendal into a northern and southern part of coarse-grained porphyritic granite.

3.3 FIELD WORK

3.3.1 Soil sampling

Soil samples were collected from the four sampling locations over a period of four days. An excavator was used to dig a total of fourteen pits on the three farms and cemetery, namely four on Audacia and Eikendal respectively and three on Ernie Els and Jamestown cemetery respectively. The positions of the test pits are illustrated in figures 3.4-3.7. The locations of the pits were chosen to fall within the granite areas of the farms and cemetery as the study focuses on the collapsibility of residual granite.

The laboratory tests require undisturbed samples and therefore great care was taken during the collection of the samples. PVC pipes of 250mm in diameter, cut in lengths of 300mm and covered at one end with a PVC sheet, were used. The pipes were slowly pressed and rotated into the soil while clearing the surrounding soil. This is a lengthy process requiring dedication and manpower. One sample was collected from each test pit, resulting in a total of fourteen samples for laboratory testing. The samples were all taken above the water table and sealed to prevent moisture loss.

Figure 3.4: Location of the four pits on Audacia (Google Earth)

Figure 3.5: Sampling locations on Eikendal (Google Earth)

Figure 3.6: Location of the three pits on Ernie Els Wines (Google Earth)

Figure 3.7: Sampling locations on Jamestown cemetery (Google Earth)

3.3.2 Soil profiling

According to Schwartz (1985) the correct recording of the soil profile is the first step in identifying a potentially collapsible soil in the field. The soil profile is a record of the vertical succession of the different layers of a soil. Each stratum should be described in terms of its moisture condition, colour, consistency, structure, soil type and origin (Jennings et al., 1973). The soil profiles of the fourteen test pits are included in appendix A with the position of the water table and sampling depth also portrayed.

CHAPTER 4: EXPERIMENTAL WORK

4.1 INTRODUCTION

This study aims to determine the occurrence and extent of collapse settlement throughout the area of research, as well as the shear behaviour of the soils. This chapter will revolve around the experimental work carried out to reach the aims of the study.

The following laboratory tests were performed:

- Double oedometer tests
- Shear strength tests

Further, indicator analyses were carried out which entail Atterberg limits and grain size distributions.

Double oedometer tests are performed to quantify the potential collapse settlement of a soil (Schwartz, 1985). These tests were carried out on the samples collected from the research area in order to obtain a clear picture of the occurrence of the collapse problem in the area.

The Atterberg limits and particle size distributions of all the soil samples were determined according to the ASTM method, to describe and identify the soils. As problems with collapse are generally associated with silty or sandy soils of low clay content, the identification of the soils will provide a better understanding of the collapse behaviour of the soils (Brink et al., 1982).

Direct shear tests are carried out to determine the consolidated-drained shear strength of a soil. The tests were performed on the samples collected from the area of research to determine the shear strength parameters of the soils as well as the effect of shear strength on collapsibility. It was further performed to determine the volume change of the soil samples during shear.

The chapter concludes with a discussion of the effects of topography and drainage on the collapsibility of the soils. The purpose thereof is to find a possible correlation between the topography of the four sampling locations and the collapsibility of the soils.

The results of the double oedometer tests, indicator analyses, and direct shear tests will be presented and interpreted next.

4.2 LABORATORY RESULTS AND INTERPRETATIONS

4.2.1 Double oedometer testing

Double oedometer tests, in accordance with USBR Test No 5700, were carried out on all fourteen soil samples collected from the demarcated study area to determine if the soils are in fact collapsible (Earth Manual Part 2, 1990). Twenty eight tests were completed, fourteen on saturated samples and fourteen on samples of natural moisture content. The data from these tests were used to plot a load-settlement graph for each sample. The saturated and natural samples were plotted on the same graph, with stress (in kN/m^2) on the x-axis, using a log scale, and void ratio on the y-axis. In order to interpret the curves and determine whether the soils are collapsible, the curves were superimposed by moving the saturated curve towards the natural curve. This was done as no in-situ curves were drawn. The double oedometer test interpretations described in section 2.7 of the literature study will not be carried out as this interpretation method needs only to be used in foundation design and not for the purpose of determining collapsibility. The data sheets for the double oedometer tests are included in Appendix A.

The results of each of the fourteen test pits will be discussed individually. The load-settlement graph and the graph illustrating the superimposed compression curves of each test pit will be presented and interpreted forthwith.

(a) Audacia

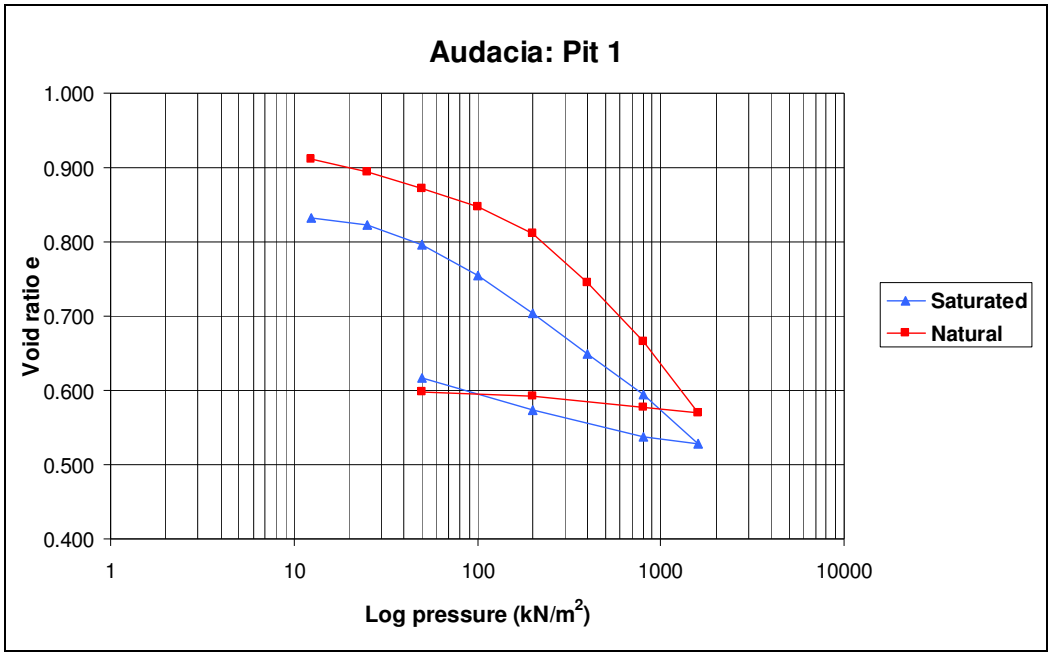

Figure 4.1: Void ratio versus log pressure of Audacia pit 1

The graph shows a relatively small difference in the dry densities of the saturated and the natural samples. The natural sample has a higher void ratio and thus a lower dry density than the saturated sample. This relatively small difference of 65 kg/m^3 in the dry density of the soil, illustrates the homogeneity of the soil. (Small differences in dry density may also occur in homogeneous soil).

The two compression curves follow more or less the same trend. During unloading the saturated curve increases more than the natural curve due to the availability of water.

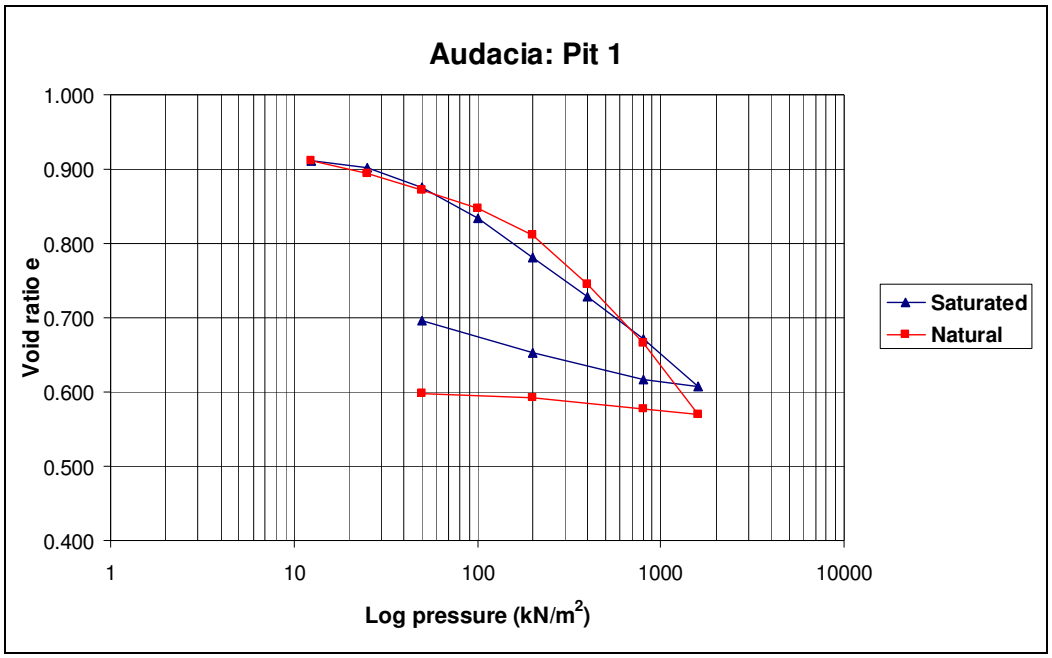

Figure 4.2: Superimposed compression curves of Audacia pit 1

As mentioned the graph illustrates a correlation between the two compression curves. At 200kN/m^2 however, the saturated sample is compressed 1.65% more than the natural sample. Yet, at maximum pressure the natural sample is compressed an additional 2.3% compared to the saturated sample. Overall the soil can be classified as a non collapsible soil. The small differences between the saturated and natural curves can be ascribed to the variability of the soil. Experimental errors can also be the cause of the difference.

Brink et al. (1982) indicated that collapse may occur in any open textured silty or sandy soil which has a high void ratio (low dry density) and yet has a relatively high shear strength at a low moisture content owing to the colloidal or other coatings which surround the individual grains. One would expect collapse to occur in the soil from Audacia pit 1, given that the soil has properties that could lead to collapse; namely a low dry density (900 to 1600 kg/m^3). This is however not the case.

In order to assist in finding a possible explanation for the double oedometer result, the grain size distribution and Atterberg limits of the soil were determined. These indicator tests were carried out to identify the soil and thus provide a better

understanding of the behaviour of the soil, and will be presented and discussed in the next section.

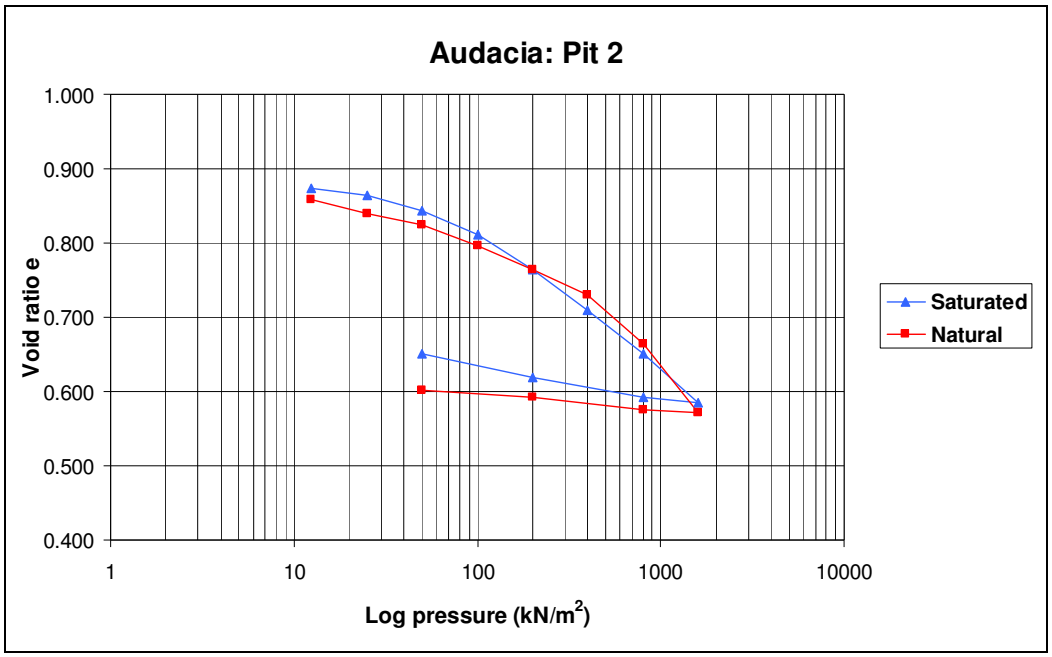

Figure 4.3: Compression curves of Audacia pit 2

From the graph it is evident that the two curves follow similar paths apart from the larger increase in void ratio of the saturated curve during unloading. A similarity in the dry densities of the saturated and natural samples is also visible.

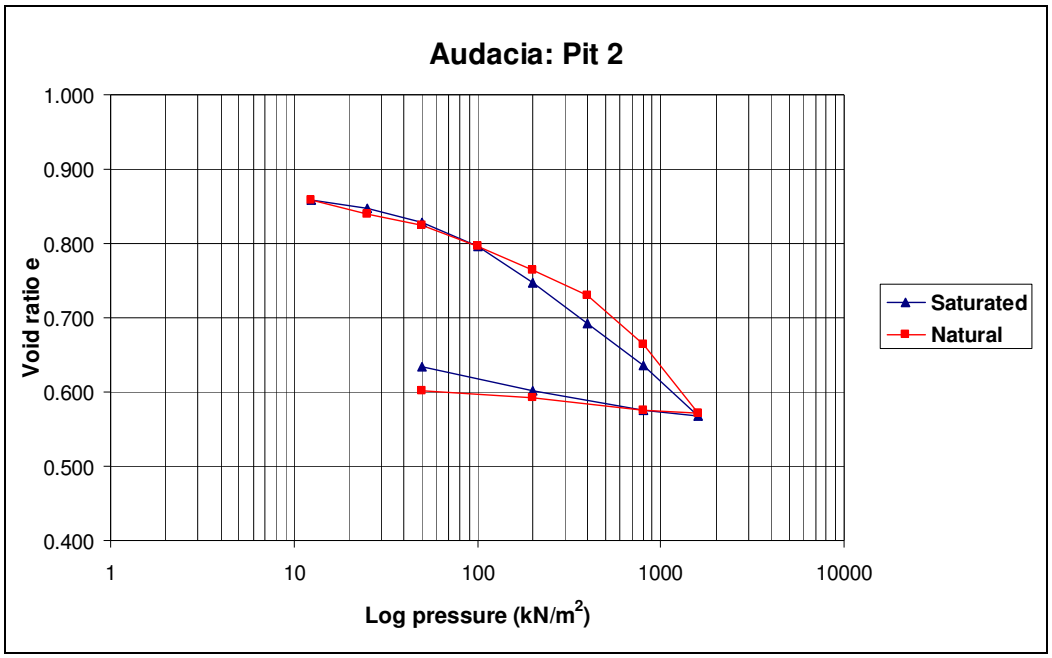

Figure 4.4: Superimposed compression curves of Audacia pit 2

From the graph it is clear that at lower pressures a close correlation exists between the two compression curves. At higher pressures signs of collapse become visible. At 200kN/m^2 the saturated sample is compressed 0.91% more than the natural sample. According to the guiding values of collapse potential given by Jennings and Knight (1975), the soil can be classified as a non collapsible soil. One would however expect collapse to occur in the soil from Audacia pit 2, given that the soil has a low dry density. The unexpected result will be addressed further in terms of the particle size distribution and Atterberg limits in the next section.

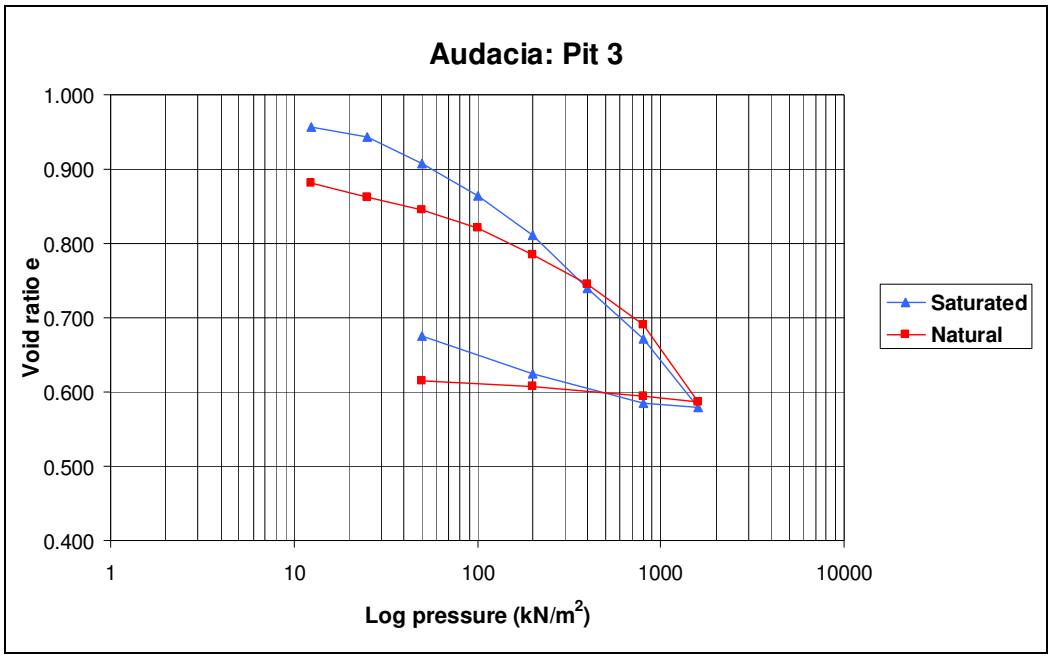

Figure 4.5: Void ratio versus log pressure of Audacia pit 3

From the graph it is apparent that the saturated sample has a higher void ratio than the natural sample. This is unusual as one would expect the saturated sample to have a higher dry density than the natural sample as the higher water content should increase the compressibility of the material. Although the two samples were taken from the same test pit, the natural sample was carved from slightly denser material than the saturated sample, which resulted in the outcome.

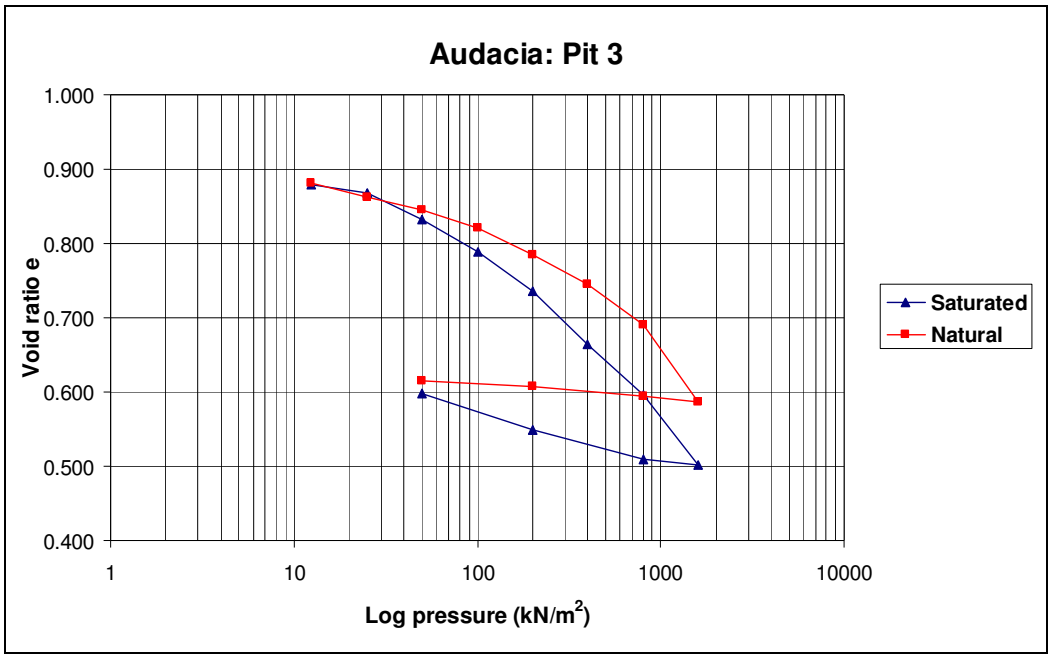

Figure 4.6: Graph of superimposed consolidation curves of Audacia pit 3

The graph shows that the saturated sample is compressed moderately more than the natural sample. A difference of 2.75% was calculated in the compression of the saturated and natural curves at 200kN/m^2. The saturated sample may have been compressed more partly as a result of the lower initial density. The soil can be classified as a moderately collapsible soil. This result was anticipated due to the low dry density of the soil. However, dry density is not the only factor to consider when studying collapse settlement and therefore the result will be discussed further in the next section.

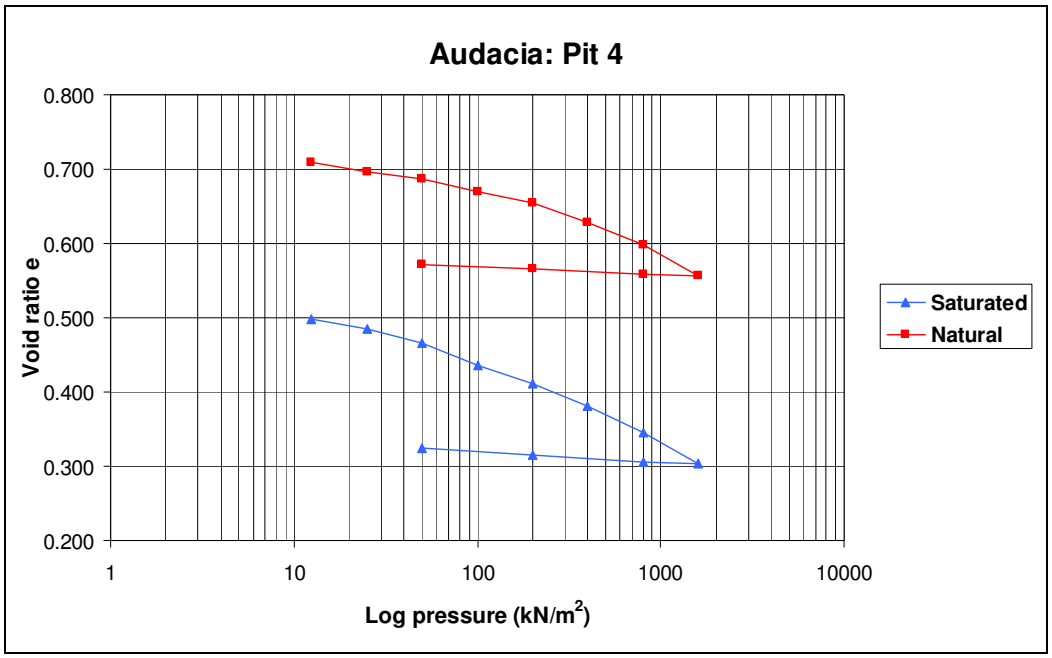

Figure 4.7: Consolidation curves of Audacia pit 4

An appreciable difference in the dry densities of the saturated and natural samples is visible. The saturated sample is much denser than the natural sample. This is as a result of the heterogeneous material from which the samples were carved.

Given that the void ratio of the saturated sample is very low (such a low void ratio is not common for a natural soil), the data from the double oedometer test were reviewed and found credible. The result is indicative of the very dense soils present on parts of Audacia.

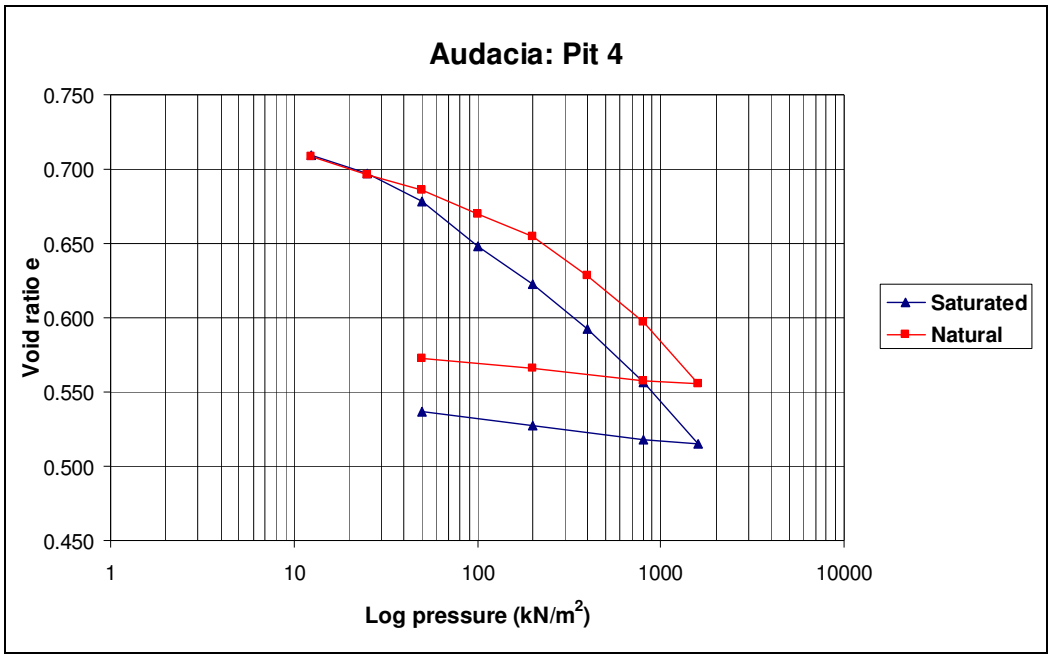

Figure 4.8: Superimposed saturated and natural curves of Audacia pit 4

From the graph it is evident that the saturated sample undergoes more compression than the natural sample. At 200kN/m^2 the saturated sample is compressed an additional 1.87% compared to the natural sample. The soil can therefore be classified as a moderately collapsible soil. The occurrence of collapse was unexpected due to the high dry density of the saturated sample. The oedometer data were carefully examined and found to be accurate.

(b) Eikendal

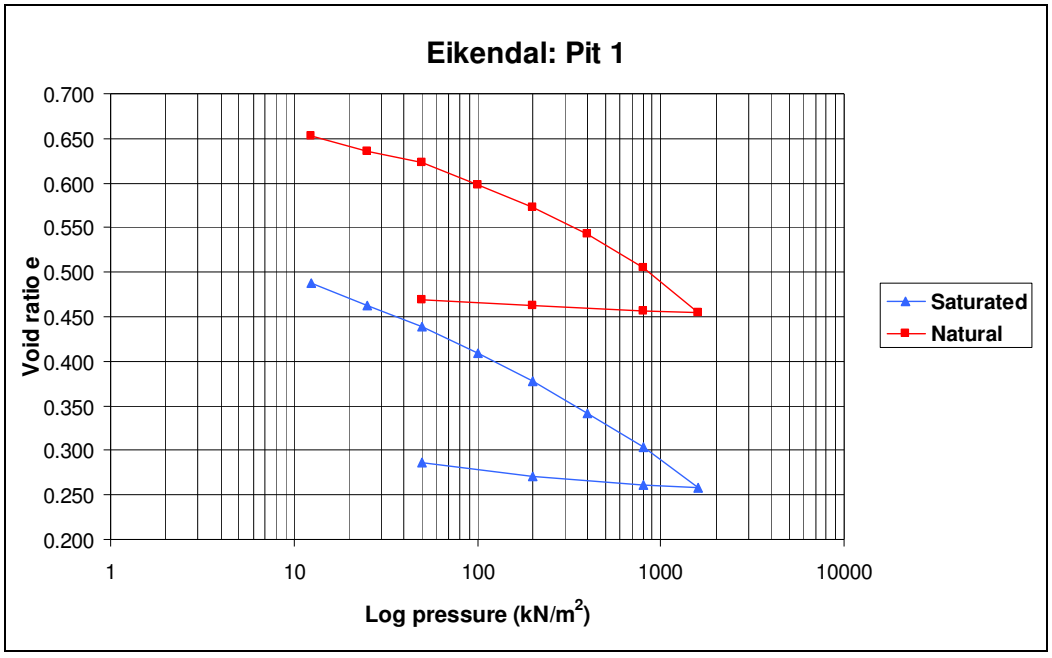

Figure 4.9: Load-settlement graph of Eikendal pit 1

A substantial difference in void ratio is visible between the saturated and natural samples. The natural sample has a much lower dry density than the saturated sample. The high dry density of the saturated sample signifies the very dense soils present on parts of Eikendal.

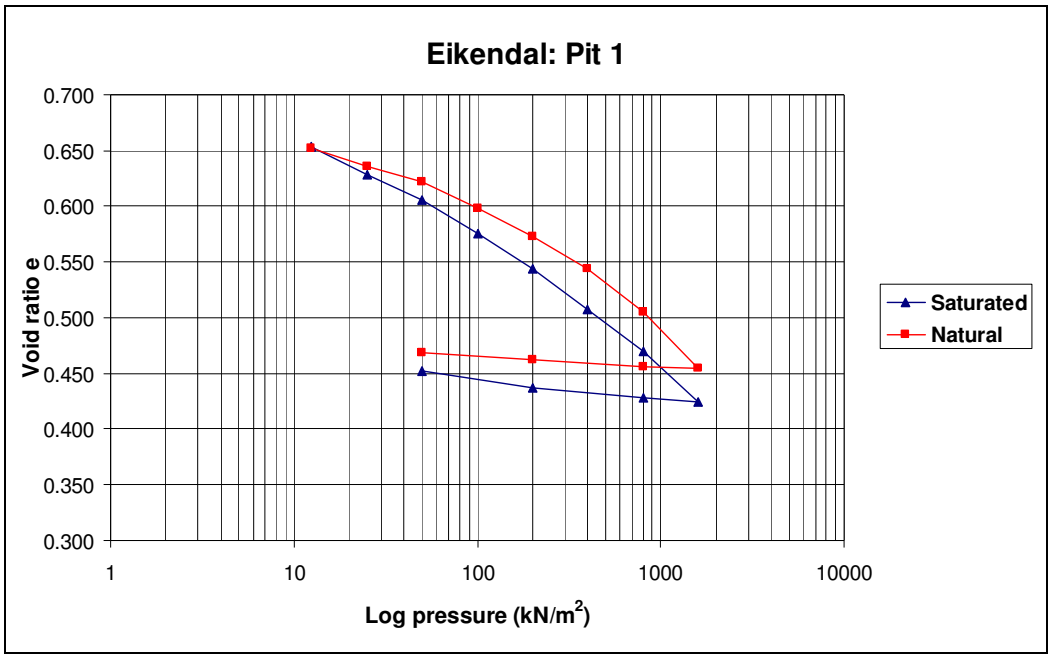

Figure 4.10: Superimposed consolidation curves of Eikendal pit 1

The graph shows that the saturated sample is compressed moderately more than the natural sample. A difference of 1.78% was calculated in the compression of the saturated and natural curves at 200kN/m^2. The high dry density of the saturated sample made the moderate collapse of the soil unforeseen.

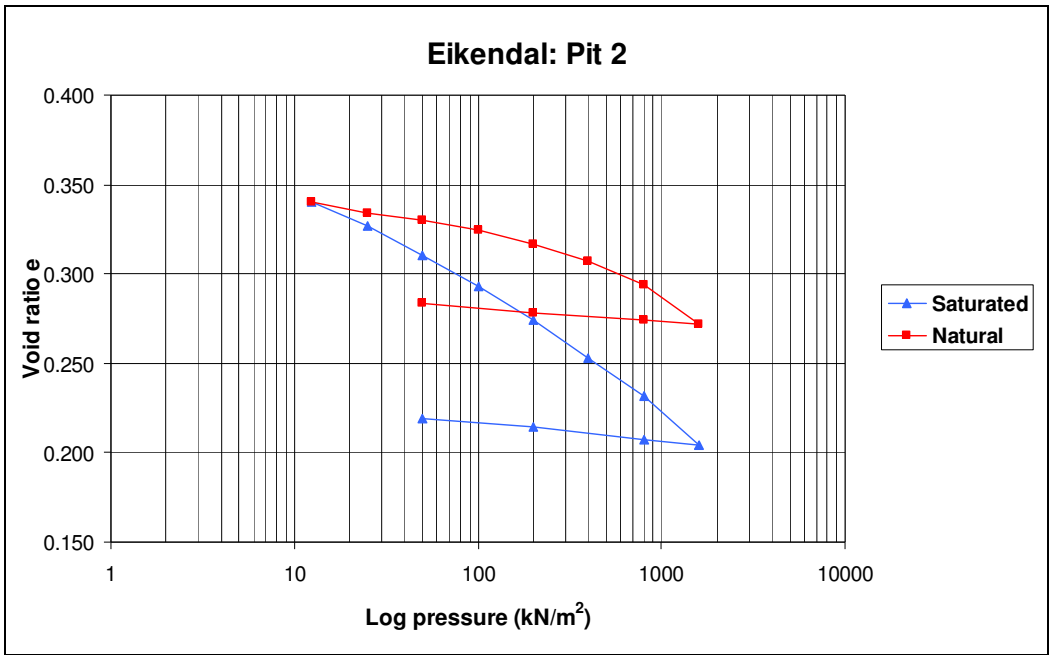

Figure 4.11: Compression curves of Eikendal pit 2

From the graph it is clear that the saturated and natural samples have the same dry density. Unlike most natural soils, the dry density of the soil is extremely high (around 2000 kg/m^3), and as a result the data from the double oedometer test were reviewed and found to be accurate.

A fairly large difference in compression is visible between the saturated and natural curves. At 200kN/m^2 the saturated sample is compressed 3.26% more than the natural sample**.** The moderate collapse of the soil was unexpected due to the high dry density of the soil.

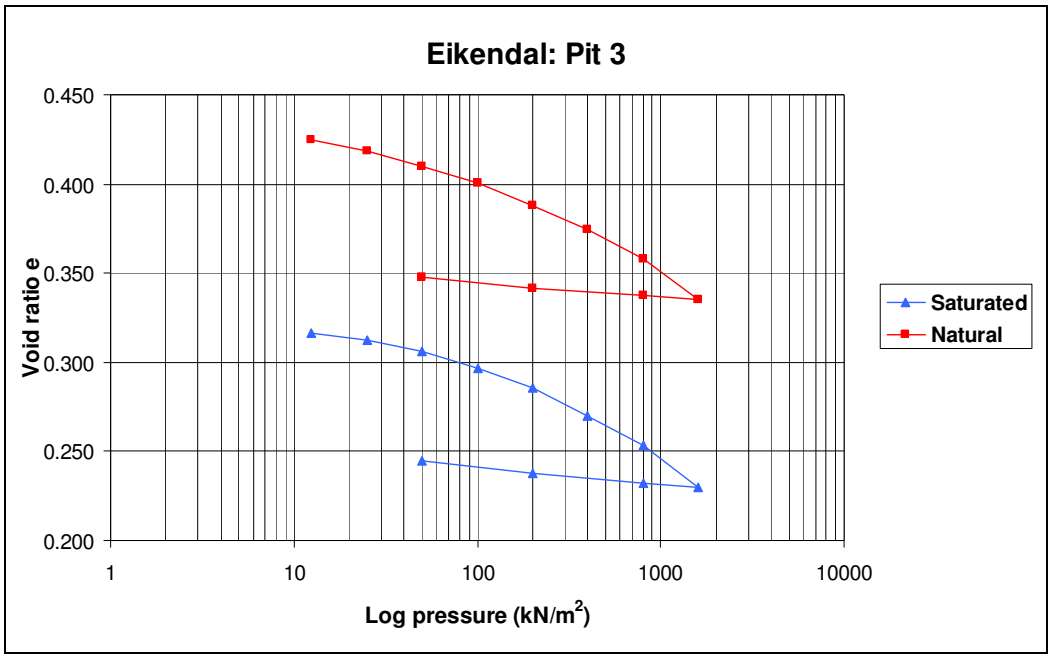

Figure 4.12: Void ratio versus log pressure of Eikendal pit 3

An appreciable difference in void ratio is noticeable between the saturated and natural curves. This is due to the heterogeneity of the soil from which the samples were carved. The void ratios of the saturated and natural samples are very low, with a minimum value of 0.316 for the saturated sample. As in the case of Eikendal pit 1 and 2, this is indicative of the very dense soils present on the farm.

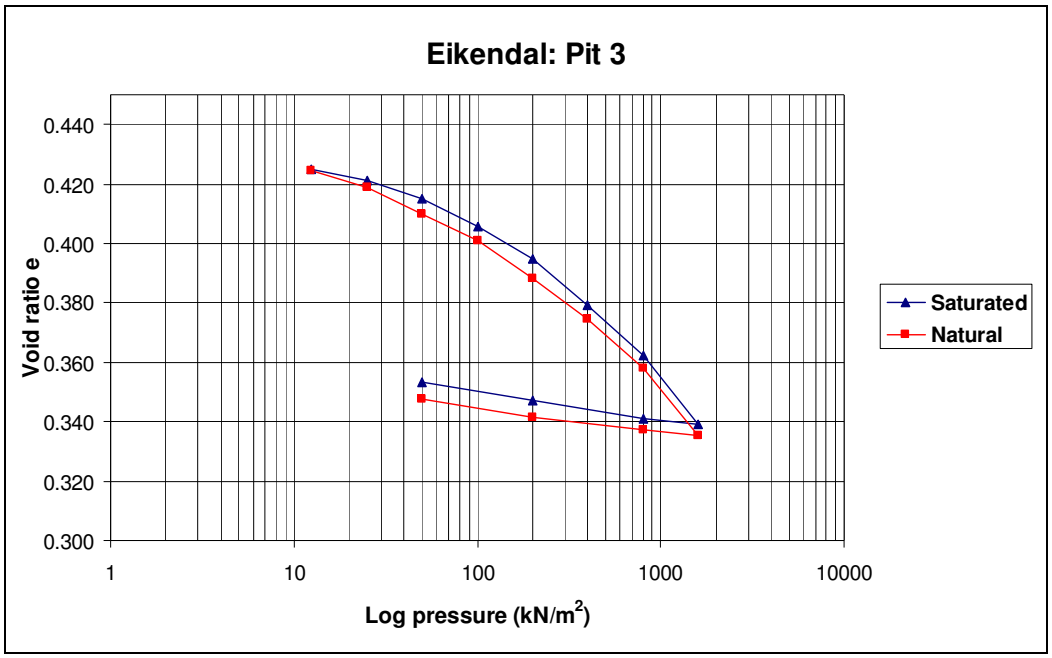

Figure 4.13: Superimposed saturated and natural curves of Eikendal pit 3

The graph illustrates a correlation between the saturated and natural samples. At 200kN/m^2 the saturated sample is compressed 0.50% more than the natural sample. The soil from Eikendal pit 3 can be classified as a non collapsible soil. This result was anticipated because of the low dry density of the soil.

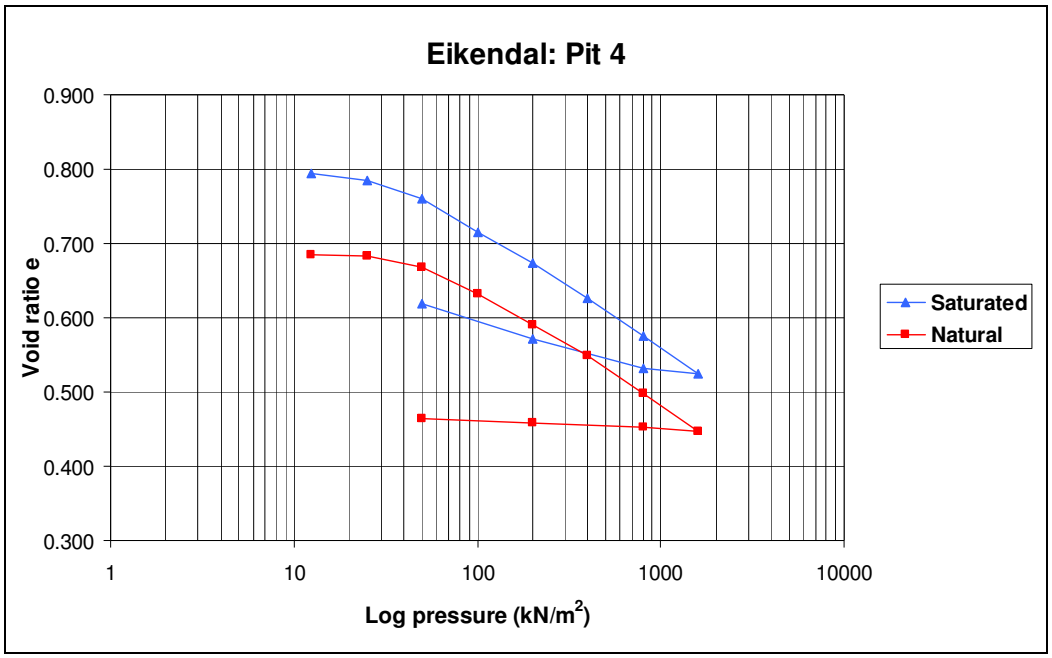

Figure 4.14: Graph of compression curves of Eikendal pit 4

From the graph it is clear that a fairly large difference in dry density exists between the saturated and natural samples. The saturated sample has a higher void ratio and thus a lower dry density than the natural sample. It is also noticeable that the soil from Eikendal pit 4 has a much lower dry density than the other samples from Eikendal.

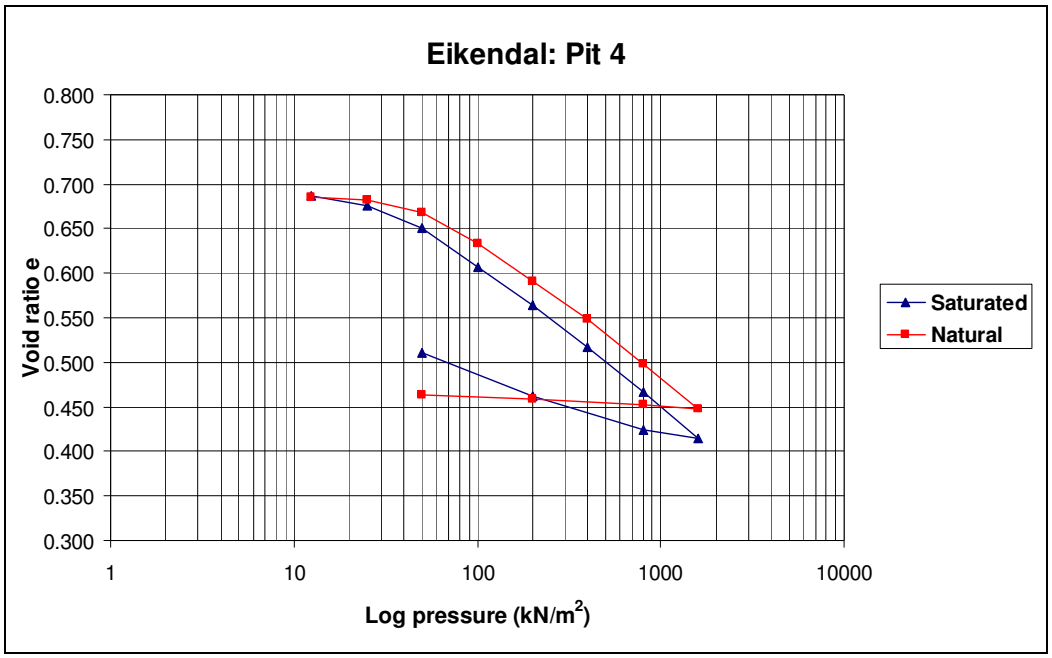

Figure 4.15: Superimposed consolidation curves of Eikendal pit 4

The graph shows that the saturated sample is compressed moderately more than the natural sample. A difference of 1.70% was calculated in the compression of the saturated and natural curves at 200kN/m^2. The sample has a low dry density and as a result the moderate collapse of the soil was expected.

(c) Ernie Els Wines

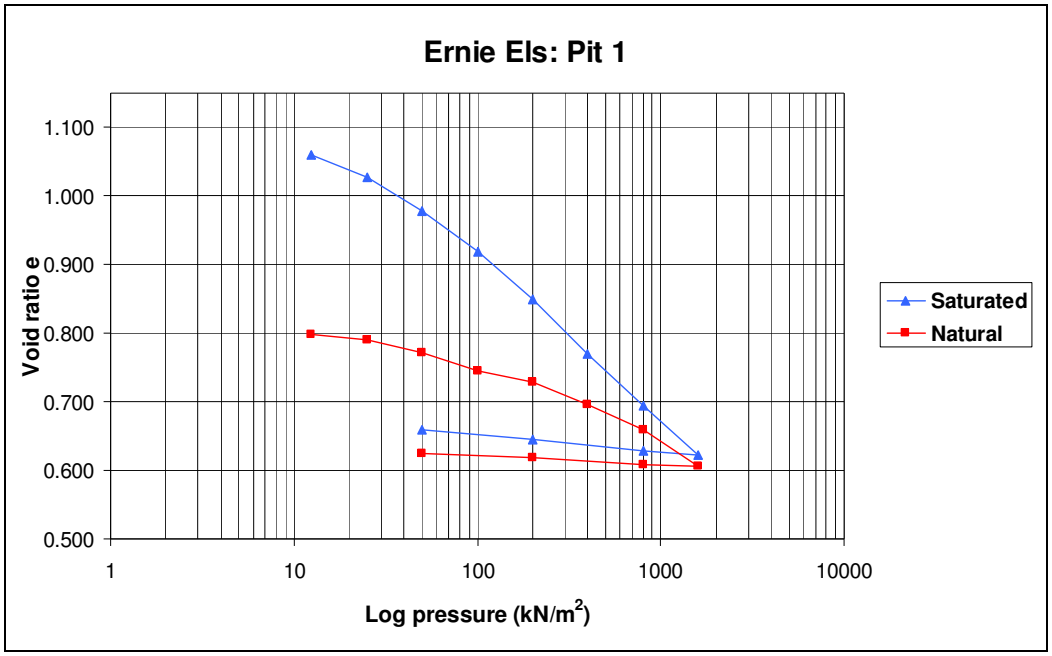

Figure 4.16: Consolidation curves of Ernie Els pit 1

A substantial difference in initial dry density is noticeable between the saturated and natural samples. The saturated sample has a much higher void ratio than the natural sample. This is as a result of the variability of the soil. During unloading the saturated and natural curves increase by more or less the same amount, despite the availability of water.

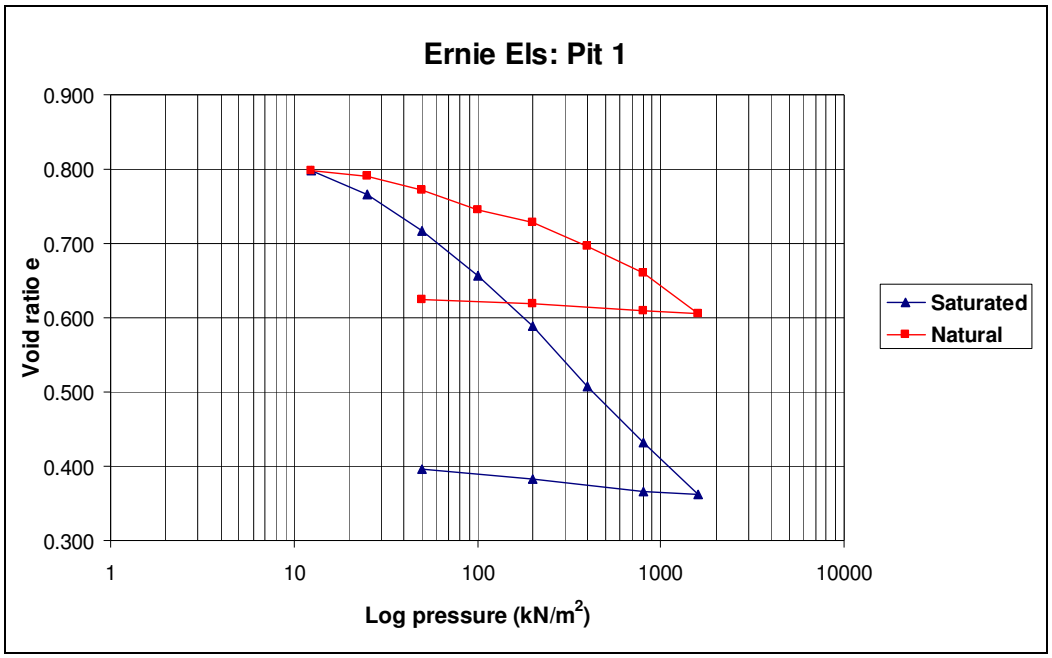

Figure 4.17: Graph of superimposed consolidation curves of Ernie Els pit 1

A large difference in compression is noticeable between the two samples. At 200kN/m^2 the saturated sample is compressed 8.16% more than the natural sample. The soil can be classified as a highly collapsible soil. This result was probable because of the low dry density of the soil. However, collapse settlement of 8.16% is very unusual for the Stellenbosch area. Values between 2% and 5% are more acceptable (Du Plessis, 2010). This unusual result will be addressed in the next section.

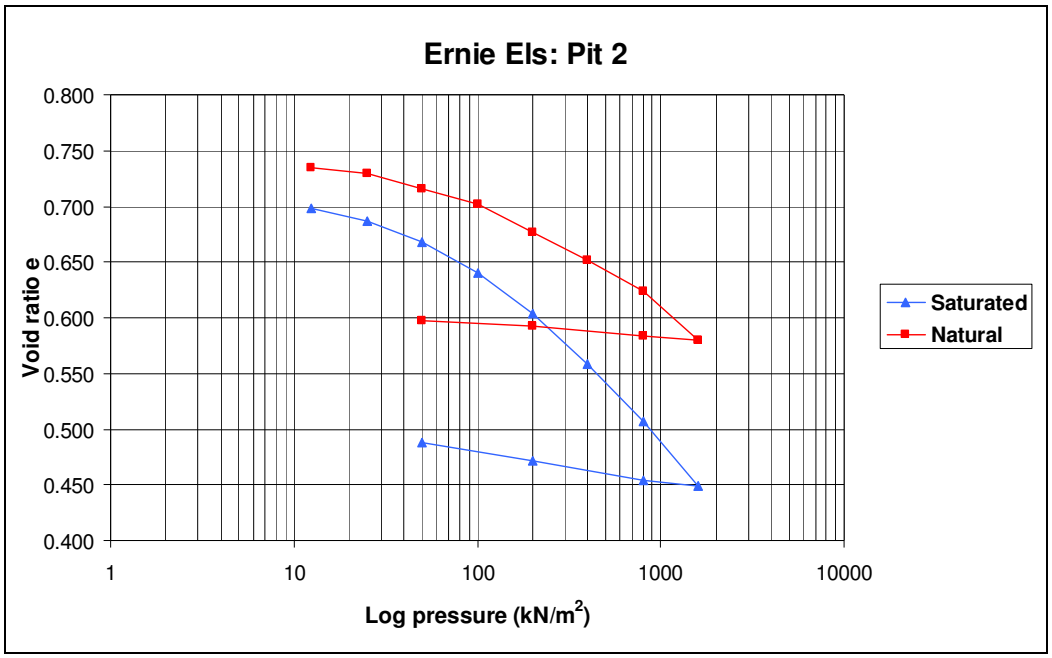

Figure 4.18: Void ratio versus log pressure of Ernie Els pit 2

The graph shows a small difference in the dry densities of the saturated and natural samples, which indicates the homogeneity of the soil.

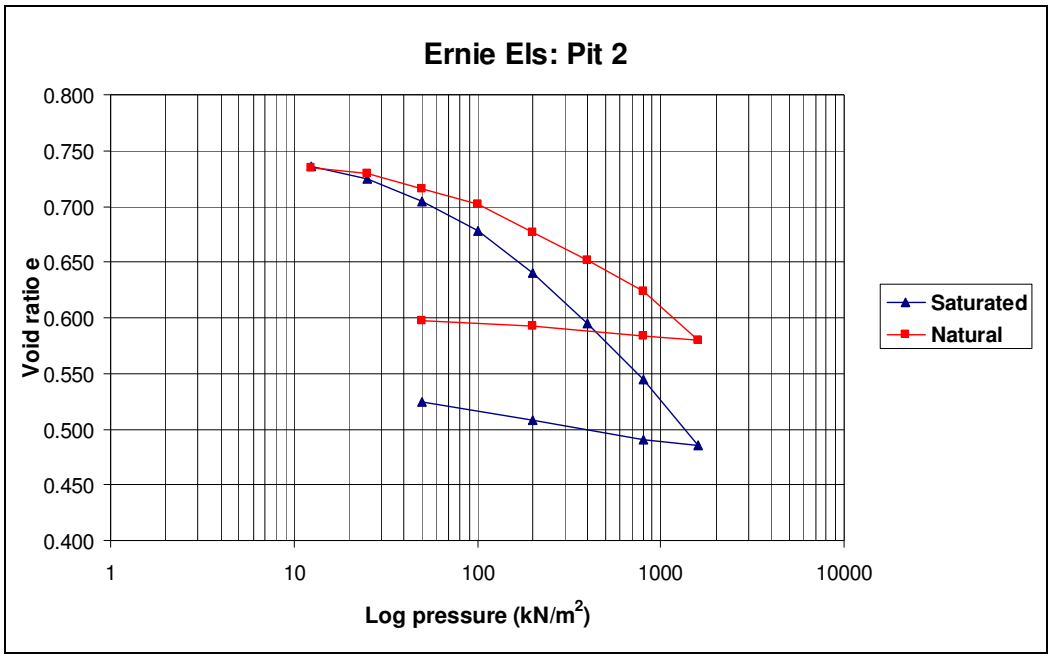

Figure 4.19: Superimposed saturated and natural curves of Ernie Els pit 2

The graph shows that the saturated sample is compressed moderately more than the natural sample. A difference of 2.10% was calculated in the compression of the saturated and natural curves at 200kN/m^2. As was expected due to the low dry density of the soil, the soil can be classified as moderately collapsible.

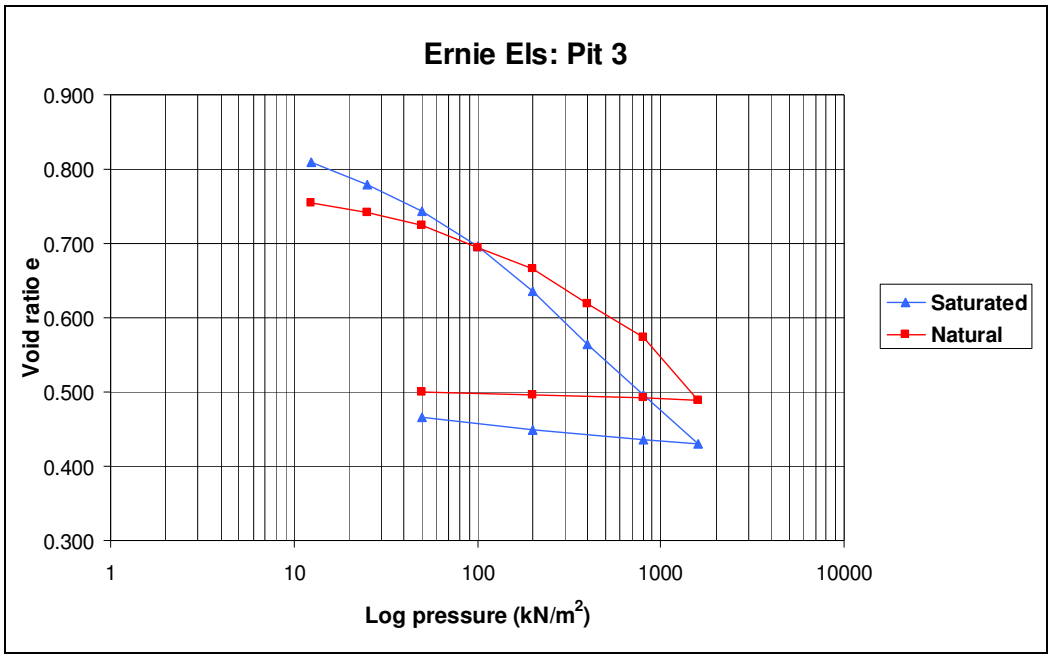

Figure 4.20: Void ratio versus log pressure of Ernie Els pit 3

From the graph it is apparent that the two samples have relatively similar dry densities. It is also noticeable that the soils from Ernie Els pits 1, 2 and 3 have low dry densities. This is the only farm where soils with a high dry density were absent.

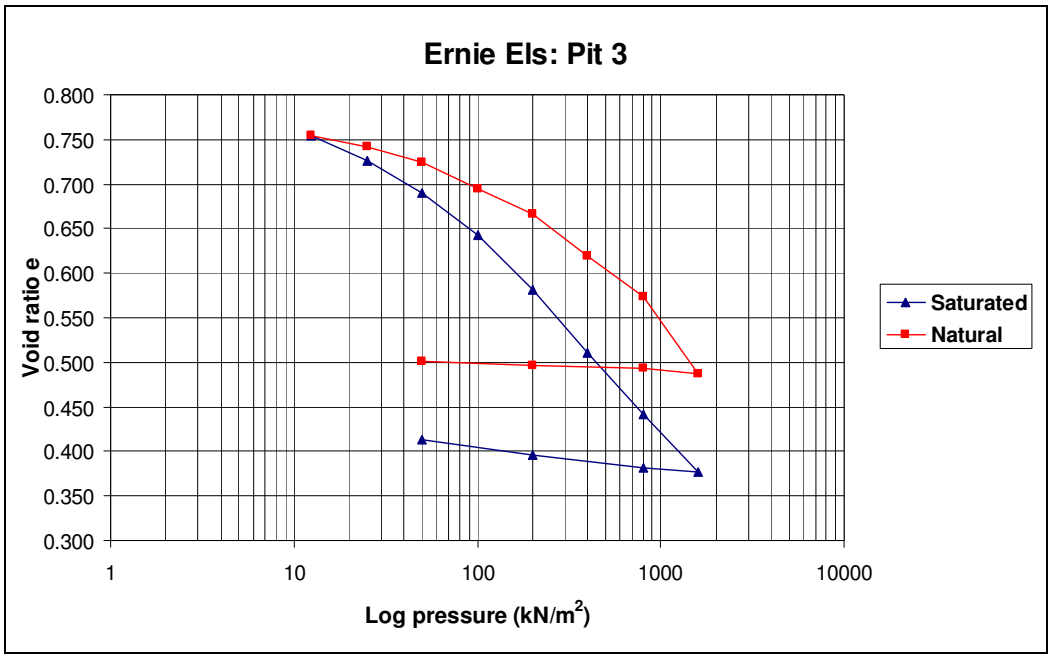

Figure 4.21: Superimposed consolidation curves of Ernie Els pit 3

The graph illustrates that the saturated sample is compressed markedly more than the natural sample. At 200kN/m^2 the saturated sample is compressed 5.04% more than the natural sample and can accordingly be classified as a highly collapsible soil. This result was anticipated as the soil has a low dry density.

(d) Jamestown cemetery

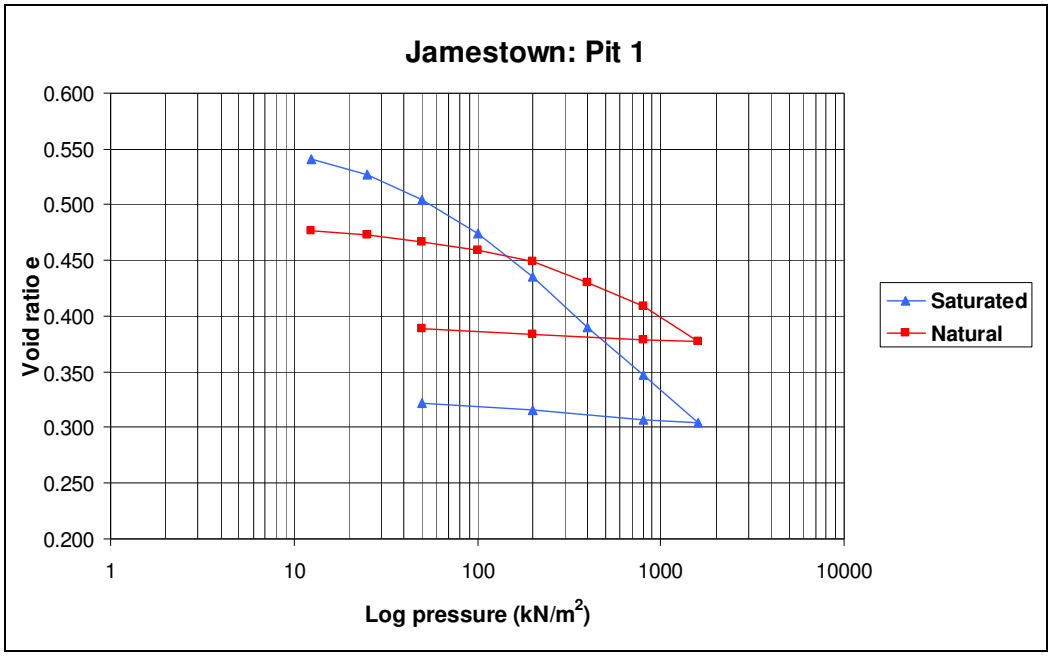

Figure 4.22: Graph of void ratio versus log pressure of Jamestown pit 1

From the graph it is clear that the void ratios of the saturated and natural samples are very low. This is indicative of the very dense soils present in parts of Jamestown cemetery.

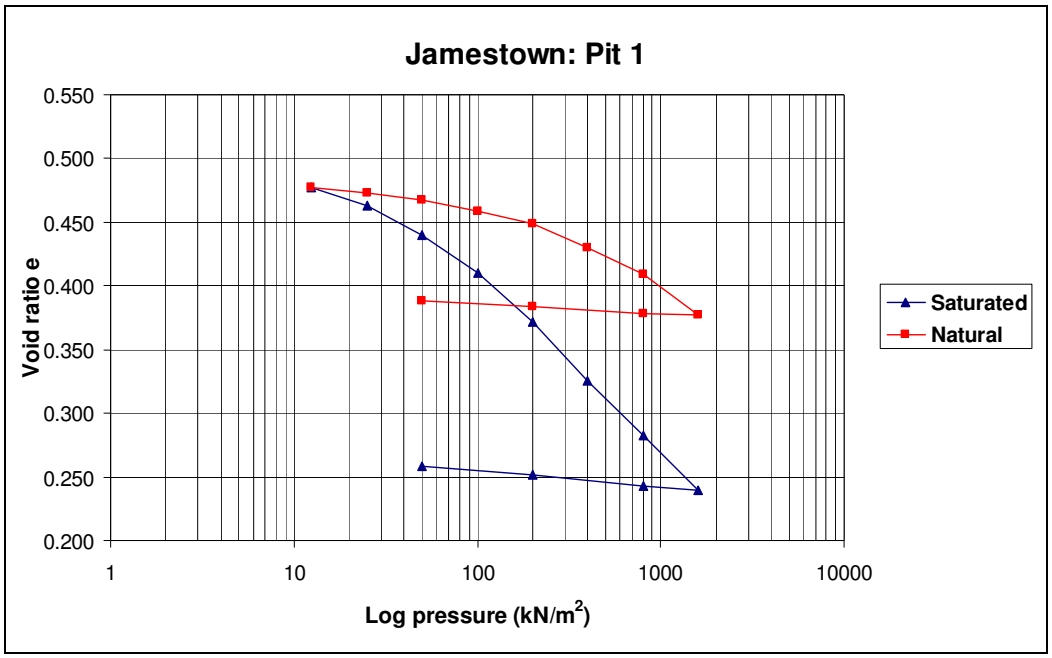

Figure 4.23: Superimposed saturated and natural curves of Jamestown pit 1

From the graph it is apparent that a large difference in compression exists between the saturated and natural samples. At 200kN/m^2 the saturated sample is compressed 5.38% more than the natural sample. According to Jennings and Knight (1975), the soil can be classified as a highly collapsible soil. The occurrence of collapse was unexpected because of the high dry density of the soil.

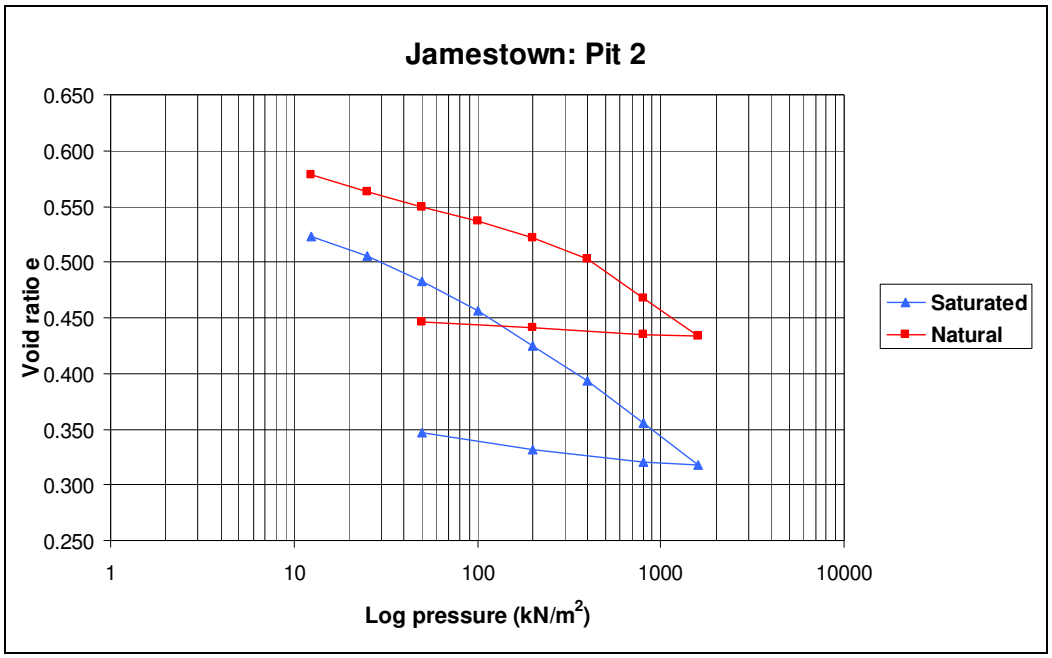

Figure 4.24: Load-settlement graph of Jamestown pit 2

The graph shows that the void ratios of the saturated and natural samples are fairly low. As in the case of Jamestown pit 1, this is indicative of the dense soils present in parts of Jamestown cemetery.

Figure 4.25: Superimposed compression curves of Jamestown pit 2

The graph illustrates that the saturated sample endures moderately more compression than the natural sample. At 200kN/m^2 the saturated sample is compressed an additional 2.70% compared to the natural sample. The high dry density of the soil made the moderate collapse of the soil unforeseen.

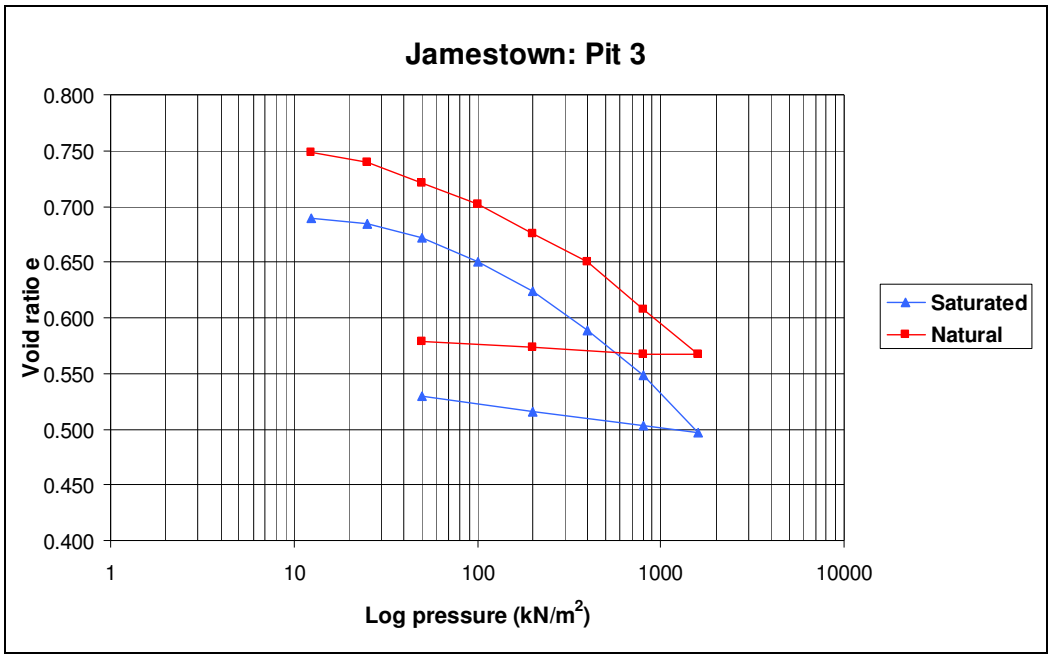

Figure 4.26: Void ratio versus log pressure of Jamestown pit 3

From the graph it is evident that the two curves follow similar paths apart from the larger increase in void ratio of the saturated curve during unloading. The relatively small difference in the dry densities of the two samples illustrates the homogeneity of the soil.

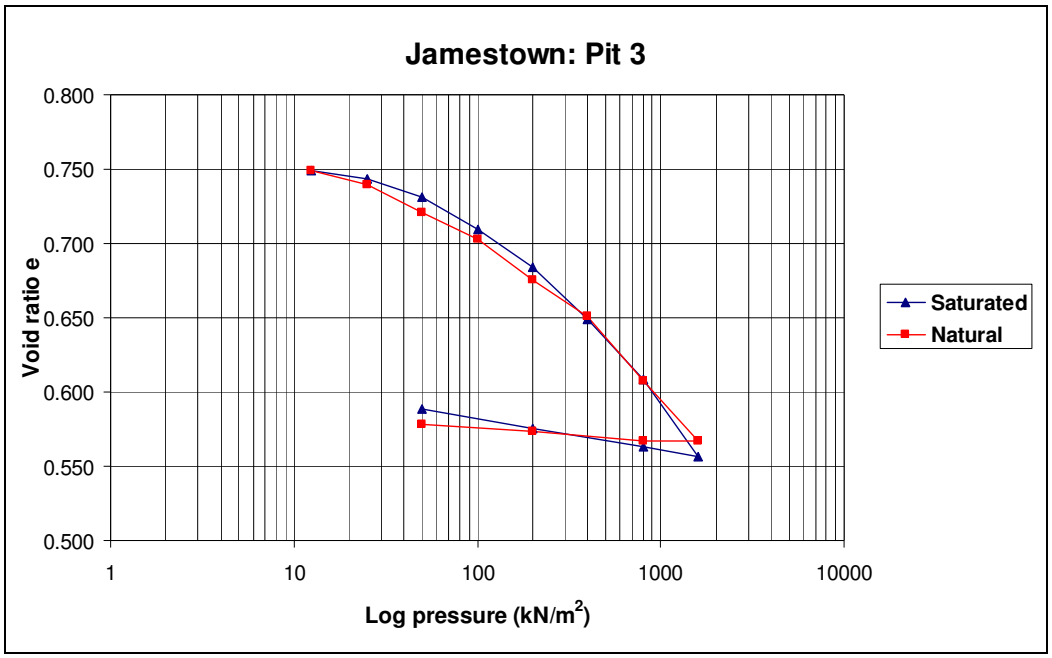

Figure 4.27: Graph of superimposed compression curves of Jamestown pit 3

As mentioned the graph illustrates a correlation between the two compression curves. A difference of 0.53% was calculated in the compression of the saturated and natural curves at 200kN/m^2. The soil can be classified as a non collapsible soil. One would however expect collapse to occur in the soil from Jamestown pit 3, given that the soil has a low dry density.

4.2.1.1 Conclusions

Of the fourteen soil samples collected from the demarcated study area, ten were found to be collapsible. Three of the four soil samples from Eikendal showed collapse, whereas two of the three samples collected at Jamestown cemetery and two of the four samples collected at Audacia showed collapse. At Ernie Els, all three samples were found to be collapsible. Consequently, collapsible soils are present in all four locations.

Of the ten soils that showed collapse, seven are moderately collapsible and three highly collapsible. A moderately collapsible soil has a collapse potential of between 1% and 5% and a highly collapsible soil a collapse potential of between 5% and 10%. It was established that the soils from Ernie Els have the highest collapse potential. Two of the three soil samples showed collapse of more than 5% and the other sample showed moderate collapse. The two soil samples from Jamestown cemetery that showed collapse are respectively moderately collapsible and highly collapsible. The two soil samples from Audacia and three soil samples from Eikendal that showed collapse, are only moderately collapsible. No severely collapsible soils were found in any of the sampling locations.

From the above it is apparent that Ernie Els presents the highest risk in terms of the quantity and severity of collapsible soils. The three remaining sampling areas, which present a moderate risk, are very similar in terms of the amount and severity of collapse.

Soils with very high dry densities were found on Audacia, Eikendal and Jamestown cemetery. The soils from Eikendal were established to be the densest, with a maximum density of 2059 kg/m^3. The soils from Jamestown cemetery were the second densest, followed by Audacia and lastly Ernie Els.

Five of the ten soils that showed collapse have low dry densities. These soils conform in terms of the definition of a collapsible soil. The other five soils that illustrated collapse have high dry densities. Collapse settlement in these soils was not expected

and contradicts typical collapse behaviour. Of the four soils that did not collapse, one has a high dry density and three have low dry densities. The three soils with the low dry densities were expected to collapse.

All three soil samples collected at Ernie Els conform in terms of typical collapse behaviour; however an unusually high collapse value was calculated for Ernie Els pit 1. Two of the four soil samples from Eikendal showed unexpected collapse. Of the four soil samples collected at Audacia, one showed typical collapse behaviour, whereas the results of the other three samples were unforeseen. The results of the three soil samples collected at Jamestown cemetery were also unexpected.

Jennings and Knight (1975) warn of the danger of assuming that all soils with a low dry density will show collapse or, vice versa, that all soils with a high dry density will not collapse. However, soils with a collapsible fabric very often have a low dry density, and thus the behaviour of some of the soils is unusual. This atypical behaviour will be studied by means of indicator analyses in the next section. The six soils that showed typical collapse behaviour will also be discussed and interpreted further, in view of factors other than dry density that may influence collapse settlement.

4.2.2 Indicator analyses

The Atterberg limits and particle size distributions of the fourteen soil samples were determined according to the ASTM method. These indicator tests were carried out to describe and classify the soils under question. Since problems with collapse are generally associated with silty or sandy soils of low clay content, the description and classification of the soils will assist in interpreting the double oedometer results (Brink et al., 1982).

4.2.2.1 Atterberg limits

The Atterberg limits were determined according to ASTM number D4318-84 (1992) - Standard test method for liquid limit, plastic limit, and plasticity index of soil.

The Atterberg limits are a fundamental measure of the nature of fine-grained soils. Depending on its water content, a soil may appear in four states: solid, semi-solid, plastic, and liquid. In each state the consistency and performance of the soil is different and so are its engineering properties. The boundary between each state can thus be defined based on a change in the soil's behaviour (http://en.wikipedia.org, 2010). In the ground, the majority of fine soils exist in the plastic state. Plasticity is due to the presence of a significant amount of clay mineral particles (or organic material) in the soil. The upper and lower limits of the range of water content over which the soil displays plastic behaviour are defined as the liquid limit (LL) and the plastic limit (PL), respectively. The shrinkage limit (SL) is the water content where additional loss of moisture will not result in any more volume reduction. The water content range itself is defined as the plasticity index (PI), (Craig, 2004), i.e:

$$PI = LL - PL$$

The liquid limit, linear shrinkage, plastic limit and plasticity index of each of the fourteen soil samples is tabulated below.

Table 4.1: Atterberg limits

Sample No.	Liquid limit (%)	Linear shrinkage (%)	Plastic limit (%)	Plasticity index (%)
Audacia 1	52.54	6.0	37.91	14.63
Audacia 2	41.23	4.67	34.10	7.13
Audacia 3	61.61	6.0	49.50	12.11
Audacia 4	39.0	6.0	28.57	10.43
Eikendal 1	38.13	6.0	27.75	10.38
Eikendal 2	25.78	3.33	18.44	7.34
Eikendal 3	40.16	4.0	31.67	8.49
Eikendal 4	49.81	6.0	34.78	15.03
Ernie Els 1	46.90	8.67	36.84	10.06
Ernie Els 2	41.73	6.0	32.48	9.25
Ernie Els 3	44.01	8.0	33.10	10.91
Jamestown1	26.25	3.33	19.10	7.15
Jamestown2	32.74	5.33	23.53	9.21
Jamestown3	49.2	6.67	37.31	11.89

4.2.2.2 Particle size analysis

The particle size analysis was carried out according to ASTM number D422-63 (1992).

The particle size analysis of a soil sample entails determining the percentage by mass of particles within the different size ranges. It is presented as a curve on a semilogarithmic plot, with the ordinates being the percentage by mass of particles smaller than the size given by the abscissa. The flatter the distribution curve, the larger the range of particle sizes in the soil; the steeper the curve, the smaller the size range. A soil can be described as well graded if there is no excess of particles in any size range and if no intermediate sizes are lacking. A soil is described as a uniformly graded soil if a high proportion of the particles have sizes within narrow limits. If smaller and larger particles are present, but particles of intermediate size are absent, the soil can be described as gap-graded (Craig, 2004).

The general slope and shape of the grain size distribution curve can be described by means of the *coefficient of uniformity* (Cu) and the *coefficient of gradation* (Cz), defined as follows:

$Cu = D_{60}/D_{10}$

$Cz = D^2_{30}/ (D_{60}.D_{10})$

The higher the value of the uniformity coefficient, the larger the range of particle sizes in the soil. A well graded soil has a coefficient of gradation of between 1 and 3 (Craig, 2004).

The particle size analysis was done in agreement with the ASTM method. The Unified Soil Classification System is however used to place the soils in groups on the basis of grading and plasticity. The data were therefore converted to comply with the Unified Soil Classification System. The particle size distributions of the fourteen soil samples are presented in table 4.2 below.

Table 4.2: Grain size distributions

Sample No	Clay < 0.002	Silt 0.002 - 0.06	Fine sand 0.06 - 0.2	Med sand 0.2 - 0.6	Coarse sand 0.6 - 2	Gravel > 2
Audacia 1	29	25	2	7	17	20
Audacia 2	21	31	11	16	18	4
Audacia 3	27	27	5	9	15	17
Audacia 4	32	9	11	20	24	4
Eikendal 1	38	15	6	11	21	9
Eikendal 2	9	12	3	14	32	30
Eikendal 3	25	16	7	11	24	17
Eikendal 4	43	16	4	6	18	13
Ernie Els 1	27	24	10	12	16	11
Ernie Els 2	21	18	15	13	24	9
Ernie Els 3	25	22	7	13	24	9
Jamestown 1	21	6	14	27	26	6
Jamestown 2	30	9	11	16	24	10
Jamestown 3	41	25	8	12	11	3

The grain size distribution graphs of the fourteen soil samples will subsequently be presented and interpreted. The particle size distributions and calculated plasticity indexes will be used to classify each soil by means of the Unified Soil Classification System. The double oedometer results will further be interpreted with the aid of the aforementioned results.

The moisture contents of the soils will also be discussed in relation with the double oedometer results. The moisture contents, dry densities and collapse potentials of the fourteen soil samples are tabulated below.

Table 4.3: Moisture contents, dry densities and collapse potentials

Sample Nr	Moisture content (%)	Dry density (kg/m^3)		Collapse potential (%)
		Natural	Saturated	
Audacia 1	23.47	1414	1479	<1
Audacia 2	27.34	1458	1445	0.91
Audacia 3	25.51	1441	1386	2.75
Audacia 4	13.52	1586	1810	1.87
Eikendal 1	9.42	1640	1822	1.78
Eikendal 2	5.45	2022	2022	3.26
Eikendal 3	13.44	1902	2059	0.50
Eikendal 4	22.37	1608	1510	1.70
Ernie Els 1	18.71	1507	1322	8.16
Ernie Els 2	20.81	1562	1596	2.10
Ernie Els 3	17.03	1544	1498	5.04
Jamestown 1	14.17	1834	1759	5.38
Jamestown 2	14.79	1717	1783	2.70
Jamestown 3	25.0	1550	1605	0.53

a) Audacia

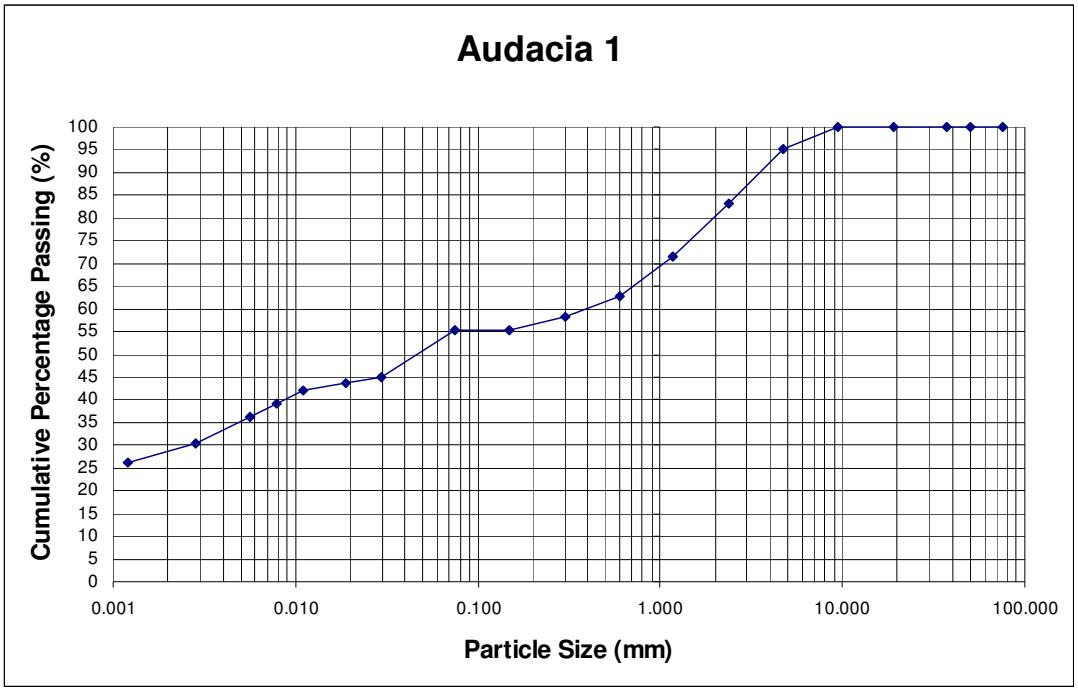

Figure 4.28: Particle size distribution graph of Audacia pit 1

From the graph we can conclude that the fine particles (clay and silt) make up the largest part of the soil. Of the coarser particles, the coarse sand and gravel make up the greater part. A relatively low proportion of particles of intermediate size are present. According to the Unified Soil Classification System, the soil from Audacia pit 1 can be classified as inorganic silt of high plasticity (MH) (ASTM, 1999).

Collapse did not occur in the soil from Audacia pit 1. This result was unexpected since the soil has properties that could lead to collapse; namely a low dry density. However, collapsible soils normally contain a high proportion of coarse particles with few fines in between, due to intense leaching in the soil. Yet, this soil contains ample clays and silts and less coarse material. The lack of leaching in the soil might have prevented a collapsible fabric from forming, thus inhibiting collapse settlement.

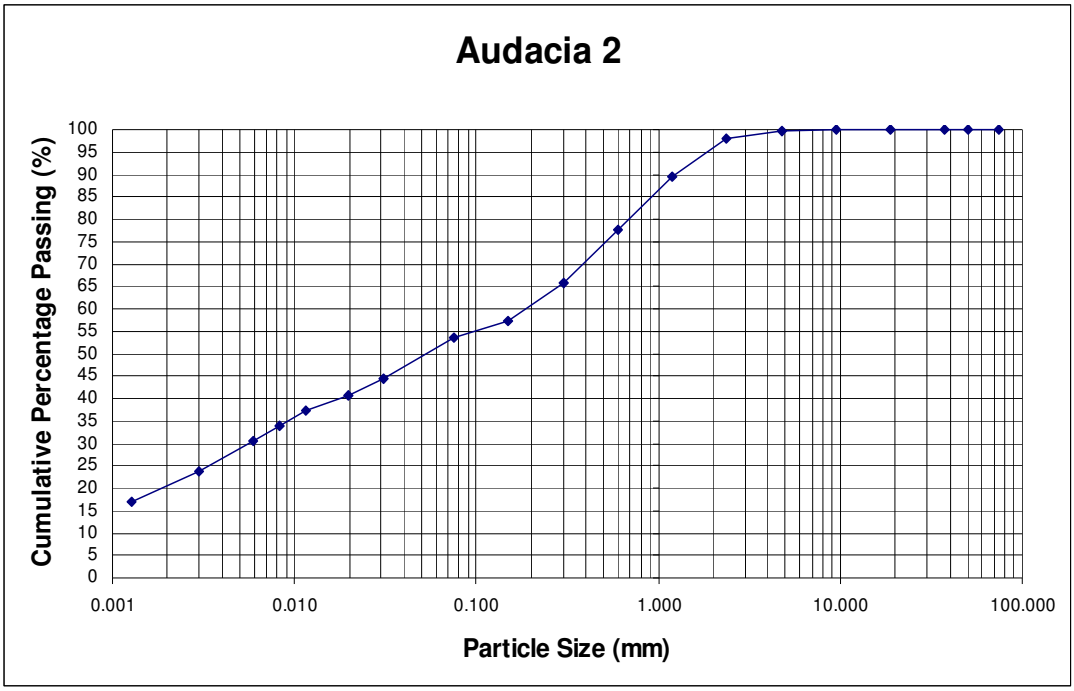

Figure 4.29: Grain size distribution curve of Audacia pit 2

From the graph it is evident that the fine particles (clay and silt) make up more than half of the soil content. There are more or less equal amounts of the coarse particles, apart from the low proportion of gravel. The soil from Audacia pit 2 can be classified as silty fine sand with slight plasticity (ML).

Collapse did not occur in the soil from Audacia pit 2. The soil was nevertheless expected to collapse due to the low dry density of the soil. However, the high clay content of the soil is usually indicative of a non collapsible soil. The lack of leaching in the soil therefore may have prevented a collapsible fabric from forming, thus inhibiting collapse settlement. The relatively even distribution of particles sizes and high moisture content of the soil could also have contributed to why the soil did not collapse.

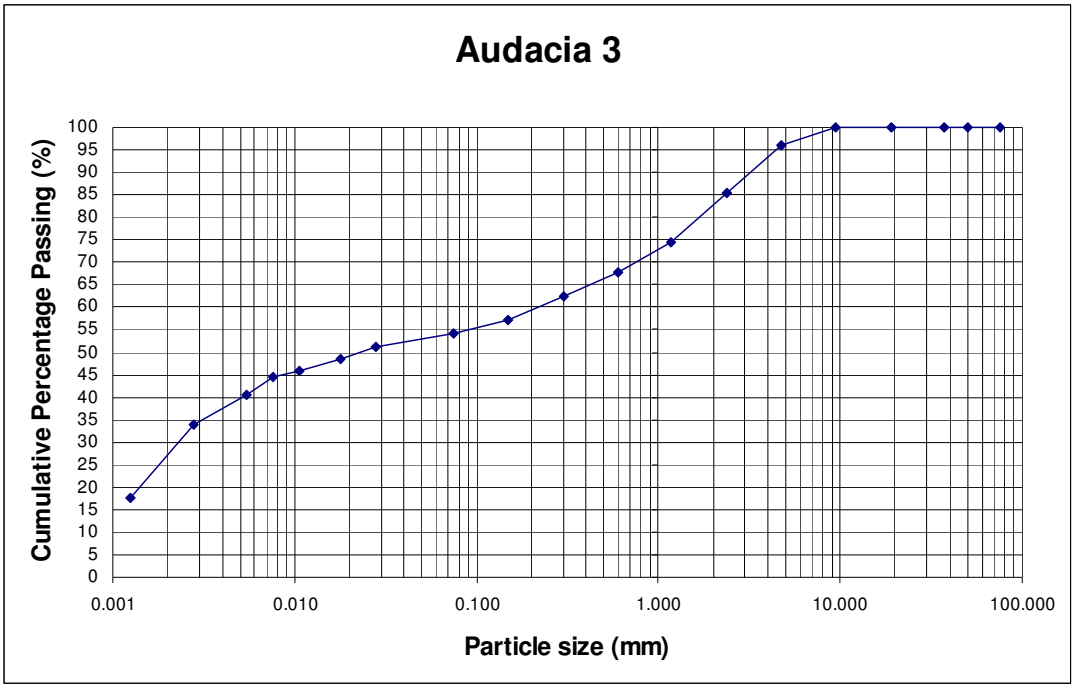

Figure 4.30: Grain size distribution graph of Audacia pit 3

The graph shows that the largest fraction of the soil consists of clay and silt. Of the coarse particles, the coarse sand and gravel form the greater part. The proportions of fine sand and medium sand are relatively low. The soil from Audacia pit 3 can be classified as inorganic silt of high plasticity (MH).

The moderate collapse that occurred in the soil from Audacia pit 3 was anticipated due to the low dry density of the soil. The soil nonetheless has a high clay content and a lower proportion of coarse particles, which is uncharacteristic of a collapsible soil. The low dry density of the soil however could have made the soil vulnerable to collapse even though the clay content is high.

This is in contrast with the results from Audacia pit 1 and Audacia pit 2, where the soils also have low dry densities and high clay contents, but collapse does not occur. The soils from Audacia pit 1 and Audacia pit 3 also have similar moisture contents and grading. No explanation could be found for the difference in behaviour.

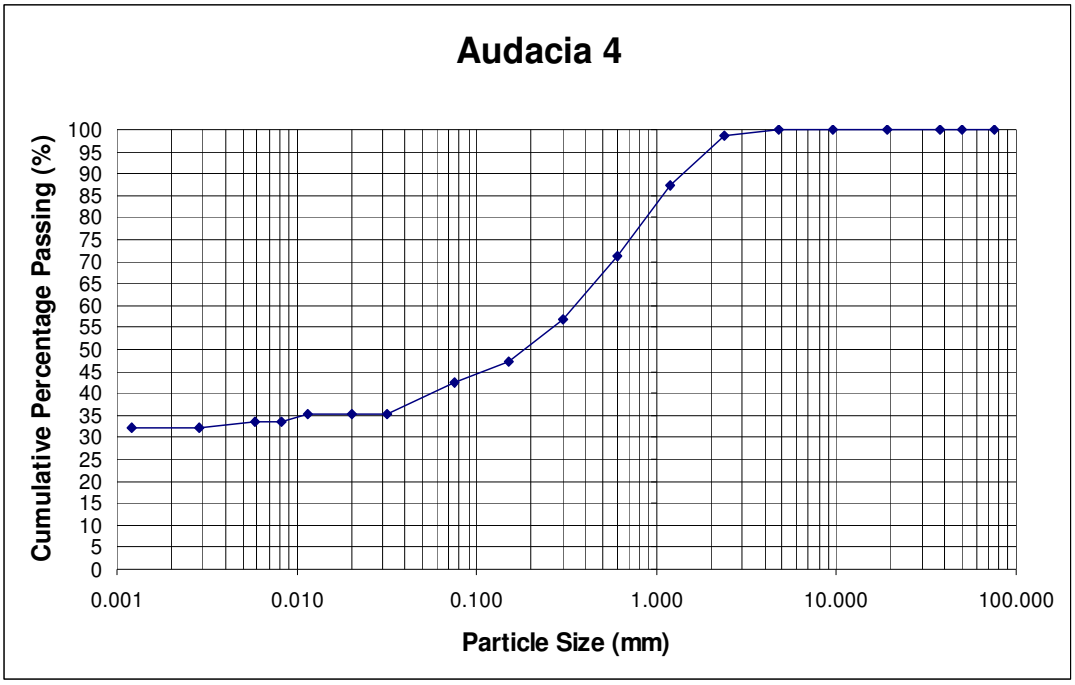

Figure 4.31: Grading curve of Audacia pit 4

From the graph it is evident that the soil from Audacia pit 4 has a very high clay content. Fairly low quantities of silt and fine sand are present in the soil. Of the coarser particles, the medium and coarse sand are well represented. A low proportion of gravel is observed. Based on its material characteristics, the soil can be classified as silty sand (SM).

Moderate collapse occurred in the soil from Audacia pit 4. This result was unexpected due to the high dry density of the soil. The high clay content makes this result even more unusual. However, the relatively low moisture content and poor grading of the soil might have contributed to the collapse settlement. In view of the fact that the soil is only moderately collapsible and not highly collapsible, the result can be considered as acceptable.

b) Eikendal

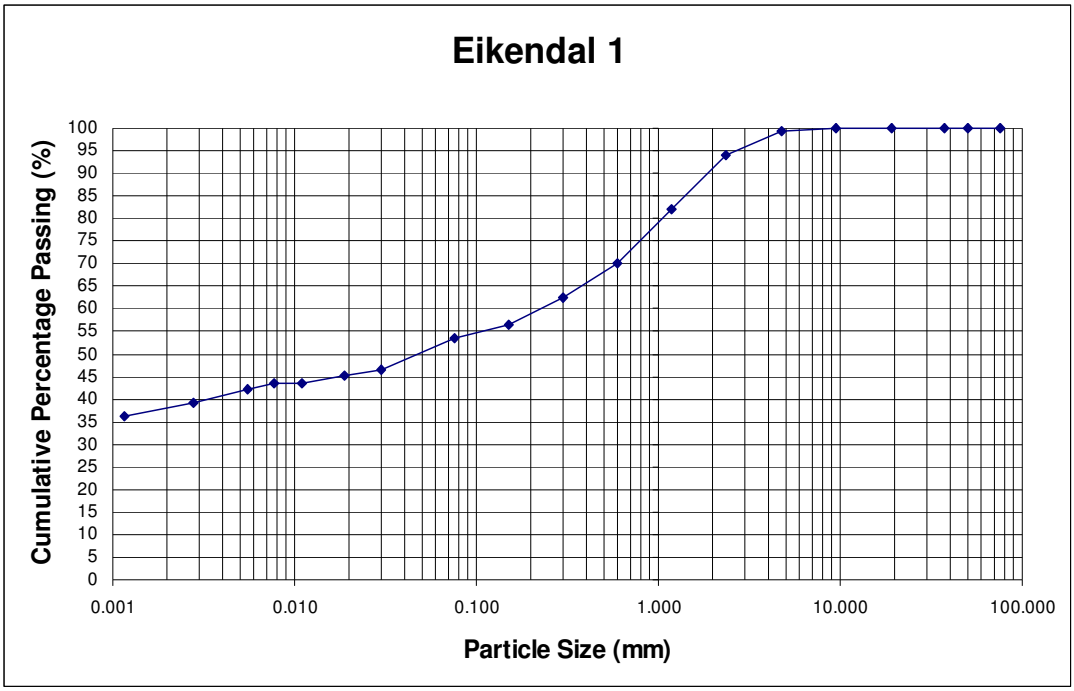

Figure 4.32: Particle size distribution curve of Eikendal pit 1

From the graph it is clear that the clay comprises almost 40% of the soil content. A fair amount of silt and coarse sand are observed in the soil, with lower quantities of fine sand, medium sand and gravel. The soil from Eikendal pit 1 can be classified as silty fine sand with slight plasticity (ML)

In view of the high dry density and high clay content of the soil from Eikendal pit 1, the moderate collapse of the soil is considered very unusual. As with Audacia pit 4 the low moisture content and poor grading might have contributed to the collapse. The soil from Audacia pit 4 and Eikendal pit 1 might also be generally more compressible soils than the rest of the soil sampled.

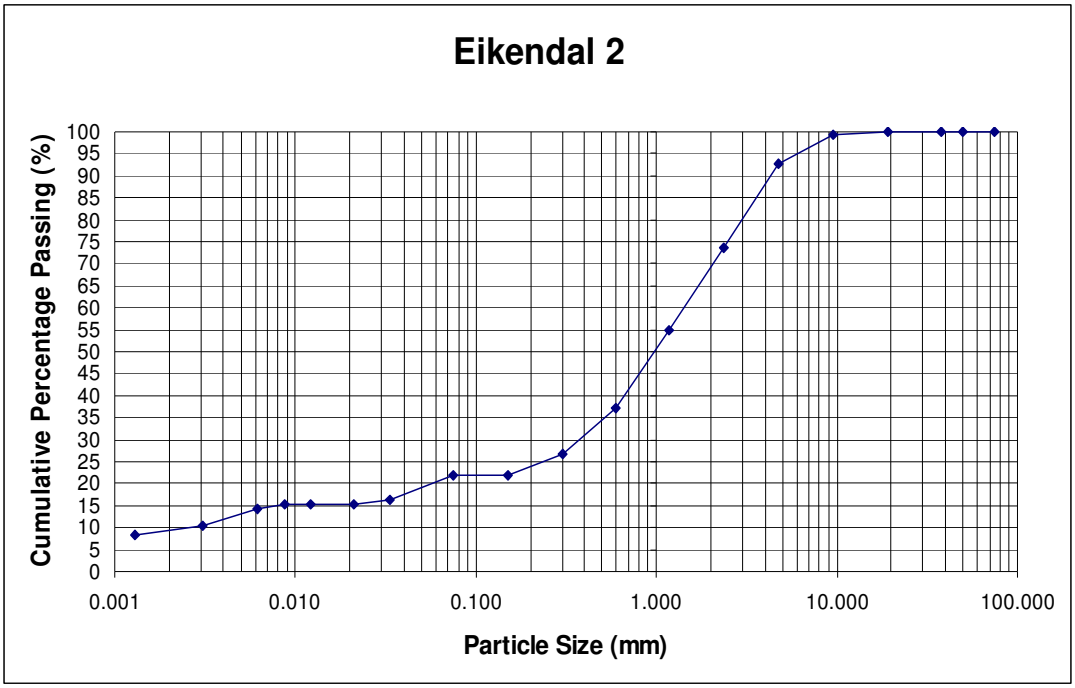

Figure 4.33: Grading curve of Eikendal pit 2

The graph shows that a large fraction of the soil particles has sizes within narrow limits. The coarse sand and gravel make up the largest part of the soil. The remaining particle sizes are present in low quantities. Based on its grading and plasticity, the soil from Eikendal pit 2 can be classified as clayey sand (SC).

The moderate collapse that occurred in the soil from Eikendal pit 2 was unexpected because of the very high dry density of the soil. The distribution of particle sizes however complies fully with what is expected from a collapsible soil. The high proportion of coarse particles with few fines in between creates a structure which is vulnerable to collapse. This, together with the very low moisture content of the soil might have contributed to the collapse settlement.

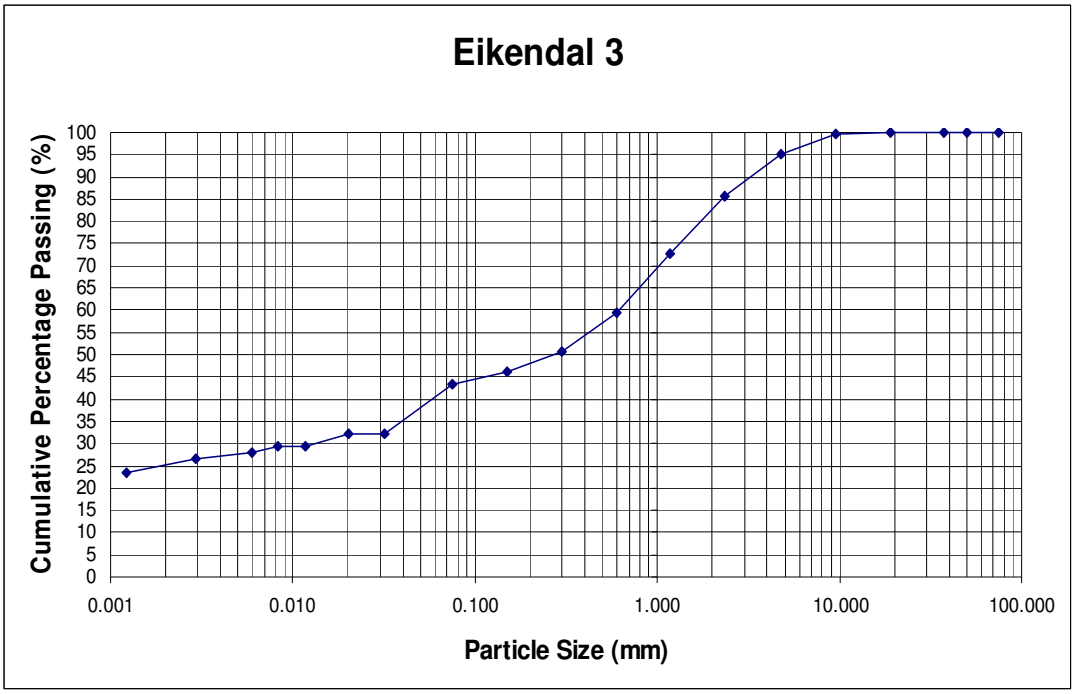

Figure 4.34: Grain size distribution graph of Eikendal pit 3

The graph shows that all the particle sizes are relatively well represented in the soil. The clay content is the highest followed by the coarse sand. Lower proportions of particles of intermediate size and gravel are present in the soil. The soil from Eikendal pit 3 can be classified as silty sand (SM).

Collapse did not occur in the soil from Eikendal pit 3. This result was anticipated due to the very high dry density of the soil. The high clay content and low moisture content also concur with the result.

This is in contrast with the results from Audacia pit 4 and Eikendal pit 1 where moderate collapse occurred, as both soils also have high dry densities, high clay contents, low moisture contents and relatively even grain size distributions. No explanation could be found for the difference in behaviour.

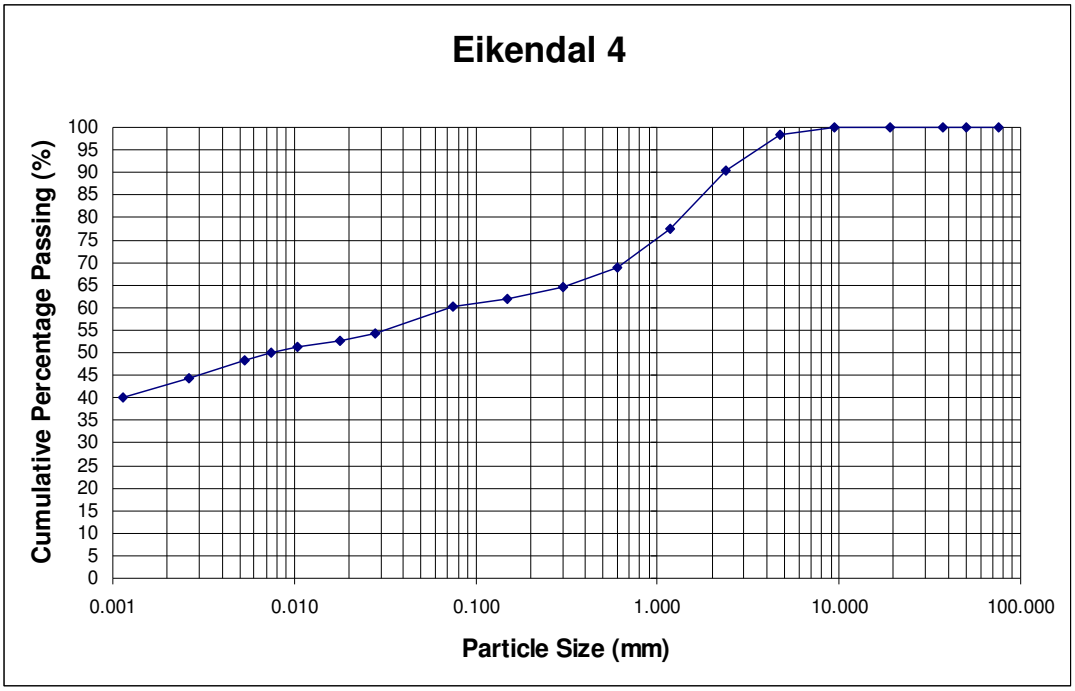

Figure 4.35: Particle size distribution of Eikendal pit 4

From the graph it is evident that more than 40% of the soil consists of clay. A fair amount of silt, coarse sand and gravel are observed, with a lower percentage of intermediate sizes. Based on its material characteristics, the soil from Eikendal pit 4 can be classified as silty fine sand with slight plasticity (ML).

The moderate collapse that occurred in the soil from Eikendal pit 4 was probable due to the low dry density of the soil. The exceptionally high clay content is unusual in view of the result. Considering the low dry density of the soil, collapse is however still possible.

This is in contrast with the result from Audacia pit 1. The soil from Audacia pit 1 has a much lower clay content than the soil from Eikendal pit 4. Both soils also have low dry densities, high moisture contents and similar grading, yet the soil from Eikendal pit 4 showed moderate collapse whereas the soil from Audacia pit 1 did not collapse. No explanation could be found for the contrasting results.

c) Ernie Els Wines

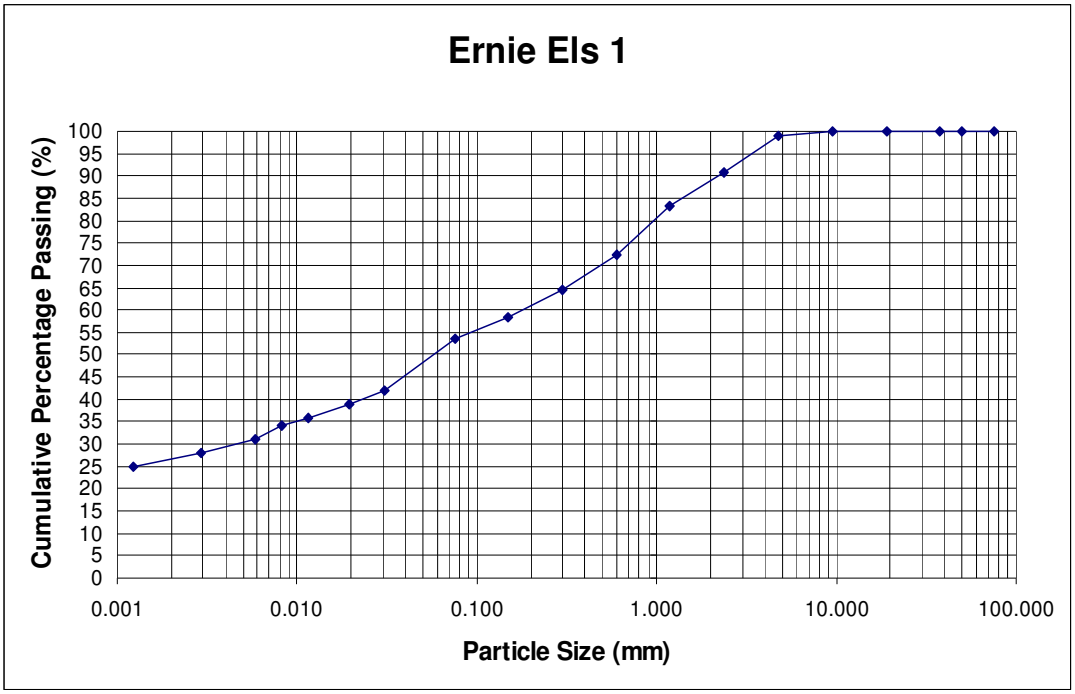

Figure 4.36: Grading curve of Ernie Els pit 1

From the graph it is clear that the fine particles (clay and silt) make up more than 50% of the soil content. There are more or less equal amounts of the coarse particles. The soil from Ernie Els pit 1 can be classified as silty fine sand with slight plasticity (ML).

The soil from Ernie Els pit 1 is highly collapsible. The low dry density of the soil made this a probable result. In view of the characteristics of a collapsible soil, the abundant clays and silts present in the soil are unusual. Yet, the low dry density of the soil could have made the soil susceptible to collapse even though the clay content is high.

However, a collapse settlement value of 8.16% was calculated for the saturated sample, which is unusually high for the Stellenbosch area. It is therefore possible that the soil was not sampled in residual granite, but in reworked residual granite. Reworked residual granite is formed by biotic action, creating a collapsible soil fabric. This may be the cause of the high percentage of collapse settlement in the soil from Ernie Els pit 1.

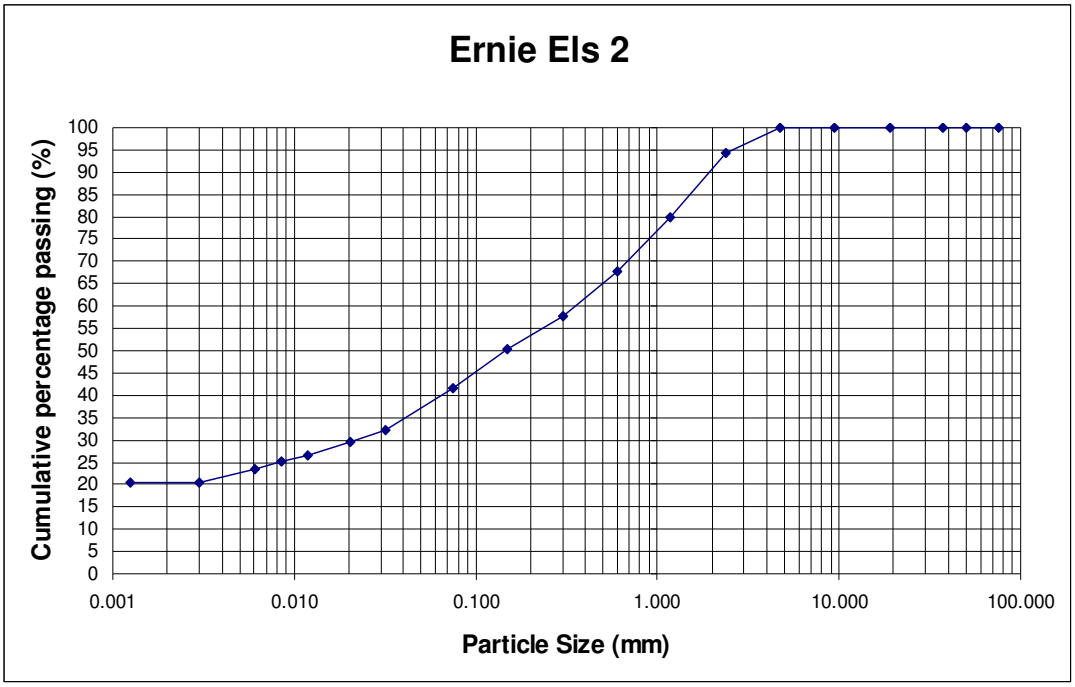

Figure 4.37: Grain size distribution curve of Ernie Els pit 2

The graph shows that the particle sizes are all well represented. There are no excess of particles in any size range. The soil from Ernie Els pit 2 can be classified as silty sand (SM).

The low dry density of the soil from Ernie Els pit 2 made the moderate collapse of the soil probable. The proportion of clay is however still higher, and the coarse grains lower than one would expect from a collapsible soil. A high clay content however does not necessarily imply that collapse will not occur. The low dry density of the soil can make it susceptible to collapse.

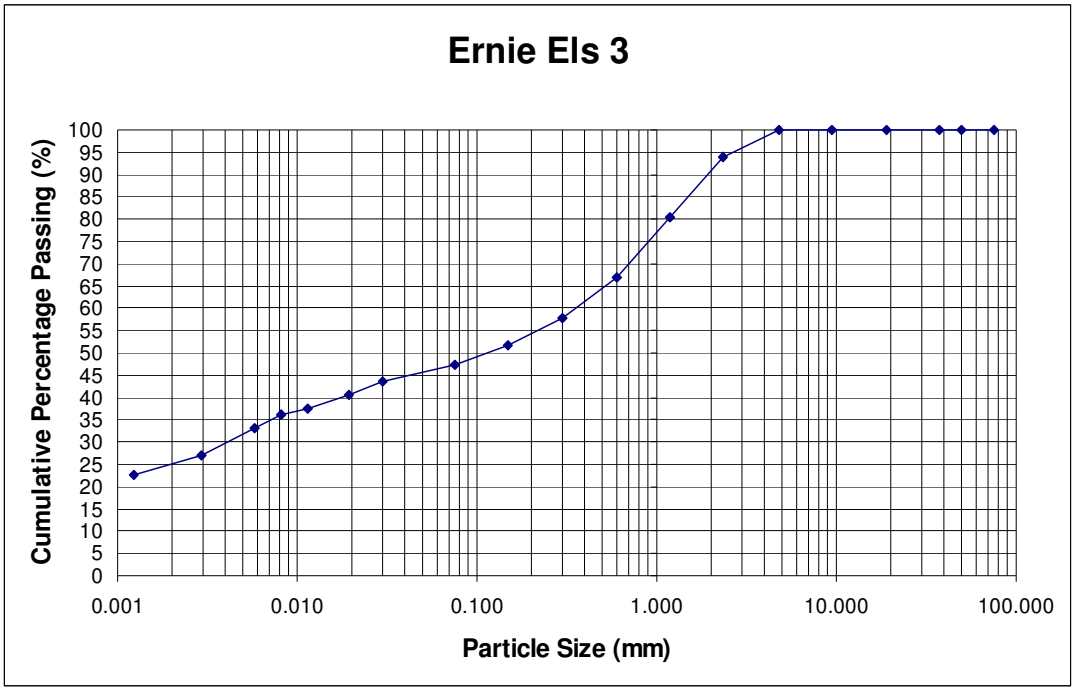

Figure 4.38: Grading curve of Ernie Els pit 3

From the graph it is clear that the clay and silt particles make up almost half of the soil content. Of the coarse particles, the coarse sand forms the largest part, whereas the remaining particle sizes are present in low proportions. Based on its grading and plasticity, the soil from Ernie Els pit 3 can be classified as silty sand (SM).

The soil from Ernie Els pit 3 is highly collapsible. The low dry density of the soil made this a probable result. The high clay and silt content is nonetheless unusual in view of the result. Considering the low dry density of the soil, collapse is however possible. Even though the soil is highly collapsible, the collapse settlement value of 5.04% is still acceptable for the Stellenbosch area.

The soil from Ernie Els pit 2, which is moderately collapsible, contains less clay than the soil from Ernie Els pit 3, which is highly collapsible. This result may seem unusual. However, the soil from Ernie Els pit 2 has a higher moisture content and more evenly distributed particle sizes than that of Ernie Els pit 3. These factors might have caused the soil from Ernie Els pit 2 to be more resistant to collapse than the soil from Ernie Els pit 3.

d) Jamestown cemetery

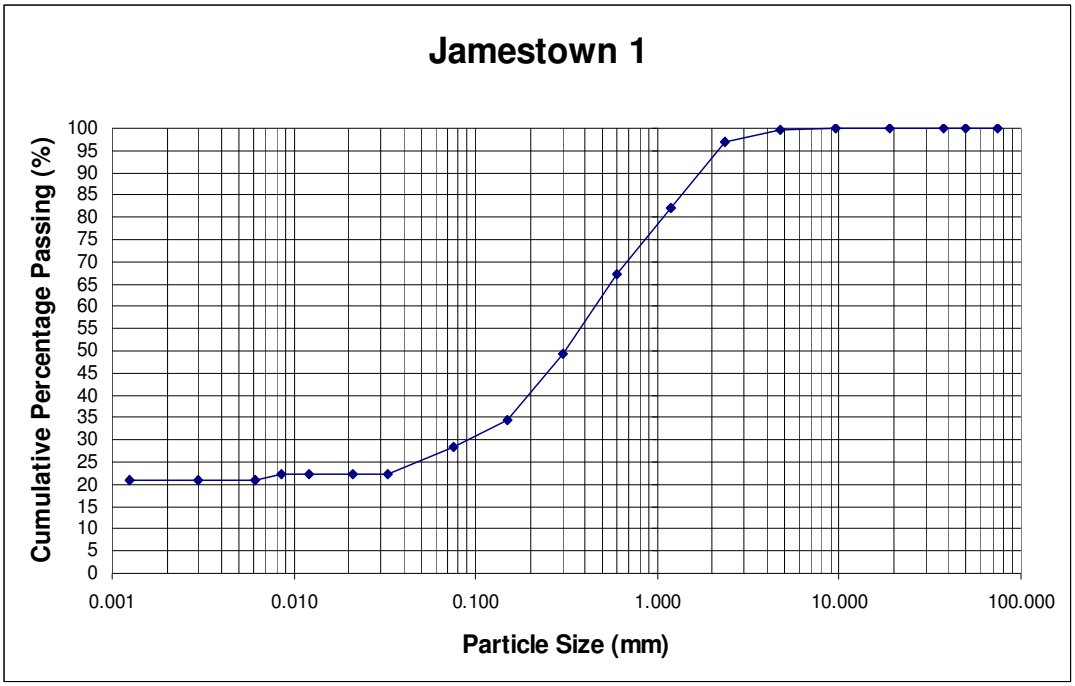

Figure 4.39: Grain size distribution graph of Jamestown pit 1

The graph shows that the medium and coarse sand make up more than half of the soil content. The clay and fine sand are also well represented. Low proportions of silt and gravel are present in the soil. The soil from Jamestown pit 1 can be classified as clayey sand (SC).

The high dry density of the soil from Jamestown pit 1 made the moderate collapse of the soil atypical. The high content of coarse particles and lower proportion of fine particles, however, comply with what is expected from a collapsible soil. This, as well as the uneven distribution of particle sizes, could have caused the soil to collapse.

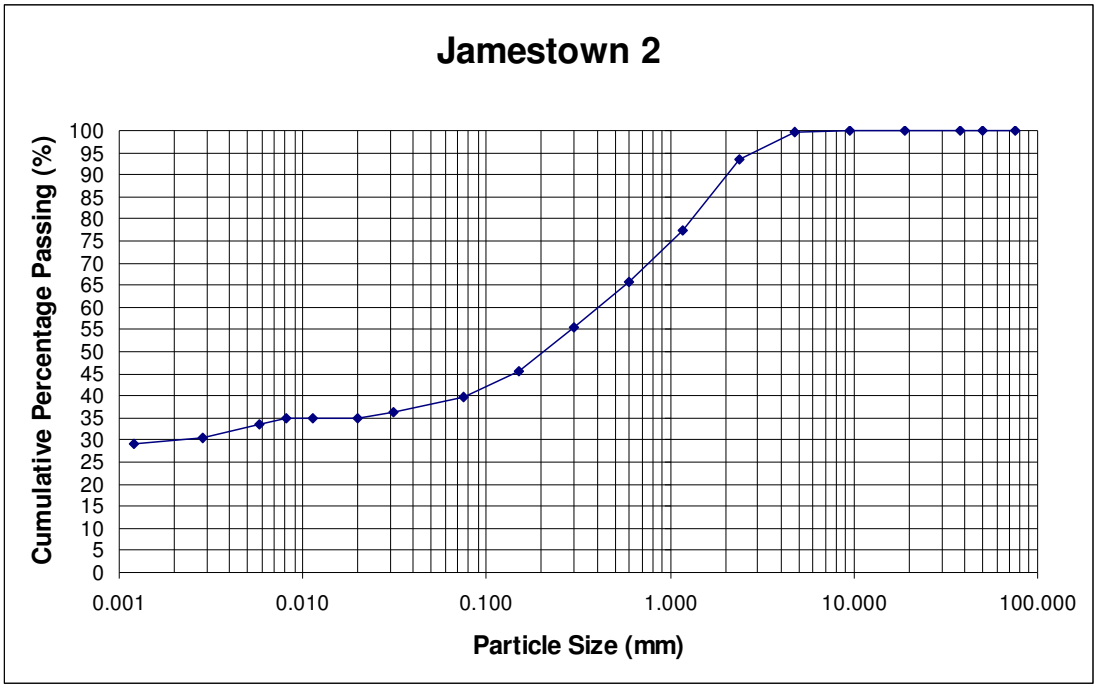

Figure 4.40: Particle size distribution of Jamestown pit 2

From the figure it is evident that the clay forms a large part of the soil content. A moderate amount of medium and coarse sand is present in the soil, with relatively low proportions of silt, fine sand and gravel. Based on its material characteristics, the soil from Jamestown pit 2 can be classified as clayey sand (SC).

In view of the high dry density and high clay content of the soil from Jamestown pit 2, the moderate collapse of the soil is considered very unusual. Yet, the relatively low moisture content and poor grading of the soil may have caused it to collapse. In view of the fact that the soil is only moderately collapsible and not highly collapsible, the result can be considered as acceptable.

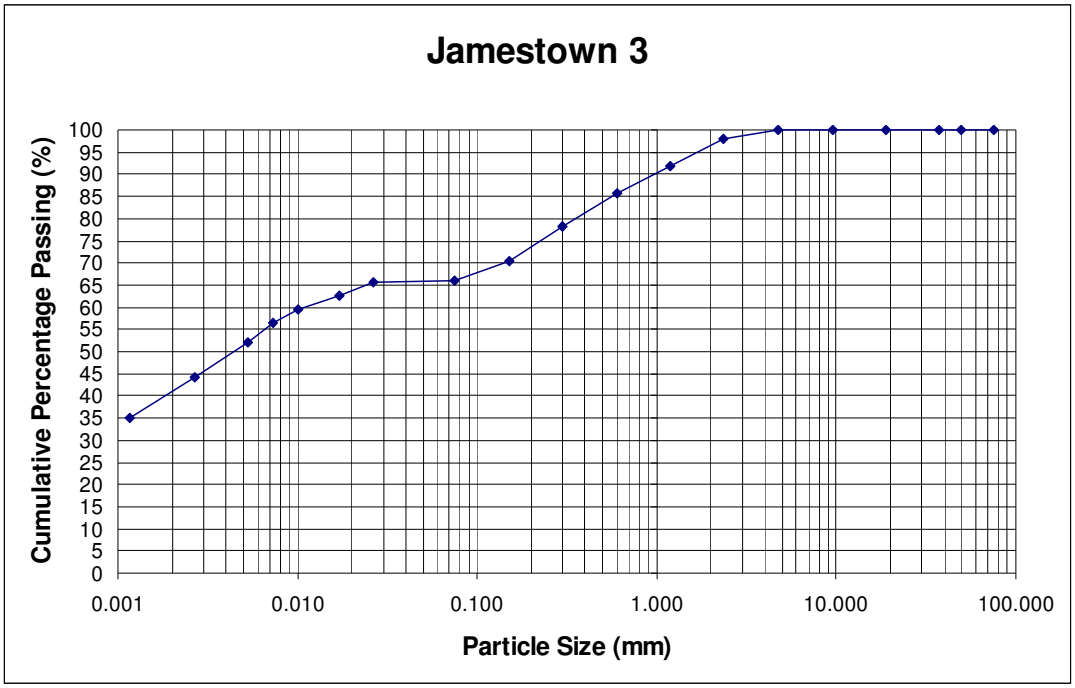

Figure 4.41: Grading curve of Jamestown pit 3

From the graph we can conclude that the fine particles (clay and silt) make up more than 60% of the soil content. Very low quantities of the coarser particles are present in the soil. The soil from Jamestown pit 3 can be classified as silty fine sand with slight plasticity (ML).

Collapse did not occur in the soil from Jamestown pit 3. This result was unexpected since the soil has properties that could lead to collapse; namely a low dry density. As mentioned above, the soil has a very high clay and silt content and sparse coarse particles. The behaviour of the soil is therefore understandable since a lack of leaching in the soil probably prevented a collapsible fabric from forming, thus inhibiting collapse settlement. The high moisture content of the soil may also have contributed to the soil not collapsing.

4.2.2.3 Conclusions

Schwartz (1985) states the following: "Collapse problems are generally associated with silty or sandy soils of low clay content. It is important to take into consideration that a high clay content does not necessarily imply that collapse will not occur. Soils with a collapsible fabric frequently have a low dry density." Jennings and Knight (1975) however warn of the danger of assuming that all soils with a low dry density will show collapse or, vice versa, that all soils with a high dry density will not collapse.

This indicates the complex nature and unpredictability of collapsible soils. This was also visible in the test results, where in some instances odd results and clear contrasts were found. Even though possible explanations for the behaviour of the soils were given in terms of dry density, moisture content and grading, a clear correlation could not be found between collapse settlement and these properties.

4.2.3 Shear strength testing

Shear strength tests, in accordance with USBR Test No 5725, were carried out on ten of the fourteen soil samples collected from the study area to determine the shear behaviour of the soils (Earth Manual Part 2, 1990). Only ten samples were included in the study as the soil from four test pits, namely Eikendal 1, Eikendal 2, Ernie Els 1 and Jamestown 1 was insufficient. All tests were performed in a 60 x 60 x 20mm direct shear device. The tests were carried out on saturated samples as well as on samples at natural moisture content at normal pressures of 50kPa, 100kPa and 150kPa. Six tests were thus carried out on each of the ten soil samples to determine the following:

a) **Shear strength parameters of the soils**

For each of the ten soil samples a graph of normal stress versus maximum shear strength was drawn to determine cohesion, c, and the angle of internal friction, ϕ, of the soil.

b) **Shear resistance versus shear displacement**

To determine the shear stress and shear displacement at which the samples failed, graphs of shear stress versus displacement were plotted for the ten soil samples.

c) **Volume change during shear**

For each test pit a graph of vertical deformation versus shear displacement was plotted to determine the additional settlement of the soil during shear.

4.2.3.1 Shear strength parameters

As mentioned above graphs of normal stress versus maximum shear strength were plotted for all ten soil samples to determine the shear strength parameters of the soils and also the influence of collapsibility on the shear strength of the soils. The tests were carried out at normal pressures of 50kPa, 100kPa and 150kPa on saturated samples and on samples at natural moisture content. The graphs of four tests pits namely Audacia 1, Eikendal 3, Ernie Els 3 and Jamestown 2 are presented below in representation of the four farms. One should however note that for the saturated samples, c' and ϕ' are being determined, and for the natural samples, c_u and ϕ_u, as the natural samples are considered to be unconsolidated-undrained.

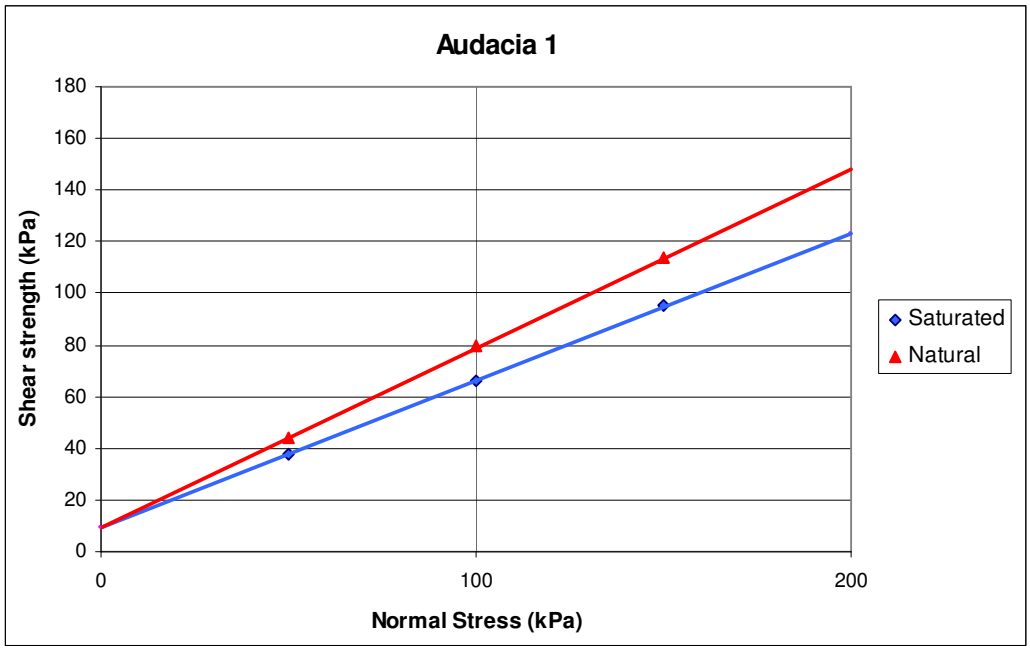

Figure 4.42: Normal stress versus maximum shear strength for Audacia pit 1

From figure 4.42 it can be seen that the saturation of the soil affected the shear strength of the soil from Audacia pit 1. The natural sample has a higher shear strength than the saturated sample because of the negative pore water pressure in the natural sample as well as the effect of saturation on the clay. This result was expected for a non collapsible soil like Audacia pit 1 as a soil at natural moisture content will generally have a higher shear strength than a saturated soil. For the saturated sample c' and ϕ' are determined as 9 kN/m^2 and 29.7° respectively and for the natural sample

c_u and ϕ_u are determined as 9 kN/m^2 and 34.8°. One should however be cautious when using the ϕ_u value in calculations as the soil is not saturated. If the water table rises, the ϕ_u value might decrease, thus affecting the safety factor.

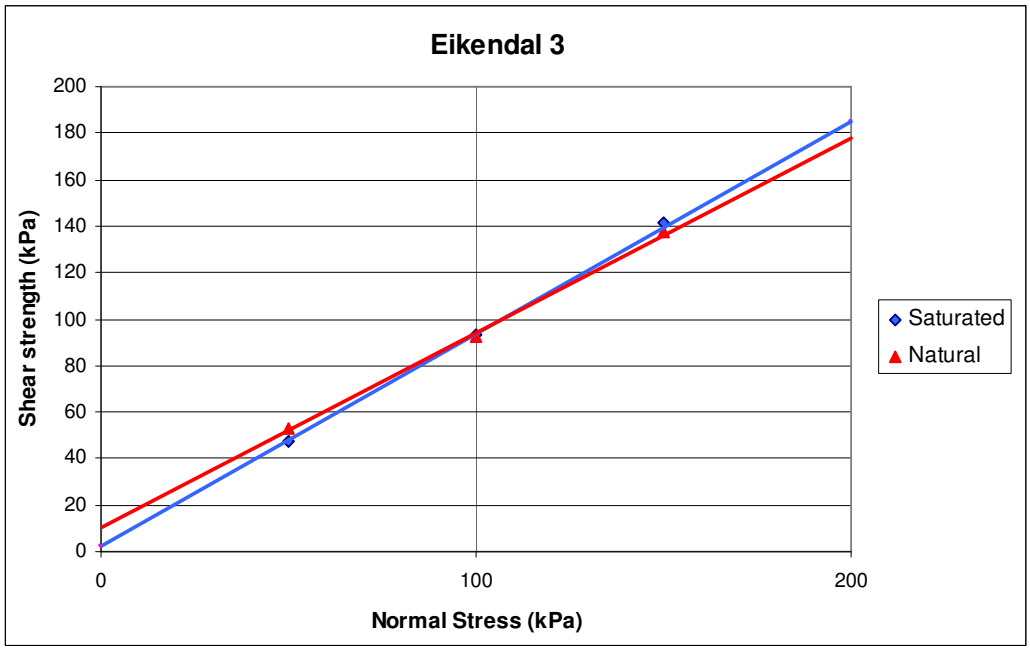

Figure 4.43: Normal stress versus maximum shear strength for Eikendal pit 3

From figure 4.43 it is evident that the shear strength of the saturated and natural samples from Eikendal pit 3 is very similar. The saturated sample however has a slightly higher shear strength than the natural sample where the normal stress exceeds 100kPa. This result correlates with the double oedometer results where the natural sample undergoes more compression than the saturated sample. The parameters c' and ϕ' of the saturated sample are determined as 2 kN/m^2 and 42.5° respectively and the c_u and ϕ_u of the natural sample as 10 kN/m^2 and 40° respectively.

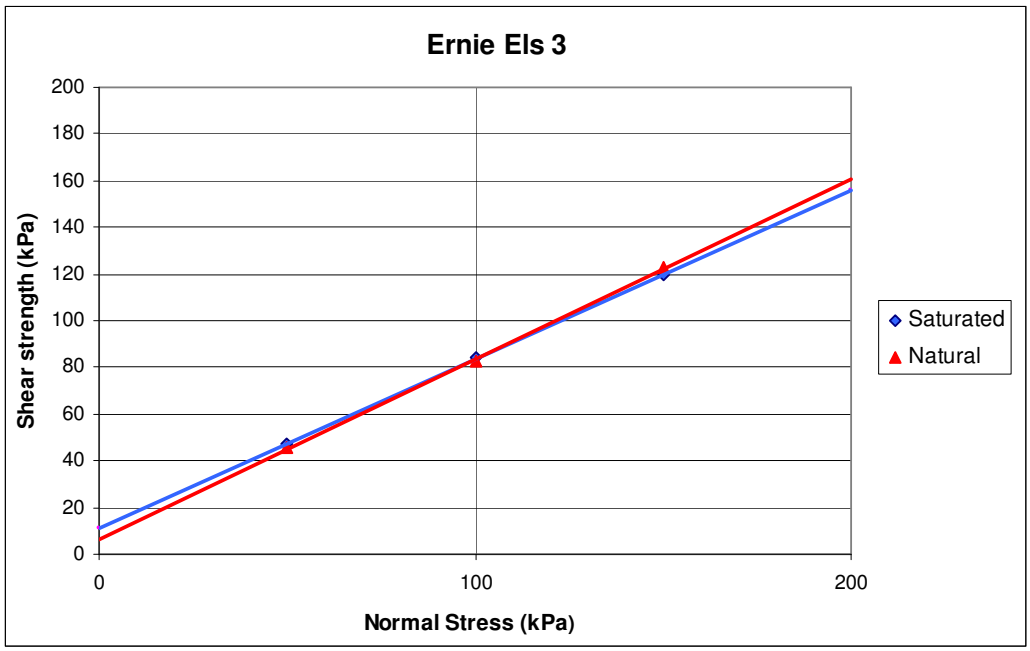

Figure 4.44: Normal stress versus maximum shear strength for Ernie Els pit 3

From figure 4.44 it can be seen that the saturation of the soil did not affect the shear strength of the soil from Ernie Els pit 3. The shear strength of the saturated and natural samples is very similar even though the soil was classified as highly collapsible. For a highly collapsible soil one would expect the saturated sample to have a notably lower shear strength than the natural sample. The c' and ϕ' of the saturated sample are calculated as 11 kN/m^2 and 35.9° respectively and the c_u and ϕ_u of the natural sample as 6 kN/m^2 and 37.8° respectively. It is thus clear that the amount of collapse does not always affect the shear strength of a soil.

Figure 4.45: Normal stress versus maximum shear strength for Jamestown pit 2

From figure 4.45 it can be seen that the natural sample from Jamestown pit 2 has a higher shear strength than the saturated sample. The presence of a collapsible fabric in the soil resulted in the decrease in shear strength upon saturation. The c' and ϕ' are calculated as 9 kN/m^2 and 39.7˚ and the c_u and ϕ_u as 5 kN/m^2 and 44.3˚.

In order to find possible explanations for the outcome of the afore-mentioned four graphs a table with the following properties was compiled:

Table 4.4: General laboratory results

Sample Nr	Moisture Content (%)	Clay (%)	Collapse (%)	ϕ' (Sat)	ϕ_u (Natural)
Audacia 1	23.47	29	< 1.0	29.7	34.8
Audacia 2	27.34	21	0.91	-	-
Audacia 3	25.51	27	2.75	-	-
Audacia 4	13.52	32	1.87	-	-
Eikendal 3	13.44	25	0.50	42.5	40.0
Eikendal 4	22.37	43	1.70	-	-
Ernie Els 2	20.81	21	2.10	-	-
Ernie Els 3	17.03	25	5.04	35.9	37.8
Jamestown 2	14.79	30	2.70	39.7	44.3
Jamestown 3	25.0	41	0.53	-	-

After analyzing the properties as illustrated in table 4.4 it can be concluded that no parallel could be found between the shear strength results and any of these properties.

It can further be concluded that a direct correlation between the collapsibility and the shear strength of the soils could not be found. It was expected that the presence of a collapsible fabric would result in an immediate decrease of shear strength if saturation occurs (Brink, 1985). This was however not the case in all instances.

The difference in shear behaviour can also be seen in the shear resistance versus shear displacement graphs in the next section.

4.2.3.2 Shear resistance versus shear displacement

Graphs of shear stress versus shear displacement were drawn of all ten saturated samples as well as of samples at natural moisture content, at a normal pressure of 100kPa, to investigate the probability of a correlation between collapsibility and shear behaviour further. The graph of Audacia pit 1 is presented below as an example. The remaining nine graphs are included in appendix C.

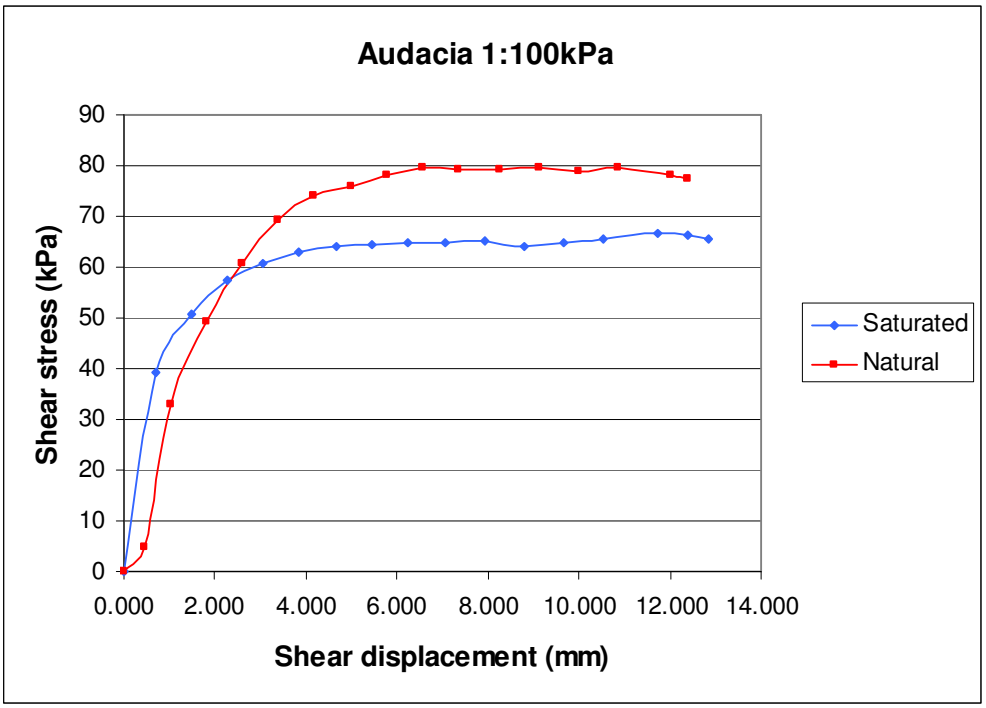

Figure 4.46: Shear stress versus shear displacement of Audacia pit 1

This graph is typical of a non collapsible soil where a difference in ϕ' and ϕ_u occurs. The saturated sample failed at a shear stress of 66.5 kPa at a displacement of 12.388mm and the natural sample failed at a shear stress of 79.8 kPa at a displacement of 9.120mm.

When comparing all ten graphs we can conclude that the amount of collapse does not always affect the shear strength of a soil. As with the results from the shear strength versus normal stress graphs, a clear correlation could not be found between the collapsibility and the shear behaviour of the soils.

4.2.3.3 Volume change during shear

Ten graphs of vertical deformation versus shear displacement at a normal pressure of 100kPa were drawn to study the vertical deformation of the soil samples during shear and further to attempt to reinforce the collapse results from the double oedometer tests. It should be noted that the difference in initial vertical deformation upon saturation was not included in the graphs. The graphs of two collapsible soils namely Eikendal pit 4 and Ernie Els pit 2 and two non collapsible soils namely Audacia pit 2 and Eikendal pit 3 are presented and interpreted below. The remaining six graphs are included in appendix C.

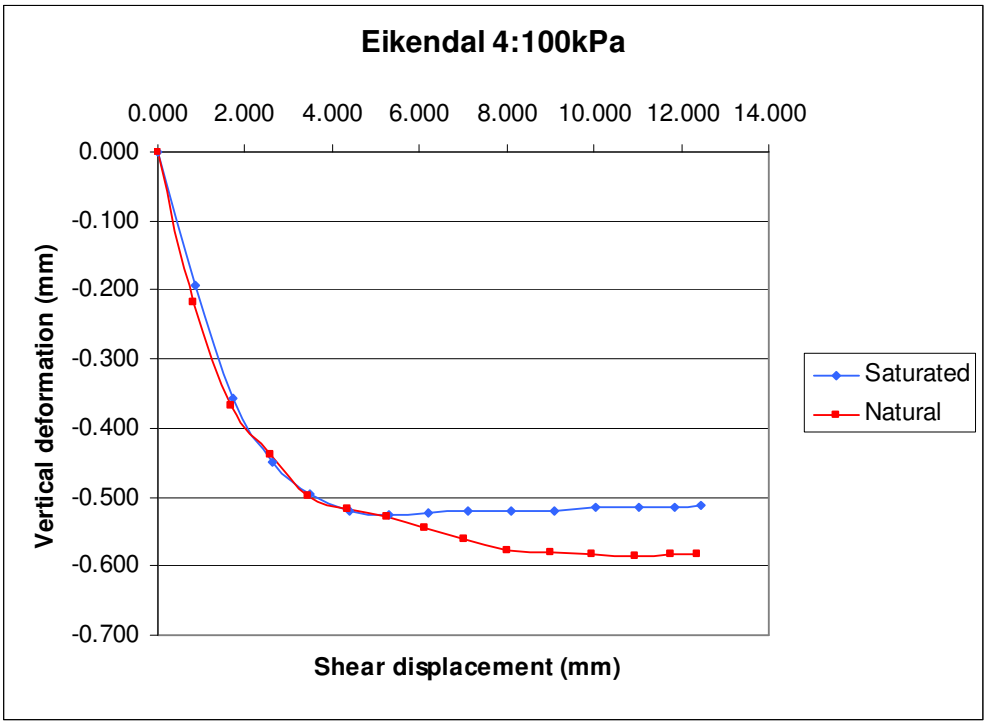

Figure 4.47: Vertical deformation versus shear displacement of Eikendal pit 4

From figure 4.47 we can determine the maximum saturated deformation in the sample from Eikendal pit 4 as 0.525mm and the maximum dry deformation as 0.586mm. It can be seen that the natural sample undergoes more vertical deformation than the saturated sample during shear. This was not expected as the soil was classified as moderately collapsible and therefore the saturated sample was expected to undergo additional volume change compared to the natural sample during shear. The

compression of the natural sample can be ascribed to the breaking of the bonds between the soil particles as a result of the shear process.

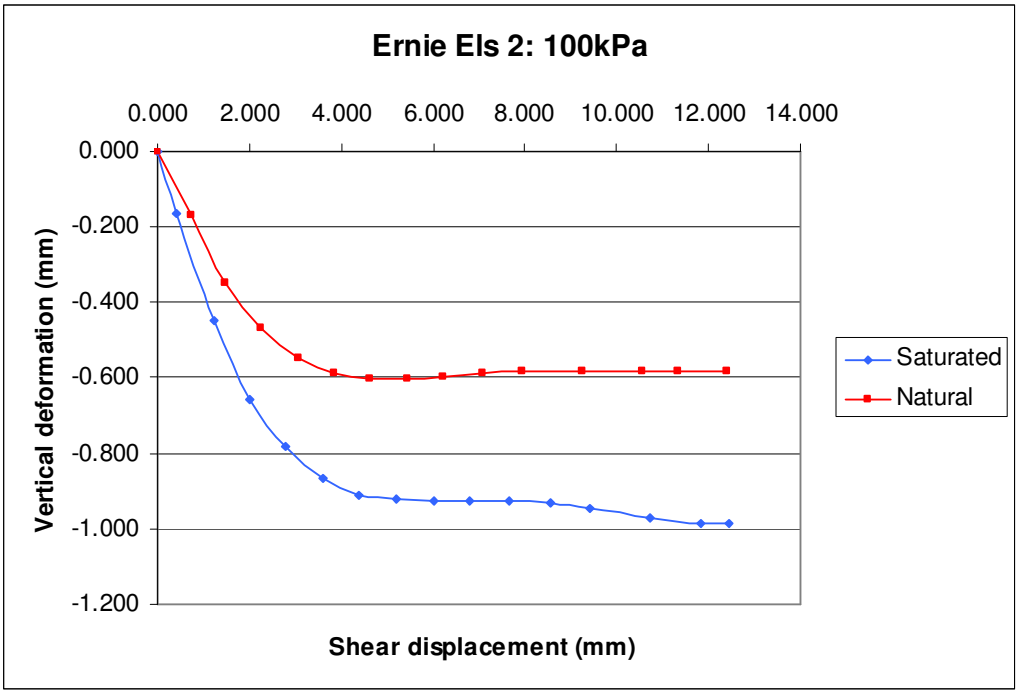

Figure 4.48: Vertical deformation versus shear displacement of Ernie Els pit 2

From figure 4.48 it can be seen that the saturated sample from Ernie Els pit 2 undergoes more vertical deformation than the natural sample. The maximum saturated deformation is 0.986mm and the maximum dry deformation 0.602mm. The difference in vertical deformation can be ascribed to the additional compression of the saturated sample during shear. This result coincides with the classification of the soil as moderately collapsible.

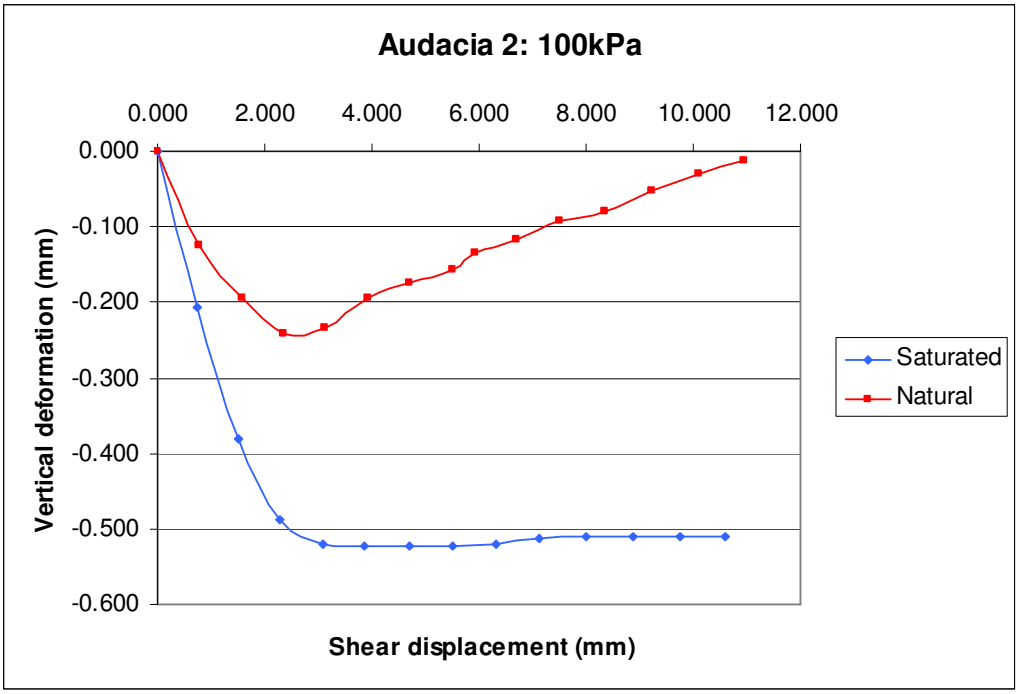

Figure 4.49: Vertical deformation versus shear displacement of Audacia pit 2

Although the soil from Audacia pit 2 was classified as non collapsible, it is evident from figure 4.49 that the saturated sample undergoes much more vertical compression than the natural sample. The maximum saturated deformation is determined as 0.524mm and the maximum dry deformation as 0.242mm. As this is a non collapsible soil, the vertical deformation of the two samples was expected to be more similar. The saturated sample nevertheless showed additional settlement whereas the natural sample was deformed minimally and then dilated to its original volume.

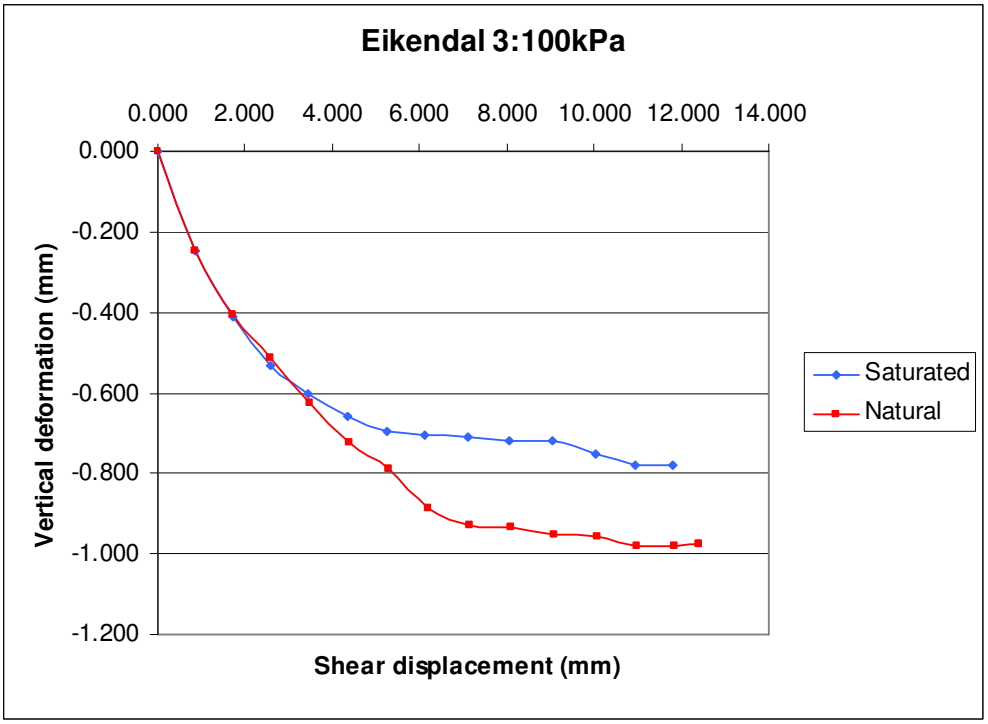

Figure 4.50: Vertical deformation versus shear displacement of Eikendal pit 3

From figure 4.50 it can be seen that the natural sample from Eikendal pit 3 compressed more than the saturated sample. A difference of 0.198mm exists in maximum deformation between the saturated and natural samples. The natural sample compressed as a result of the breaking of the particle bonds. This result was expected as it is a non collapsible soil.

When comparing the four vertical deformation versus shear displacement graphs it can be concluded that a clear correlation could not be found between collapse settlement determined by double oedometer testing and vertical deformation during shear strength testing. Soils that collapsed in the consolidometer did not necessarily show additional volume change during shear, and vice versa. The behaviour of the natural samples is also very unpredictable. This is in accordance with the overall result found when comparing all ten graphs.

4.2.3.4 Conclusions

While studying the shear behaviour of the soils from the study area, the following conclusions were reached:

- The presence of a collapsible fabric does not always result in an immediate decrease of shear strength if saturation occurs.
- Shear strength testing does not provide an adequate method for the determination of a collapsible soil.
- Soils can be very unpredictable and therefore one can very rarely make assumptions about the behaviour of a soil without doing the necessary testing.

4.3 EFFECTS OF TOPOGRAPHY AND DRAINAGE ON THE COLLAPSIBILITY OF SOIL

Topography and drainage play a major role in the development of a collapsible soil structure. Under topographical conditions which favour easy internal drainage, much of the clay is washed out and the characteristic structure of a collapsing soil develops. The quartz and the unweathered orthoclase form the solid particles which are held in position by bridges of kaolinite. The formation of such a structure depends on the local topography and climate. Apparently, gradients between 5˚ and 15˚ provide the conditions most conducive to the formation of collapsible structures. In these ranges gravitational pull has a maximum effect on seepage, resulting in much of the colloidal kaolinite being washed or leached out of the soil (Weinert, 1980).

The topography of the area demarcated for this thesis is undulating. Gradients ranging from 0˚ to 15˚ were observed. In the next section the question of whether a correlation exists between the topography of the four sampling locations and the collapsibility of the soils will be explored. As mentioned above, climate also has an effect on the collapsibility of soil, but will not be included in this study as the four sampling locations are in close proximity within the Stellenbosch area. In this area warm humid conditions prevail which are optimum for the formation of collapsible structures (Engelbrecht, 2008).

The topography of the three farms and cemetery from which the samples were collected is described below:

- Audacia

The soil samples from Audacia were collected from a slope with a gradient of more or less 13˚. It is a suitable location for a collapsible soil structure to form and therefore collapse is likely.

- Eikendal

The even topography of Eikendal impedes easy internal drainage and thus only small amounts of clay are being washed or leached out of the soil, preventing the formation of a collapsible soil structure. For this reason collapse settlement is not likely in the soil from Eikendal.

- Ernie Els

Collapse settlement is probable in the soil sampled from Ernie Els as the samples were collected from a slope with a gradient of more or less 13˚.

- Jamestown cemetery

The soil samples from Jamestown cemetery were collected on a slope with a gradient of more or less 7˚. Collapse is therefore likely to occur.

The degree of collapsibility of each of the fourteen soil samples and the topography of the respective sampling locations are tabulated below. The gradients of the slopes of Audacia, Ernie Els and Jamestown cemetery fall within the ideal ranges for the formation of a collapsible soil fabric i.e. between 5˚ and 15˚, therefore a differentiation is only made between even ground and slopes. As the soil samples were collected in a relatively concentrated area in the middle of each slope, the position on the slope needs not to be taken into account. The samples were collected from a concentrated area as permission for sampling was restricted to certain areas. The collapsibility of the soil is categorized as not collapsible, moderately collapsible and highly collapsible.

Table 4.5: Collapsibility versus topography

	Audacia	Ernie Els	Eikendal	Jamestown
Slope	Sample 1 Not collapsible	Sample 1 Highly collapsible	–	Sample 1 Highly collapsible
	Sample 2 Not collapsible	Sample 2 Moderately collapsible	–	Sample 2 Moderately collapsible
	Sample 3 Moderately collapsible	Sample 3 Highly collapsible	–	Sample 3 Not Collapsible
	Sample 4 Moderately collapsible	–	–	–
Even	–	–	Sample 1 Moderately collapsible	–
	–	–	Sample 2 Moderately collapsible	–
	–	–	Sample 3 Not Collapsible	–
	–	–	Sample 4 Moderately collapsible	–

From the table it can be seen that no clear correlation could be found between the collapsibility of the soils and topography of the four sampling locations. Of the ten samples collected from a slope, seven showed collapse and three did not show collapse. Although the majority of samples collapsed, a convincing trend was not found. Of the four samples collected on level ground, only one sample did not collapse. The moderate collapse of the remaining three samples support the premise of the lack of a correlation found between collapsibility and topography.

Within the limited study area and number of samples collected it was not possible to obtain an undisputed result.

CHAPTER 5: CONCLUSIONS AND RECOMMENDATIONS

5.1 INTRODUCTION

The study was undertaken to determine the occurrence and extent of collapse settlement in the demarcated study area situated on the R44 between Stellenbosch and Somerset West. The aim of the study was achieved through the experimental work which included double oedometer testing. The objective to determine the reasons for the collapse behaviour of the soils was not reached. The outcomes of further objectives together with the conclusions and recommendations that follow from the research conducted will be discussed forthwith.

5.2 CONCLUSIONS

The following conclusions can be drawn concerning the double oedometer tests and indicator analyses.

- Double oedometer testing confirmed the presence of collapsible soils on Audacia, Eikendal, Ernie Els Wines and in the Jamestown cemetery. Soils ranging from moderately collapsible to highly collapsible were found. Collapsible soils are thus prevalent in the study area and therefore the necessary testing should always be carried out when dealing with the design of foundations.

- Ernie Els Wines presents the highest threat in terms of quantity and severity of collapsible soils and extra caution should be taken during future developments on the farm.

- Various authors have stated that collapse will most likely not occur if the soil has a dry density exceeding 1600kg/m^3 (Brink, 1985). The laboratory results showed that collapse is in fact possible at dry densities of up to 2022kg/m^3. It should be remembered that if a soil has a dry density exceeding 1600kg/m^3 the possibility of collapse should not be excluded.

- The double oedometer results were used in an attempt to obtain a relationship between collapse settlement and a combination of easily determined properties such as dry density (void ratio), moisture content and grading, but no meaningful conclusions have emerged. Collapse can thus not be identified or ruled out by studying these properties.

The shear behaviour of the soils was evaluated, resulting in the following conclusions:

- It was expected that the presence of a collapsible fabric would result in an immediate decrease in shear strength if saturation occurs (Brink, 1985). The shear strength results however showed that this is not the case in all instances. A relationship between collapsibility and shear strength can thus not be assumed.

- An attempt was made to obtain a correlation between the shear strength of the soils and a number of variables such as moisture content, clay content and collapsibility. A parallel between these properties and the angle of internal friction of the soils could not be found. The shear strength of a soil can thus not be determined by studying only the moisture content, clay content and collapsibility.

- In an attempt to reinforce the double oedometer results, the vertical deformation of the soil samples was studied during shear strength testing. A correlation between the collapse settlement determined during the double oedometer testing and the volume change during shear strength testing could not be found. Collapse settlement can therefore not be predicted by studying the vertical deformation of a soil during shear.

The effects of topography and drainage on the collapsibility of soils were also investigated, with the following conclusions:

- A direct relationship between the collapsibility of the soils and the topography of the four sampling locations did not emerge. The incidence of collapse was found to be similar on slopes and even ground. The assumption that collapse is more likely to occur on a slope than on even ground was therefore not proven. However, the gradients of all three slopes fall within the ideal ranges for the formation of a collapsible soil fabric, therefore, had the study area included more steeply sloping terrain, the result may well have been different.

The reason for the inconclusive results could be ascribed to the relatively small study area and limited number of samples.

5.2.1 General conclusions

The difficulty in defining the mechanisms of collapse which involves the interaction of a number of complex variables appears to be a common finding for studies on this subject (Brink, 1985). This renders the prediction and understanding of the collapse phenomenon particularly problematic. It can be concluded that soils are very unpredictable and assumptions concerning the behaviour of a soil can rarely be made.

When performing a site investigation for future developments in or close to the demarcated study area and when dealing with residual granite in general, collapse should always be a concern and quantified. The first step in identifying a potentially collapsible soil is the correct recording of the soil profile (Schwartz, 1985). Various in-situ tests such as the “sausage” test and the plate-loading test can be carried out to determine if collapse settlement is a possibility and if further laboratory testing is indicated.

5.3 RECOMMENDED FUTURE RESEARCH

The following recommendations are made based on the conclusions:

5.3.1 Recommendations related to field work

It is recommended that:

- the demarcated study area be enlarged in order to broaden the area of research. The increased data obtained will increase the likelihood of a more conclusive result.

- more sampling areas be included in the existing demarcated study area to enable a more thorough research and therefore obtain a more accurate representation of the collapse problem in the study area.

- more test pits be included on each sampling location in order to increase the knowledge of the occurrence and extent of the collapse problem on each sampling location.

- more undisturbed samples be collected from each test pit and more tests performed to increase the accuracy of the results.

- some samples be taken at greater depths in order to determine the extent of the collapse horizon.

5.3.2 Recommendations related to experimental work

- By collecting more samples from each test pit, the accuracy of the results can be increased in the following manner:

    - Double oedometer testing: testing two saturated and two natural samples from each test pit instead of just one of each.

- Shear strength testing: doubling the number of shear strength tests carried out on the soil from each test pit.

- It is recommended that in future research the type of clay minerals in the soil be determined. As reddish kaolinitic soils form in well drained conditions and blackish montmorillonitic clays form in weakly drained circumstances, the type of clay minerals in the soil can be an indication of the collapsibility of the soil (Engelbrecht, 2008). Therefore this can provide explanations concerning the collapse results.

5.3.3 General recommendations

As was determined in the research study, no correlation could be found between shear strength and the collapsibility of the soils, therefore, if doubling the number of shear strength tests still does not show a correlation between the two mentioned factors, shear strength tests do not need to be included in future studies concerning collapsible soils.

Given the fact that residual granite soils have been found to be associated with a number of problematic characteristics, other than collapse, and the fact that these characteristics might be inter-connected, it is recommended that any future study concerning the collapse phenomenon be expanded to cover all aspects of residual granite.

References

Aitchison, G.D. 1973. Problems of soil mechanics and construction on structurally unstable soils. Proceedings, 8th International Conference on Soil Mechanics and Foundation Engineering, Moscow.

American Society for Testing and Materials. 1992. Annual Book of ASTM Standards, Sec.4, Vol.04.08, West Conshohoken, Pa.

American Society for Testing and Materials. 1999. Annual Book of ASTM Standards, Sec.4, Vol.04.08, West Conshohoken, Pa.

Army Code No 71044. Her Majesty's Stationary Office. 1976. Applied geology for engineers. Military Engineering Volume xv. London: Army Publications.

Atterberg Limits [Online]. Available: http://en.wikipedia.org/wiki/Atterberglimits. [2010, February 19].

Brink, A.B.A. 1978. Foundation engineering problems associated with residual soils formed by the decomposition of granite in Southern Africa. Paper presented at the Sixth Quinquennial Convention: Seminar on soil structure interaction. SAICE, Durban.

Brink, A.B.A. 1996. Engineering geology of Southern Africa: Volume 1. South Africa: Building publications.

Brink, A.B.A. 1981. Engineering geology of Southern Africa: Volume 2. South Africa: Building Publications.

Brink, A.B.A. 1985. Engineering geology of Southern Africa: Volume 4 Post-Gondwana deposits. South Africa: Building Publications.

Brink, A.B.A., Partridge, T.C. & Williams, A.A.B. 1982. Soil survey for engineering. Oxford: Oxford University Press.

Byrne, G., Everett, J.P. & Schwartz, K. 1995. A guide to practical geotechnical engineering in Southern Africa: 3rd edition. South Africa: Frankipile.

Chamberlin, T.C. & Salisbury, R.D. 1914. Geology shorter course. Chicago: Henry Holt & Company.

Craig, R.F. 2004. Craig's soil mechanics: 7th edition. USA: Spon Press.

Das, B.M. 2004. Principles of foundation engineering: 5th edition. USA: Brooks/Cole.

De Wet, M. 2009. Soil behaviour seminar. Unpublished class notes (Soil structure-fabric and its stability). Stellenbosch: University of Stellenbosch.

Dudley, J.H. 1970. Review of collapsing soils. *Journal of the Soil Mechanics and Foundations Division ASCE*, 96(SM3):925-947.

Du Plessis, F. 2010. Personal interview. 1 April, Cape Town.

Engelbrecht, J.C. 2008. Advanced foundation design seminar. Unpublished class notes (Residual soils in South Africa). Stellenbosch: University of Stellenbosch.

Goldich, S.S. 1938. A study in rock-weathering. *Journal of Geology*, 46: 17-58.

Jackson, M.L. & Sherman, G.D. 1953. Chemical weathering of minerals in soils. *Advances in Agronomy*, 5: 219-318.

Jennings, J.E., Brink, A.B.A. & Williams, A.A.B. 1973. Revised guide to soil profiling for civil engineering purposes in Southern Africa. *The Civil Engineer in South Africa,* pp3-12.

Jennings, J.E. & Knight, K.A. 1975. A guide to construction on or with materials exhibiting additional settlement due to collapse of grain structure. Proceedings, 6th Regional Conference for Africa on Soil Mechanics and Foundation Engineering, Durban.

Jenny, H. 1941. Factors of soil formation: A system of quantitative pedology. New York: McGraw-Hill.

Keller, W.D. 1957. The principles of chemical weathering: Revised edition. Columbia: Lucas Bros.

Koerner, R.M. 1984. Construction and geotechnical methods in foundation engineering. USA: McGraw-Hill, Inc.

Leygonie, F.E. 1977. Die graniete van Langebaan, Kaapprovinsie. *Annals University of Stellenbosch*, A1(2):33-105.

Mitchell, J.K. 1993. Fundamentals of soil behaviour: 2nd edition. USA: John Wiley & Sons, Inc.

Schoch, A.E., Leterrier, J. & La Roche, H.D.E. 1977. Major element geochemical trends in the Cape granites. *Transactions Geological Society of South Africa*, 80(3): 197-209.

Schulze, B.R. 1958. The climate of South Africa according to Thornthwaite's rational classification. *South African Geographical Journal*, 40:31-53

Schwartz, K. 1985. Problem soils in South Africa: Collapsible soils. *The Civil Engineer in South Africa,* pp378-391.

Sowers, G.B. & Sowers, G.F. 1953. Introductory soil mechanics and foundations. USA: The Macmillan Company.

Theron, J.N., Gresse, P.G., Siegfried, H.P. & Rogers, J. 1992. Explanation: sheet 3318 (1:250 000). Geological Survey: The geology of the Cape Town area.

Twidale, C.R. 1982. Granite landforms. The Netherlands: Elsevier Scientific Publishing Company.

Unpublished field sheet. 1:50 000 Somerset West 3418BB, Stellenbosch 3318DD. Council for Geoscience.

U.S. Department of the Interior: Bureau of Reclamation. 1990. Earth manual part 2: A water resources technical publication: 3rd edition. USBR Test No 5725. Denver: U.S. Department of the Interior.

U.S. Department of the Interior: Bureau of Reclamation. 1990. Earth manual part 2: A water resources technical publication: 3rd edition. USBR Test No 5700. Denver: U.S. Department of the Interior.

Weinert, H.H. 1980. The natural road construction materials of Southern Africa. Pretoria: H & R Academica (Pty.) Ltd.

Williams, A.A.B; Pidgeon, J.T. & Day, P.W. 1985. Problem soils in South Africa: Expansive soils. *The Civil Engineer in South Africa,* pp367-407.

Zeevaert, L. 1983. Foundation engineering for difficult subsoil conditions: 2nd edition. USA: Van Nostrand Reinhold Company Inc.

Appendix A

Soil profiles

AUDACIA

HOLE No: TH1
Sheet 1 of 1

JOB NUMBER: 20019GG

Scale 1:20

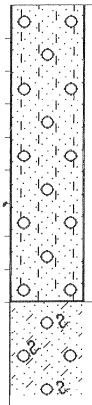

0.00 Slightly moist dark brown medium dense intact gravelly to silty SAND; TRANSPORTED (probably ALLUVIUM).

0.90

1.0m

Moist medium greyish brown mottled orange medium dense intact gravelly to clayey SAND with roots; RESIDUAL.

NOTES

1) No groundwater encountered.

2) One undisturbed soil sample taken at 1.0m.

CONTRACTOR :
MACHINE :
DRILLED BY :
PROFILED BY : N. GILDENHUYS

TYPE SET BY : SHEILA
SETUP FILE : k&t-hole.SET

INCLINATION : Vertical
DIAM :
DATE :
DATE : 30-03-10

DATE : 01/04/10 11:35
TEXT : ..\DATA\G20019-1.TXT

ELEVATION : N/A
X-COORD : N/A
Y-COORD : N/A

HOLE No: TH1

D016

dot.PLOT 4004 J&W

AUDACIA

HOLE No: TH2
Sheet 1 of 1

JOB NUMBER: 20019GG

Scale 1:20

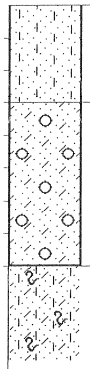

0.00 Slightly moist dark brown medium dense intact silty SAND; TRANSPORTED (probably ALLUVIUM).

0.30 Slightly moist medium brown medium dense fissured gravelly to clayey SAND; TRANSPORTED.

0.80 Moist light brownish orange mottled red dense fissured clayey to silty SAND with roots; RESIDUAL.

0.90m ■

NOTES

1) No groundwater encountered.

2) One undisturbed soil sample taken at 0.90m.

CONTRACTOR :
MACHINE :
DRILLED BY :
PROFILED BY : N. GILDENHUYS

TYPE SET BY : SHEILA
SETUP FILE : k&t-hole.SET

INCLINATION : Vertical
DIAM :
DATE :
DATE : 30-03-10

DATE : 01/04/10 11:37
TEXT : ..\DATA\G20019-2.TXT

ELEVATION : N/A
X-COORD : N/A
Y-COORD : N/A

HOLE No: TH2

D016

dot.PLOT 4004 J&W

AUDACIA

HOLE No: TH3
Sheet 1 of 1

JOB NUMBER: 20019GG

Scale 1:20

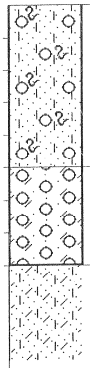

1.0m

0.00 Slightly moist medium brown medium dense intact gravelly to silty SAND with roots; TRANSPORTED (probably ALLUVIUM).

0.50 Slightly moist medium brown medium dense fissured clayey to sandy QUARTZ GRAVEL; TRANSPORTED.

0.80 Moist light reddish brown mottled white medium dense fissured silty to clayey SAND; RESIDUAL.

NOTES

1) No groundwater encountered.

2) One undisturbed soil sample taken at 1.0m.

CONTRACTOR :
MACHINE :
DRILLED BY :
PROFILED BY : N. GILDENHUYS

TYPE SET BY : SHEILA
SETUP FILE : k&t-hole.SET

INCLINATION : Vertical
DIAM :
DATE :
DATE : 30-03-10

DATE : 01/04/10 11:38
TEXT : ..\DATA\G20019 3.TXT

ELEVATION : N/A
X-COORD : N/A
Y-COORD : N/A

HOLE No: TH3

D016

dot.PLOT 4004 J&W

AUDACIA

HOLE No: TH4
Sheet 1 of 1

JOB NUMBER: 20019GG

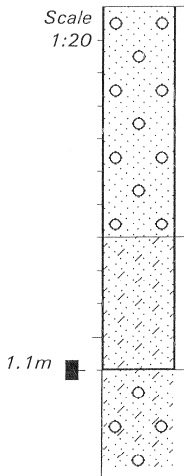

0.00 Slightly moist medium dark brown medium dense intact gravelly SAND; TRANSPORTED (probably ALLUVIUM).

0.70 Slightly moist medium brown medium dense fissured clayey SAND; TRANSPORTED.

1.10 Moist light brown mottled dark brown medium dense fissured gravelly to clayey SAND; RESIDUAL.

NOTES

1) No groundwater encountered.

2) One undisturbed soil sample taken at 1.1m.

CONTRACTOR :
MACHINE :
DRILLED BY :
PROFILED BY : N. GILDENHUYS
TYPE SET BY : SHEILA
SETUP FILE : k&t-hole.SET

INCLINATION : Vertical
DIAM :
DATE :
DATE : 30-03-10
DATE : 01/04/10 11:39
TEXT : ..\DATA\G20019-4.TXT

ELEVATION : N/A
X-COORD : N/A
Y-COORD : N/A

HOLE No: TH4

D016

dot.PLOT 4004 J&W

EIKENDAL

HOLE No: TH1
Sheet 1 of 1

JOB NUMBER: 20019GG

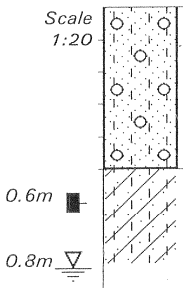

0.00 Very moist medium brown medium dense intact gravelly to silty SAND; TRANSPORTED (probably ALLUVIUM).

0.50 Wet medium brownish orange firm intact silty to sandy CLAY; RESIDUAL.

NOTES

1) Perched water table at 0.8m.

2) One undisturbed soil sample taken at 0.6m.

CONTRACTOR :
MACHINE :
DRILLED BY :
PROFILED BY : N. GILDENHUYS

TYPE SET BY : SHEILA
SETUP FILE : k&t-hole.SET

INCLINATION : Vertical
DIAM :
DATE :
DATE : 30-03-10

DATE : 01/04/10 11:43
TEXT : ..\DATA\G20019-8.TXT

ELEVATION : N/A
X-COORD : N/A
Y-COORD : N/A

HOLE No: TH1

D016

dot.PLOT 4004 J&W

EIKENDAL

HOLE No: TH2
Sheet 1 of 1

JOB NUMBER: 20019GG

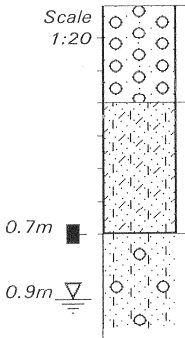

Moist dark brown medium dense intact sandy GRAVEL; TRANSPORTED (probably ALLUVIUM).

Very moist light greyish orange dense fissured silty to clayey SAND; TRANSPORTED.

Very moist light brownish orange mottled grey dense fissured silty to gravelly SAND; RESIDUAL.

NOTES

1) Perched water table at 0.9m.

2) One undisturbed soil sample taken at 0.7m.

CONTRACTOR :
MACHINE :
DRILLED BY :
PROFILED BY : N. GILDENHUYS

TYPE SET BY : SHEILA
SETUP FILE : k&t-hole.SET

INCLINATION : Vertical
DIAM :
DATE :
DATE : 30-03-10

DATE : 01/04/10 11:44
TEXT : ..\DATA\G20019-9.TXT

ELEVATION : N/A
X-COORD : N/A
Y-COORD : N/A

HOLE No: TH2

D016

dot.PLOT 4004 J&W

EIKENDAL

HOLE No: TH3
Sheet 1 of 1

JOB NUMBER: 20019GG

Scale 1:20

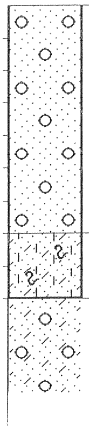

0.00 Moist dark brown medium dense intact gravelly SAND; TRANSPORTED (probably ALLUVIUM).

0.70 Very moist light greyish brown dense fissured silty to clayey SAND with roots; TRANSPORTED.

0.90 Very moist light brownish orange mottled grey very dense intact clayey to gravelly SAND; RESIDUAL.

NOTES

1) Perched water table at 1.2m.

2) one undisturbed soil sample taken at 1.0m.

CONTRACTOR :
MACHINE :
DRILLED BY :
PROFILED BY : N. GILDENHUYS

TYPE SET BY : SHEILA
SETUP FILE : k&t-hole.SET

INCLINATION : Vertical
DIAM :
DATE :
DATE : 30-03-10

DATE : 01/04/10 11:47
TEXT : ..\DATA\G20019~2.TXT

ELEVATION : N/A
X-COORD : N/A
Y-COORD : N/A

HOLE No: TH3

D016

dot.PLOT 4004 J&W

EIKENDAL

HOLE No: TH4
Sheet 1 of 1

JOB NUMBER: 20019GG

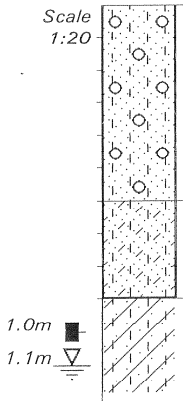

0.00 Moist medium brown mottled dark brown medium dense fissured gravelly to silty SAND; TRANSPORTED (probably ALLUVIUM).

0.60 Very moist light brownish grey dense fissured silty to clayey SAND; TRANSPORTED.

0.90 Very moist light orange brown mottled grey firm intact silty to sandy CLAY; RESIDUAL.

NOTES

1) Perched water table at 1.1m.

2) One undisturbed soil sample taken at 1.0m.

CONTRACTOR :
MACHINE :
DRILLED BY :
PROFILED BY : N. GILDENHUYS

TYPE SET BY : SHEILA
SETUP FILE : k&t-hole.SET

INCLINATION : Vertical
DIAM :
DATE :
DATE : 30-03-10

DATE : 01/04/10 11:48
TEXT : ..\DATA\G20019~3.TXT

ELEVATION : N/A
X-COORD : N/A
Y-COORD : N/A

HOLE No: TH4

D016

dot.PLOT 4004 J&W

ERNIE ELS WINES

HOLE No: TH1
Sheet 1 of 1

JOB NUMBER: 20019GG

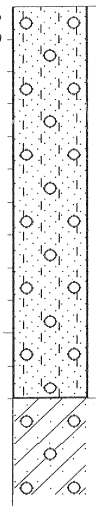

0.00 — Moist light to medium brown medium dense intact silty to gravelly SAND; TRANSPORTED (probably ALLUVIUM).

1.20 — Moist medium reddish brown firm intact gravelly to sandy CLAY; REWORKED RESIDUAL.

NOTES

1) No groundwater encountered.

2) One undisturbed soil sample taken at 1.3m.

CONTRACTOR :
MACHINE :
DRILLED BY :
PROFILED BY : N. GILDENHUYS

TYPE SET BY : SHEILA
SETUP FILE : k&t-hole.SET

INCLINATION : Vertical
DIAM :
DATE :
DATE : 30-03-10

DATE : 01/04/10 11:54
TEXT : ..\DATA\G20019-A.TXT

ELEVATION : N/A
X-COORD : N/A
Y-COORD : N/A

HOLE No: TH1

D016

dot.PLOT 4004 J&W

ERNIE ELS WINES

HOLE No: TH2
Sheet 1 of 1

JOB NUMBER: 20019GG

Scale 1:20

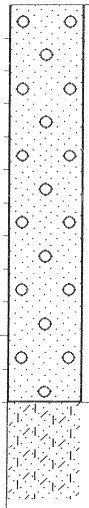

0.00 Slightly moist medium reddish brown medium dense intact gravelly SAND; TRANSPORTED (probably ALLUVIUM).

1.20

1.3m

Slightly moist light reddish brown medium dense fissured silty to clayey SAND; RESIDUAL.

NOTES

1) No groundwater encountered.

2) One undisturbed soil sample taken at 1.3m.

CONTRACTOR :
MACHINE :
DRILLED BY :
PROFILED BY : N. GILDENHUYS

INCLINATION : Vertical
DIAM :
DATE :
DATE : 30-03-10

ELEVATION : N/A
X-COORD : N/A
Y-COORD : N/A

HOLE No: TH2

TYPE SET BY : SHEILA
SETUP FILE : k&t-hole.SET

DATE : 01/04/10 11:41
TEXT : ..\DATA\G20019-6.TXT

D016

dot.PLOT 4004 J&W

ERNIE ELS WINES

HOLE No: TH3
Sheet 1 of 1

JOB NUMBER: 20019GG

Scale 1:20

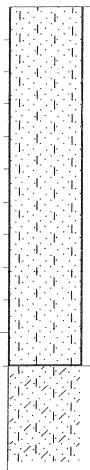

0.00 Slightly moist medium to dark brownish orange medium dense fissured silty SAND; TRANSPORTED (probably ALLUVIUM).

1.10

1.2m

Slightly moist light to medium brown dense fissured silty to clayey SAND; RESIDUAL.

NOTES

1) No groundwater encountered.

2) One undisturbed soil sample taken at 1.2m.

CONTRACTOR :
MACHINE :
DRILLED BY :
PROFILED BY : N. GILDENHUYS

TYPE SET BY : SHEILA
SETUP FILE : k&t-hole.SET

INCLINATION : Vertical
DIAM :
DATE :
DATE : 30-03-10

DATE : 01/04/10 11:42
TEXT : ..\DATA\G20019-7.TXT

ELEVATION : N/A
X-COORD : N/A
Y-COORD : N/A

HOLE No: TH3

D016

dot.PLOT 4004 J&W

JAMESTOWN CEMETERY

HOLE No: TH1
Sheet 1 of 1

JOB NUMBER: 20019GG

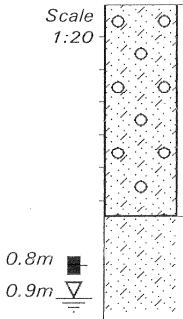

0.00 Very moist medium brown medium dense fissured gravelly to clayey SAND; TRANSPORTED (probably ALLUVIUM).

0.65 Wet light brown dense fissured clayey SAND; RESIDUAL.

NOTES

1) Perched water table at 0.9m.

2) One undisturbed soil sample taken at 0.8m.

CONTRACTOR :
MACHINE :
DRILLED BY :
PROFILED BY : N. GILDENHUYS
TYPE SET BY : SHEILA
SETUP FILE : k&t-hole.SET

INCLINATION : Vertical
DIAM :
DATE :
DATE : 30-03-10
DATE : 01/04/10 11:49
TEXT : ..\DATA\G20019~4.TXT

ELEVATION : N/A
X-COORD : N/A
Y-COORD : N/A

HOLE No: TH1

D016

dot.PLOT 4004 J&W

JAMESTOWN CEMETERY

HOLE No: TH2
Sheet 1 of 1

JOB NUMBER: 20019GG

Scale 1:20

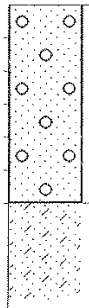

0.8m

0.00 Slightly moist dark brown mottled light brown loose fissured gravelly SAND; TRANSPORTED (probably ALLUVIUM).

0.60 Very moist medium browish orange dense fissured clayey SAND; RESIDUAL.

NOTES

1) No groundwater encountered.

2) One undisturbed soil sample taken at 0.8m.

CONTRACTOR :
MACHINE :
DRILLED BY :
PROFILED BY : N. GILDENHUYS
TYPE SET BY : SHEILA
SETUP FILE : k&t-hole.SET

INCLINATION : Vertical
DIAM :
DATE :
DATE : 30-03-10
DATE : 01/04/10 11:51
TEXT : ..\DATA\G2F5E9~1.TXT

ELEVATION : N/A
X-COORD : N/A
Y-COORD : N/A

HOLE No: TH2

D016

dot.PLOT 4004 J&W

JAMESTOWN CEMETERY

HOLE No: TH3
Sheet 1 of 1

JOB NUMBER: 20019GG

Scale 1:20

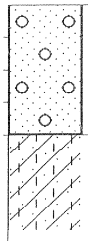

0.7m

0.00 Dry light brown loose fissured gravelly SAND; TRANSPORTED (probably ALLUVIUM).

0.40 Slightly moist light brownish orange soft fissured sandy to silty CLAY; RESIDUAL.

NOTES

1) No groundwater encountered.

2) One undisturbed soil sample taken at 0.7m.

CONTRACTOR :
MACHINE :
DRILLED BY :
PROFILED BY : N. GILDENHUYS

TYPE SET BY : SHEILA
SETUP FILE : k&t-hole.SET

INCLINATION : Vertical
DIAM :
DATE :
DATE : 30-03-10

DATE : 01/04/10 11:52
TEXT : ..\DATA\G2F9E9~1.TXT

ELEVATION : N/A
X-COORD : N/A
Y-COORD : N/A

HOLE No: TH3

D016

dot.PLOT 4004 J&W

Appendix B

Double oedometer testing

Data sheet

B-1: Audacia pit 1

Table B-1.1: Natural water content

Mass tin (g)	234.51
Mass tin + wet soil (g)	482.47
Mass tin + dry soil (g)	435.34
Water content (%)	23.47

Table B-1.2: Ring properties

Diameter (mm)	71.37
Mass (g)	83.40
Height (mm)	20

Table B-1.3: Consolidation test results for saturated sample

Pressure	Reading (mm)		ΔH	H	$H-H_s$	e
(kN/m^2)	start	end	(mm)	(mm)	(mm)	$(H-H_s)/H_s$
12.5	-	9.467	-	20.000	9.080	0.832
25	9.467	9.357	-0.110	19.890	8.970	0.821
50	9.357	9.071	-0.286	19.604	8.684	0.795
100	9.071	8.617	-0.454	19.150	8.230	0.754
200	8.617	8.057	-0.560	18.590	7.670	0.702
400	8.057	7.464	-0.593	17.997	7.077	0.648
800	7.464	6.861	-0.603	17.394	6.474	0.593
1600	6.861	6.157	-0.704	16.690	5.770	0.528
800	6.157	6.246	0.089	16.779	5.859	0.537
200	6.246	6.643	0.397	17.176	6.256	0.573
50	6.643	7.111	0.468	17.644	6.724	0.616

Table B-1.4: Consolidation test results for natural sample

Pressure	Reading (mm)		ΔH	H	$H-H_s$	e
(kN/m^2)	start	end	(mm)	(mm)	(mm)	$(H-H_s)/H_s$
12.5	-	9.315	-	20.000	9.530	0.910
25	9.315	9.136	-0.179	19.821	9.351	0.893
50	9.136	8.916	-0.220	19.601	9.131	0.872
100	8.916	8.644	-0.272	19.329	8.859	0.846
200	8.644	8.279	-0.365	18.964	8.494	0.811
400	8.279	7.582	-0.697	18.267	7.797	0.745
800	7.582	6.753	-0.829	17.438	6.968	0.666
1600	6.753	5.755	-0.998	16.440	5.970	0.570
800	5.755	5.820	0.065	16.505	6.035	0.576
200	5.820	5.985	0.165	16.670	6.200	0.592
50	5.985	6.052	0.067	16.737	6.267	0.599

Table B-1.5: Water content after test

Saturated sample		**Natural sample**	
Mass tin (g)	235.58	Mass tin (g)	234.51
Mass tin + wet specimen + ring (g)	470.22	Mass tin + wet specimen + ring (g)	455.23
Mass tin + dry specimen + ring (g)	437.31	Mass tin + dry specimen + ring (g)	431.38
Water content after test (%)	16.31	Water content after test (%)	12.11

Saturated sample:

$H_s = M_s/A/G_s\rho_w$ (mm) with

M_s = Mass dry specimen = 118.33g

$A = \pi D^2/4 = \pi(71.37)^2/4 = 4000mm^2$

$\rho_w = 10^{-3}$ g/mm^3
$G_s = 2.71$

Thus, H_s = 10.92 mm

Natural sample:

$H_s = M_s/A/G_s\rho_w$ (mm) with

M_s = Mass dry specimen = 113.47g

$A = \pi D^2/4 = \pi(71.37)^2/4 = 4000mm^2$

$\rho_w = 10^{-3}$ g/mm^3
$G_s = 2.71$

Thus, H_s = 10.47mm

B-2: Audacia pit 2

Table B-2.1: Natural water content

Mass tin (g)	179.27
Mass tin + wet soil (g)	379.20
Mass tin + dry soil (g)	336.27
Water content (%)	27.34

Table B-2.2: Ring properties

Diameter (mm)	71.37
Mass (g)	83.40
Height (mm)	20

Table B-2.3: Consolidation test results for saturated sample

Pressure	Reading (mm)		ΔH	H	$H-H_s$	e
(kN/m^2)	start	end	(mm)	(mm)	(mm)	$(H-H_s)/H_s$
12.5	-	9.509	-	20.000	9.330	0.874
25	9.509	9.394	-0.115	19.885	9.215	0.864
50	9.394	9.181	-0.213	19.672	9.002	0.844
100	9.181	8.841	-0.340	19.332	8.662	0.812
200	8.841	8.331	-0.510	18.822	8.152	0.764
400	8.331	7.745	-0.586	18.236	7.566	0.709
800	7.745	7.130	-0.615	17.621	6.951	0.651
1600	7.130	6.418	-0.712	16.909	6.239	0.585
800	6.418	6.490	0.072	16.981	6.311	0.591
200	6.490	6.779	0.289	17.270	6.600	0.619
50	6.779	7.119	0.340	17.610	6.940	0.650

Table B-2.4: Consolidation test results for natural sample

Pressure	Reading (mm)		ΔH	H	$H-H_s$	e
(kN/m^2)	start	end	(mm)	(mm)	(mm)	$(H-H_s)/H_s$
12.5	-	9.490	-	20.000	9.230	0.857
25	9.490	9.305	-0.185	19.815	9.045	0.840
50	9.305	9.142	-0.163	19.652	8.882	0.825
100	9.142	8.836	-0.306	19.346	8.576	0.796
200	8.836	8.483	-0.353	18.993	8.223	0.764
400	8.483	8.124	-0.359	18.634	7.864	0.730
800	8.124	7.406	-0.718	17.916	7.146	0.664
1600	7.406	6.406	-1.000	16.916	6.146	0.571
800	6.406	6.462	0.056	16.972	6.202	0.576
200	6.462	6.642	0.180	17.152	6.382	0.593
50	6.642	6.742	0.100	17.252	6.482	0.602

Table B-2.5: Water content after test

Saturated sample		**Natural sample**	
Mass tin (g)	179.30	Mass tin (g)	152.23
Mass tin + wet specimen + ring (g)	410.90	Mass tin + wet specimen + ring (g)	373.98
Mass tin + dry specimen + ring (g)	378.36	Mass tin + dry specimen + ring (g)	352.34
Water content after test (%)	16.35	Water content after test (%)	10.81

Saturated sample:

$H_s = M_s/A/G_s\rho_w$ (mm) with

M_s = Mass dry specimen = 115.66g

$A = \pi D^2/4 = \pi(71.37)^2/4 = 4000mm^2$

$\rho_w = 10^{-3}$ g/mm^3
$G_s = 2.71$

Thus, H_s = 10.67mm

Natural sample:

$H_s = M_s/A/G_s\rho_w$ (mm) with

M_s = Mass dry specimen = 116.71g

$A = \pi D^2/4 = \pi(71.37)^2/4 = 4000mm^2$

$\rho_w = 10^{-3}$ g/mm^3
$G_s = 2.71$

Thus, H_s = 10.77mm

B-3: Audacia pit 3

Table B-3.1: Natural water content

Mass tin (g)	179.28
Mass tin + wet soil (g)	401.47
Mass tin + dry soil (g)	356.31
Water content (%)	25.51

Table B-3.2: Ring properties of saturated sample

Diameter (mm)	70
Mass (g)	83.85
Height (mm)	19

Table B-3.3: Ring properties of natural sample

Diameter (mm)	71.37
Mass (g)	83.40
Height (mm)	20

Table B-3.4: Consolidation test results for saturated sample

Pressure	Reading (mm)		ΔH	H	$H-H_s$	e
(kN/m^2)	start	end	(mm)	(mm)	(mm)	$(H-H_s)/H_s$
12.5	-	9.726	-	19.000	9.290	0.957
25	9.726	9.607	-0.119	18.881	9.171	0.944
50	9.607	9.264	-0.343	18.538	8.828	0.909
100	9.264	8.835	-0.429	18.109	8.399	0.865
200	8.835	8.328	-0.507	17.602	7.892	0.813
400	8.328	7.631	-0.697	16.905	7.195	0.741
800	7.631	6.970	-0.661	16.244	6.534	0.673
1600	6.970	6.062	-0.908	15.336	5.626	0.579
800	6.062	6.127	0.065	15.401	5.691	0.586
200	6.127	6.511	0.384	15.785	6.075	0.626
50	6.511	6.999	0.488	16.273	6.563	0.676

Table B-3.5: Consolidation test results for natural sample

Pressure	Reading (mm)		ΔH	H	$H-H_s$	e
(kN/m^2)	start	end	(mm)	(mm)	(mm)	$(H-H_s)/H_s$
12.5	-	9.403	-	20.000	9.360	0.880
25	9.403	9.213	-0.190	19.810	9.170	0.862
50	9.213	9.027	-0.186	19.624	8.984	0.844
100	9.027	8.760	-0.267	19.357	8.717	0.819
200	8.760	8.393	-0.367	18.990	8.350	0.785
400	8.393	7.959	-0.434	18.556	7.916	0.744
800	7.959	7.388	-0.571	17.985	7.345	0.690
1600	7.388	6.291	-1.097	16.888	6.248	0.587
800	6.291	6.355	0.064	16.952	6.312	0.593
200	6.355	6.506	0.151	17.103	6.463	0.607
50	6.506	6.588	0.082	17.185	6.545	0.615

Table B-3.6: Water content after test

Saturated sample		**Natural sample**	
Mass tin (g)	152.17	Mass tin (g)	235.56
Mass tin + wet specimen + ring (g)	368.80	Mass tin + wet specimen + ring (g)	455.76
Mass tin + dry specimen + ring (g)	337.34	Mass tin + dry specimen + ring (g)	434.26
Water content after test (%)	17.0	Water content after test (%)	10.82

Saturated sample:

$H_s = M_s/A/G_s\rho_w$ (mm) with

M_s = Mass dry specimen = 101.32g

$A = \pi D^2/4 = \pi(70)^2/4 = 3848.45mm^2$

$\rho_w = 10^{-3}$ g/mm^3
$G_s = 2.71$

Thus, $H_s = 9.71$mm

Natural sample:

$H_s = M_s/A/G_s\rho_w$ (mm) with

M_s = Mass dry specimen = 115.3g

$A = \pi D^2/4 = \pi(71.37)^2/4 = 4000mm^2$

$\rho_w = 10^{-3}$ g/mm^3
$G_s = 2.71$

Thus, $H_s = 10.64$mm

B-4: Audacia pit 4

Table B-4.1: Natural water content

Mass tin (g)	234.56
Mass tin + wet soil (g)	476.43
Mass tin + dry soil (g)	447.62
Water content (%)	13.52

Table B-4.2: Ring properties of saturated sample

Diameter (mm)	71.37
Mass (g)	83.40
Height (mm)	20

Table B-4.3: Ring properties of natural sample

Diameter (mm)	70
Mass (g)	83.85
Height (mm)	19

Table B-4.4: Consolidation test results for saturated sample

Pressure	Reading (mm)		ΔH	H	$H-H_s$	e
(kN/m^2)	start	end	(mm)	(mm)	(mm)	$(H-H_s)/H_s$
12.5	-	9.417	-	20.000	6.640	0.497
25	9.417	9.259	-0.158	19.842	6.482	0.485
50	9.259	9.004	-0.255	19.587	6.227	0.466
100	9.004	8.599	-0.405	19.182	5.822	0.436
200	8.599	8.260	-0.339	18.843	5.483	0.410
400	8.260	7.854	-0.406	18.437	5.077	0.380
800	7.854	7.375	-0.479	17.958	4.598	0.344
1600	7.375	6.827	-0.548	17.410	4.050	0.303
800	6.827	6.862	0.035	17.445	4.085	0.306
200	6.862	6.983	0.121	17.566	4.206	0.315
50	6.983	7.116	0.133	17.699	4.339	0.325

Table B-4.5: Consolidation test results for natural sample

Pressure	Reading (mm)		ΔH	H	$H-H_s$	e
(kN/m^2)	start	end	(mm)	(mm)	(mm)	$(H-H_s)/H_s$
12.5	-	9.549	-	19.000	7.880	0.709
25	9.549	9.410	-0.139	18.861	7.741	0.696
50	9.410	9.294	-0.116	18.745	7.625	0.686
100	9.294	9.118	-0.176	18.569	7.449	0.670
200	9.118	8.944	-0.174	18.395	7.275	0.654
400	8.944	8.649	-0.295	18.100	6.980	0.628
800	8.649	8.312	-0.337	17.763	6.643	0.597
1600	8.312	7.846	-0.466	17.297	6.177	0.555
800	7.846	7.869	0.023	17.320	6.200	0.558
200	7.869	7.964	0.095	17.415	6.295	0.566
50	7.964	8.034	0.070	17.485	6.365	0.572

Table B-4.6: Water content after test

Saturated sample		**Natural sample**	
Mass tin (g)	235.57	Mass tin (g)	152.16
Mass tin + wet specimen + ring (g)	486.44	Mass tin + wet specimen + ring (g)	360.42
Mass tin + dry specimen + ring (g)	463.75	Mass tin + dry specimen + ring (g)	351.97
Water content after test (%)	9.94	Water content after test (%)	4.23

Saturated sample:

$H_s = M_s/A/G_s\rho_w$ (mm) with

M_s = Mass dry specimen = 144.78g

$A = \pi D^2/4 = \pi(71.37)^2/4 = 4000mm^2$

$\rho_w = 10^{-3}$ g/mm^3
$G_s = 2.71$

Thus, H_s = 13.36mm

Natural sample:

$H_s = M_s/A/G_s\rho_w$ (mm) with

M_s = Mass dry specimen = 115.96g

$A = \pi D^2/4 = \pi(70)^2/4 = 3848.45mm^2$

$\rho_w = 10^{-3}$ g/mm^3
$G_s = 2.71$

Thus, H_s = 11.12mm

B-5: Eikendal pit 1

Table B-5.1: Natural water content

Mass tin (g)	179.30
Mass tin + wet soil (g)	492.14
Mass tin + dry soil (g)	465.21
Water content (%)	9.42

Table B-5.2: Ring properties

Diameter (mm)	71.37
Mass (g)	83.40
Height (mm)	20

Table B-5.3: Consolidation test results for saturated sample

Pressure	Reading (mm)		ΔH	H	$H-H_s$	e
(kN/m^2)	start	end	(mm)	(mm)	(mm)	$(H-H_s)/H_s$
12.5	-	9.447	-	20.000	6.550	0.487
25	9.447	9.114	-0.333	19.667	6.217	0.462
50	9.114	8.806	-0.308	19.359	5.909	0.439
100	8.806	8.391	-0.415	18.944	5.494	0.408
200	8.391	7.971	-0.420	18.524	5.074	0.377
400	7.971	7.483	-0.488	18.036	4.586	0.341
800	7.483	6.978	-0.505	17.531	4.081	0.303
1600	6.978	6.369	-0.609	16.922	3.472	0.258
800	6.369	6.416	0.047	16.969	3.519	0.262
200	6.416	6.536	0.120	17.089	3.639	0.271
50	6.536	6.741	0.205	17.294	3.844	0.286

Table B-5.4: Consolidation test results for natural sample

Pressure	Reading (mm)		ΔH	H	$H-H_s$	e
(kN/m^2)	start	end	(mm)	(mm)	(mm)	$(H-H_s)/H_s$
12.5	-	9.321	-	20.000	7.900	0.653
25	9.321	9.123	-0.198	19.802	7.702	0.637
50	9.123	8.956	-0.167	19.635	7.535	0.623
100	8.956	8.662	-0.294	19.341	7.241	0.598
200	8.662	8.351	-0.311	19.030	6.930	0.573
400	8.351	8.000	-0.351	18.679	6.579	0.544
800	8.000	7.536	-0.464	18.215	6.115	0.505
1600	7.536	6.921	-0.615	17.600	5.500	0.455
800	6.921	6.942	0.021	17.621	5.521	0.456
200	6.942	7.023	0.081	17.702	5.602	0.463
50	7.023	7.095	0.072	17.774	5.674	0.469

Table B-5.5: Water content after test

Saturated sample		**Natural sample**	
Mass tin (g)	235.12	Mass tin (g)	152.13
Mass tin + wet specimen + ring (g)	483.67	Mass tin + wet specimen + ring (g)	383.16
Mass tin + dry specimen + ring (g)	464.28	Mass tin + dry specimen + ring (g)	366.72
Water content after test (%)	8.46	Water content after test (%)	7.66

Saturated sample:

$H_s = M_s/A/G_s\rho_w$ (mm) with

M_s = Mass dry specimen = 145.76g

$A = \pi D^2/4 = \pi(71.37)^2/4 = 4000mm^2$

$\rho_w = 10^{-3}$ g/mm^3
$G_s = 2.71$

Thus, H_s = 13.45mm

Natural sample:

$H_s = M_s/A/G_s\rho_w$ (mm) with

M_s = Mass dry specimen = 131.19g

$A = \pi D^2/4 = \pi(71.37)^2/4 = 4000mm^2$

$\rho_w = 10^{-3}$ g/mm^3
$G_s = 2.71$

Thus, H_s = 12.10mm

B-6: Eikendal pit 2

Table B-6.1: Natural water content

Mass tin (g)	152.24
Mass tin + wet soil (g)	361.65
Mass tin + dry soil (g)	350.82
Water content (%)	5.45

Table B-6.2: Ring properties

Diameter (mm)	71.37
Mass (g)	83.40
Height (mm)	20

Table B-6.3: Consolidation test results for saturated sample

Pressure	Reading (mm)		ΔH	H	$H-H_s$	e
(kN/m^2)	start	end	(mm)	(mm)	(mm)	$(H-H_s)/H_s$
12.5	-	9.176	-	20.000	5.080	0.340
25	9.176	8.978	-0.198	19.802	4.882	0.327
50	8.978	8.727	-0.251	19.551	4.631	0.310
100	8.727	8.477	-0.250	19.301	4.381	0.294
200	8.477	8.197	-0.280	19.021	4.101	0.275
400	8.197	7.874	-0.323	18.698	3.778	0.253
800	7.874	7.557	-0.317	18.381	3.461	0.232
1600	7.557	7.152	-0.405	17.976	3.056	0.205
800	7.152	7.195	0.043	18.019	3.099	0.208
200	7.195	7.300	0.105	18.124	3.204	0.215
50	7.300	7.366	0.066	18.190	3.270	0.219

Table B-6.4: Consolidation test results for natural sample

Pressure	Reading (mm)		ΔH	H	$H-H_s$	e
(kN/m^2)	start	end	(mm)	(mm)	(mm)	$(H-H_s)/H_s$
12.5	-	9.525	-	20.000	5.070	0.340
25	9.525	9.440	-0.085	19.915	4.985	0.334
50	9.440	9.372	-0.068	19.847	4.917	0.329
100	9.372	9.298	-0.074	19.773	4.843	0.324
200	9.298	9.176	-0.122	19.651	4.721	0.316
400	9.176	9.032	-0.144	19.507	4.577	0.307
800	9.032	8.833	-0.199	19.308	4.378	0.293
1600	8.833	8.513	-0.320	18.988	4.058	0.272
800	8.513	8.544	0.031	19.019	4.089	0.274
200	8.544	8.607	0.063	19.082	4.152	0.278
50	8.607	8.689	0.082	19.164	4.234	0.284

Table B-6.5: Water content after test

Saturated sample		**Natural sample**	
Mass tin (g)	179.27	Mass tin (g)	234.52
Mass tin + wet specimen + ring (g)	437.60	Mass tin + wet specimen + ring (g)	481.45
Mass tin + dry specimen + ring (g)	424.45	Mass tin + dry specimen + ring (g)	479.71
Water content after test (%)	5.36	Water content after test (%)	0.71

Saturated sample:

$H_s = M_s/A/G_s\rho_w$ (mm) with

M_s = Mass dry specimen = 161.78g

$A = \pi D^2/4 = \pi(71.37)^2/4 = 4000mm^2$

$\rho_w = 10^{-3}$ g/mm^3
$G_s = 2.71$

Thus, H_s = 14.92mm

Natural sample:

$H_s = M_s/A/G_s\rho_w$ (mm) with

M_s = Mass dry specimen = 161.79g

$A = \pi D^2/4 = \pi(71.37)^2/4 = 4000mm^2$

$\rho_w = 10^{-3}$ g/mm^3
$G_s = 2.71$

Thus, H_s = 14.93mm

B-7: Eikendal pit 3

Table B-7.1: Natural water content

Mass tin (g)	235.56
Mass tin + wet soil (g)	474.72
Mass tin + dry soil (g)	446.39
Water content (%)	13.44

Table B-7.2: Ring properties

Diameter (mm)	71.37
Mass (g)	83.40
Height (mm)	20

Table B-7.3: Consolidation test results for saturated sample

Pressure	Reading (mm)		ΔH	H	$H-H_s$	e
(kN/m^2)	start	end	(mm)	(mm)	(mm)	$(H-H_s)/H_s$
12.5	-	9.874	-	20.000	4.800	0.316
25	9.874	9.814	-0.060	19.940	4.740	0.312
50	9.814	9.721	-0.093	19.847	4.647	0.306
100	9.721	9.581	-0.140	19.707	4.507	0.297
200	9.581	9.413	-0.168	19.539	4.339	0.285
400	9.413	9.177	-0.236	19.303	4.103	0.270
800	9.177	8.923	-0.254	19.049	3.849	0.253
1600	8.923	8.567	-0.356	18.693	3.493	0.230
800	8.567	8.596	0.029	18.722	3.522	0.232
200	8.596	8.690	0.094	18.816	3.616	0.238
50	8.690	8.786	0.096	18.912	3.712	0.244

Table B-7.4: Consolidation test results for natural sample

Pressure	Reading (mm)		ΔH	H	$H-H_s$	e
(kN/m^2)	start	end	(mm)	(mm)	(mm)	$(H-H_s)/H_s$
12.5	-	9.800	-	20.000	5.960	0.425
25	9.800	9.720	-0.080	19.920	5.880	0.419
50	9.720	9.595	-0.125	19.795	5.755	0.410
100	9.595	9.466	-0.129	19.666	5.626	0.401
200	9.466	9.289	-0.177	19.489	5.449	0.388
400	9.289	9.095	-0.194	19.295	5.255	0.374
800	9.095	8.864	-0.231	19.064	5.024	0.358
1600	8.864	8.545	-0.319	18.745	4.705	0.335
800	8.545	8.575	0.030	18.775	4.735	0.337
200	8.575	8.632	0.057	18.832	4.792	0.341
50	8.632	8.720	0.088	18.920	4.880	0.348

Table B-7.5: Water content after test

Saturated sample		**Natural sample**	
Mass tin (g)	235.56	Mass tin (g)	152.19
Mass tin + wet specimen + ring (g)	500.18	Mass tin + wet specimen + ring (g)	390.91
Mass tin + dry specimen + ring (g)	483.70	Mass tin + dry specimen + ring (g)	387.77
Water content after test (%)	6.64	Water content after test (%)	1.33

Saturated sample:

$H_s = M_s/A/G_s\rho_w$ (mm) with

M_s = Mass dry specimen = 164.74g

$A = \pi D^2/4 = \pi(71.37)^2/4 = 4000mm^2$

$\rho_w = 10^{-3}$ g/mm^3
$G_s = 2.71$

Thus, H_s = 15.20mm

Natural sample:

$H_s = M_s/A/G_s\rho_w$ (mm) with

M_s = Mass dry specimen = 152.18g

$A = \pi D^2/4 = \pi(71.37)^2/4 = 4000mm^2$

$\rho_w = 10^{-3}$ g/mm^3
$G_s = 2.71$

Thus, H_s = 14.04mm

B-8: Eikendal pit 4

Table B-8.1: Natural water content

Mass tin (g)	152.23
Mass tin + wet soil (g)	450.18
Mass tin + dry soil (g)	395.71
Water content (%)	22.37

Table B-8.2: Ring properties of saturated sample

Diameter (mm)	70
Mass (g)	83.85
Height (mm)	19

Table B-8.3: Ring properties of natural sample

Diameter (mm)	71.37
Mass (g)	83.40
Height (mm)	20

Table B-8.4: Consolidation test results for saturated sample

Pressure	Reading (mm)		ΔH	H	$H-H_s$	e
(kN/m^2)	start	end	(mm)	(mm)	(mm)	$(H-H_s)/H_s$
12.5	-	9.519	-	19.000	8.420	0.796
25	9.519	9.416	-0.103	18.897	8.317	0.786
50	9.416	9.148	-0.268	18.629	8.049	0.761
100	9.148	8.680	-0.468	18.161	7.581	0.717
200	8.680	8.224	-0.456	17.705	7.125	0.673
400	8.224	7.729	-0.495	17.210	6.630	0.627
800	7.729	7.189	-0.540	16.670	6.090	0.576
1600	7.189	6.648	-0.541	16.129	5.549	0.524
800	6.648	6.743	0.095	16.224	5.644	0.533
200	6.743	7.151	0.408	16.632	6.052	0.572
50	7.151	7.656	0.505	17.137	6.557	0.620

Table B-8.5: Consolidation test results for natural sample

Pressure	Reading (mm)		ΔH	H	$H-H_s$	e
(kN/m^2)	start	end	(mm)	(mm)	(mm)	$(H-H_s)/H_s$
12.5	-	9.572	-	20.000	8.130	0.685
25	9.572	9.535	-0.037	19.963	8.093	0.682
50	9.535	9.365	-0.170	19.793	7.923	0.667
100	9.365	8.945	-0.420	19.373	7.503	0.632
200	8.945	8.450	-0.495	18.878	7.008	0.590
400	8.450	7.950	-0.500	18.378	6.508	0.548
800	7.950	7.339	-0.611	17.767	5.897	0.497
1600	7.339	6.742	-0.597	17.170	5.300	0.447
800	6.742	6.807	0.065	17.235	5.365	0.452
200	6.807	6.875	0.068	17.303	5.433	0.458
50	6.875	6.942	0.067	17.370	5.500	0.463

Table B-8.6: Water content after test

Saturated sample		**Natural sample**	
Mass tin (g)	234.51	Mass tin (g)	235.57
Mass tin + wet specimen + ring (g)	455.41	Mass tin + wet specimen + ring (g)	470.42
Mass tin + dry specimen + ring (g)	428.74	Mass tin + dry specimen + ring (g)	447.59
Water content after test (%)	13.73	Water content after test (%)	10.77

Saturated sample:

$H_s = M_s/A/G_s\rho_w$ (mm) with

M_s = Mass dry specimen = 110.38g

$A = \pi D^2/4 = \pi(70)^2/4 = 3848.45mm^2$

$\rho_w = 10^{-3}$ g/mm^3
$G_s = 2.71$

Thus, H_s = 10.58mm

Natural sample:

$H_s = M_s/A/G_s\rho_w$ (mm) with

M_s = Mass dry specimen = 128.62g

$A = \pi D^2/4 = \pi(71.37)^2/4 = 4000mm^2$

$\rho_w = 10^{-3}$ g/mm^3
$G_s = 2.71$

Thus, H_s = 11.87mm

B-9: Ernie Els pit 1

Table B-9.1: Natural water content

Mass tin (g)	152.14
Mass tin + wet soil (g)	436.83
Mass tin + dry soil (g)	391.95
Water content (%)	18.71

Table B-9.2: Ring properties of saturated sample

Diameter (mm)	70
Mass (g)	83.85
Height (mm)	19

Table B-9.3: Ring properties of natural sample

Diameter (mm)	71.37
Mass (g)	83.40
Height (mm)	20

Table B-9.4: Consolidation test results for saturated sample

Pressure	Reading (mm)		ΔH	H	$H-H_s$	e
(kN/m^2)	start	end	(mm)	(mm)	(mm)	$(H-H_s)/H_s$
12.5	-	8.749	-	19.000	9.780	1.061
25	8.749	8.440	-0.309	18.691	9.471	1.027
50	8.440	7.989	-0.451	18.240	9.020	0.978
100	7.989	7.434	-0.555	17.685	8.465	0.918
200	7.434	6.808	-0.626	17.059	7.839	0.850
400	6.808	6.069	-0.739	16.320	7.100	0.770
800	6.069	5.367	-0.702	15.618	6.398	0.694
1600	5.367	4.717	-0.650	14.968	5.748	0.623
800	4.717	4.756	0.039	15.007	5.787	0.628
200	4.756	4.918	0.162	15.169	5.949	0.645
50	4.918	5.040	0.122	15.291	6.071	0.658

Table B-9.5: Consolidation test results for natural sample

Pressure	Reading (mm)		ΔH	H	$H-H_s$	e
(kN/m^2)	start	end	(mm)	(mm)	(mm)	$(H-H_s)/H_s$
12.5	-	9.560	-	20.000	8.880	0.799
25	9.560	9.473	-0.087	19.913	8.793	0.791
50	9.473	9.265	-0.208	19.705	8.585	0.772
100	9.265	8.960	-0.305	19.400	8.280	0.745
200	8.960	8.780	-0.180	19.220	8.100	0.728
400	8.780	8.424	-0.356	18.864	7.744	0.696
800	8.424	8.015	-0.409	18.455	7.335	0.660
1600	8.015	7.414	-0.601	17.854	6.734	0.606
800	7.414	7.451	0.037	17.891	6.771	0.609
200	7.451	7.557	0.106	17.997	6.877	0.618
50	7.557	7.633	0.076	18.073	6.953	0.625

Table B-9.6: Water content after test

Saturated sample		**Natural sample**	
Mass tin (g)	179.26	Mass tin (g)	234.55
Mass tin + wet specimen + ring (g)	380.39	Mass tin + wet specimen + ring (g)	447.70
Mass tin + dry specimen + ring (g)	359.26	Mass tin + dry specimen + ring (g)	438.48
Water content after test (%)	11.74	Water content after test (%)	4.52

Saturated sample:

$H_s = M_s/A/G_s\rho_w$ (mm) with

M_s = Mass dry specimen = 96.15g

$A = \pi D^2/4 = \pi(70)^2/4 = 3848.45mm^2$

$\rho_w = 10^{-3}$ g/mm^3
$G_s = 2.71$

Thus, $H_s = 9.22$mm

Natural sample:

$H_s = M_s/A/G_s\rho_w$ (mm) with

M_s = Mass dry specimen = 120.53g

$A = \pi D^2/4 = \pi(71.37)^2/4 = 4000mm^2$

$\rho_w = 10^{-3}$ g/mm^3
$G_s = 2.71$

Thus, $H_s = 11.12$mm

B-10: Ernie Els pit 2

Table B-10.1: Natural water content

Mass tin (g)	235.57
Mass tin + wet soil (g)	524.92
Mass tin + dry soil (g)	475.07
Water content (%)	20.81

Table B-10.2: Ring properties

Diameter (mm)	71.37
Mass (g)	83.40
Height (mm)	20

Table B-10.3: Consolidation test results for saturated sample

Pressure	Reading (mm)		ΔH	H	$H-H_s$	e
(kN/m^2)	start	end	(mm)	(mm)	(mm)	$(H-H_s)/H_s$
12.5	-	9.017	-	20.000	8.220	0.698
25	9.017	8.888	-0.129	19.871	8.091	0.687
50	8.888	8.655	-0.233	19.638	7.858	0.667
100	8.655	8.336	-0.319	19.319	7.539	0.640
200	8.336	7.904	-0.432	18.887	7.107	0.603
400	7.904	7.368	-0.536	18.351	6.571	0.558
800	7.368	6.771	-0.597	17.754	5.974	0.507
1600	6.771	6.082	-0.689	17.065	5.285	0.449
800	6.082	6.137	0.055	17.120	5.340	0.453
200	6.137	6.345	0.208	17.328	5.548	0.471
50	6.345	6.542	0.197	17.525	5.745	0.488

Table B-10.4: Consolidation test results for natural sample

Pressure	Reading (mm)		ΔH	H	$H-H_s$	e
(kN/m^2)	start	end	(mm)	(mm)	(mm)	$(H-H_s)/H_s$
12.5	-	9.816	-	20.000	8.470	0.735
25	9.816	9.756	-0.060	19.940	8.410	0.729
50	9.756	9.590	-0.166	19.774	8.244	0.715
100	9.590	9.435	-0.155	19.619	8.089	0.702
200	9.435	9.136	-0.299	19.320	7.790	0.676
400	9.136	8.854	-0.282	19.038	7.508	0.651
800	8.854	8.536	-0.318	18.720	7.190	0.624
1600	8.536	8.028	-0.508	18.212	6.682	0.580
800	8.028	8.069	0.041	18.253	6.723	0.583
200	8.069	8.171	0.102	18.355	6.825	0.592
50	8.171	8.229	0.058	18.413	6.883	0.597

Table B-10.5: Water content after test

Saturated sample		**Natural sample**	
Mass tin (g)	234.56	Mass tin (g)	235.57
Mass tin + wet specimen + ring (g)	475.88	Mass tin + wet specimen + ring (g)	456.98
Mass tin + dry specimen + ring (g)	445.62	Mass tin + dry specimen + ring (g)	443.92
Water content after test (%)	14.34	Water content after test (%)	6.27

Saturated sample:

$H_s = M_s/A/G_s\rho_w$ (mm) with

M_s = Mass dry specimen = 127.66g

$A = \pi D^2/4 = \pi(71.37)^2/4 = 4000mm^2$

$\rho_w = 10^{-3}$ g/mm^3
$G_s = 2.71$

Thus, H_s = 11.78mm

Natural sample:

$H_s = M_s/A/G_s\rho_w$ (mm) with

M_s = Mass dry specimen = 124.95g

$A = \pi D^2/4 = \pi(71.37)^2/4 = 4000mm^2$

$\rho_w = 10^{-3}$ g/mm^3
$G_s = 2.71$

Thus, H_s = 11.53mm

B-11: Ernie Els pit 3

Table B-11.1: Natural water content

Mass tin (g)	179.33
Mass tin + wet soil (g)	475.30
Mass tin + dry soil (g)	432.24
Water content (%)	17.03

Table B-11.2: Ring properties

Diameter (mm)	71.37
Mass (g)	83.40
Height (mm)	20

Table B-11.3: Consolidation test results for saturated sample

Pressure	Reading (mm)		ΔH	H	$H-H_s$	e
(kN/m^2)	start	end	(mm)	(mm)	(mm)	$(H-H_s)/H_s$
12.5	-	8.614	-	20.000	8.940	0.808
25	8.614	8.289	-0.325	19.675	8.615	0.779
50	8.289	7.894	-0.395	19.280	8.220	0.743
100	7.894	7.377	-0.517	18.763	7.703	0.696
200	7.377	6.698	-0.679	18.084	7.024	0.635
400	6.698	5.907	-0.791	17.293	6.233	0.564
800	5.907	5.149	-0.758	16.535	5.475	0.495
1600	5.149	4.428	-0.721	15.814	4.754	0.430
800	4.428	4.481	0.053	15.867	4.807	0.435
200	4.481	4.640	0.159	16.026	4.966	0.449
50	4.640	4.831	0.191	16.217	5.157	0.466

Table B-11.4: Consolidation test results for natural sample

Pressure	Reading (mm)		ΔH	H	$H-H_s$	e
(kN/m^2)	start	end	(mm)	(mm)	(mm)	$(H-H_s)/H_s$
12.5	-	9.174	-	20.000	8.600	0.754
25	9.174	9.013	-0.161	19.839	8.439	0.740
50	9.013	8.827	-0.186	19.653	8.253	0.724
100	8.827	8.491	-0.336	19.317	7.917	0.694
200	8.491	8.160	-0.331	18.986	7.586	0.665
400	8.160	7.627	-0.533	18.453	7.053	0.619
800	7.627	7.110	-0.517	17.936	6.536	0.573
1600	7.110	6.127	-0.983	16.953	5.553	0.487
800	6.127	6.184	0.057	17.010	5.610	0.492
200	6.184	6.221	0.037	17.047	5.647	0.495
50	6.221	6.276	0.055	17.102	5.702	0.500

Table B-11.5: Water content after test

Saturated sample		**Natural sample**	
Mass tin (g)	235.57	Mass tin (g)	234.53
Mass tin + wet specimen + ring (g)	463.20	Mass tin + wet specimen + ring (g)	452.99
Mass tin + dry specimen + ring (g)	438.82	Mass tin + dry specimen + ring (g)	441.45
Water content after test (%)	12.0	Water content after test (%)	5.80

Saturated sample:

$H_s = M_s/A/G_s\rho_w$ (mm) with

M_s = Mass dry specimen = 119.85g

$A = \pi D^2/4 = \pi(71.37)^2/4 = 4000mm^2$

$\rho_w = 10^{-3}$ g/mm^3
$G_s = 2.71$

Thus, H_s = 11.06mm

Natural sample:

$H_s = M_s/A/G_s\rho_w$ (mm) with

M_s = Mass dry specimen = 123.52g

$A = \pi D^2/4 = \pi(71.37)^2/4 = 4000mm^2$

$\rho_w = 10^{-3}$ g/mm^3
$G_s = 2.71$

Thus, H_s = 11.40mm

B-12: Jamestown pit 1

Table B-12.1: Natural water content

Mass tin (g)	234.53
Mass tin + wet soil (g)	514.85
Mass tin + dry soil (g)	480.06
Water content (%)	14.17

Table B-12.2: Ring properties

Diameter (mm)	71.37
Mass (g)	83.40
Height (mm)	20

Table B-12.3: Consolidation test results for saturated sample

Pressure	Reading (mm)		ΔH	H	$H-H_s$	e
(kN/m^2)	start	end	(mm)	(mm)	(mm)	$(H-H_s)/H_s$
12.5	-	9.109	-	20.000	7.020	0.541
25	9.109	8.921	-0.188	19.812	6.832	0.526
50	8.921	8.634	-0.287	19.525	6.545	0.504
100	8.634	8.240	-0.394	19.131	6.151	0.474
200	8.240	7.738	-0.502	18.629	5.649	0.435
400	7.738	7.148	-0.590	18.039	5.059	0.390
800	7.148	6.587	-0.561	17.478	4.498	0.347
1600	6.587	6.030	-0.557	16.921	3.941	0.304
800	6.030	6.072	0.042	16.963	3.983	0.307
200	6.072	6.179	0.107	17.070	4.090	0.315
50	6.179	6.264	0.085	17.155	4.175	0.322

Table B-12.4: Consolidation test results for natural sample

Pressure	Reading (mm)		ΔH	H	$H-H_s$	e
(kN/m^2)	start	end	(mm)	(mm)	(mm)	$(H-H_s)/H_s$
12.5	-	9.807	-	20.000	6.460	0.477
25	9.807	9.744	-0.063	19.937	6.397	0.472
50	9.744	9.667	-0.077	19.860	6.320	0.467
100	9.667	9.552	-0.115	19.745	6.205	0.458
200	9.552	9.424	-0.128	19.617	6.077	0.449
400	9.424	9.168	-0.256	19.361	5.821	0.430
800	9.168	8.883	-0.285	19.076	5.536	0.409
1600	8.883	8.445	-0.438	18.638	5.098	0.377
800	8.445	8.473	0.028	18.666	5.126	0.379
200	8.473	8.536	0.063	18.729	5.189	0.383
50	8.536	8.607	0.071	18.800	5.260	0.388

Table B-12.5: Water content after test

Saturated sample		**Natural sample**	
Mass tin (g)	179.25	Mass tin (g)	179.25
Mass tin + wet specimen + ring (g)	421.28	Mass tin + wet specimen + ring (g)	411.25
Mass tin + dry specimen + ring (g)	403.33	Mass tin + dry specimen + ring (g)	409.40
Water content after test (%)	8.01	Water content after test (%)	0.80

Saturated sample:

$H_s = M_s/A/G_s\rho_w$ (mm) with

M_s = Mass dry specimen = 140.68g

$A = \pi D^2/4 = \pi(71.37)^2/4 = 4000mm^2$

$\rho_w = 10^{-3}$ g/mm^3
$G_s = 2.71$

Thus, H_s = 12.98mm

Natural sample:

$H_s = M_s/A/G_s\rho_w$ (mm) with

M_s = Mass dry specimen = 146.75g

$A = \pi D^2/4 = \pi(71.37)^2/4 = 4000mm^2$

$\rho_w = 10^{-3}$ g/mm^3
$G_s = 2.71$

Thus, H_s = 13.54mm

B-13: Jamestown pit 2

Table B-13.1: Natural water content

Mass tin (g)	235.56
Mass tin + wet soil (g)	482.44
Mass tin + dry soil (g)	450.64
Water content (%)	14.79

Table B-13.2: Ring properties

Diameter (mm)	71.37
Mass (g)	83.40
Height (mm)	20

Table B-13.3: Consolidation test results for saturated sample

Pressure	Reading (mm)		ΔH	H	$H-H_s$	e
(kN/m^2)	start	end	(mm)	(mm)	(mm)	$(H-H_s)/H_s$
12.5	-	9.346	-	20.000	6.870	0.523
25	9.346	9.107	-0.239	19.761	6.631	0.505
50	9.107	8.806	-0.301	19.460	6.330	0.482
100	8.806	8.463	-0.343	19.117	5.987	0.456
200	8.463	8.059	-0.404	18.713	5.583	0.425
400	8.059	7.638	-0.421	18.292	5.162	0.393
800	7.638	7.141	-0.497	17.795	4.665	0.355
1600	7.141	6.645	-0.496	17.299	4.169	0.318
800	6.645	6.688	0.043	17.342	4.212	0.321
200	6.688	6.839	0.151	17.493	4.363	0.332
50	6.839	7.027	0.188	17.681	4.551	0.347

Table B-13.4: Consolidation test results for natural sample

Pressure	Reading (mm)		ΔH	H	$H-H_s$	e
(kN/m^2)	start	end	(mm)	(mm)	(mm)	$(H-H_s)/H_s$
12.5	-	9.253	-	20.000	7.330	0.579
25	9.253	9.065	-0.188	19.812	7.142	0.564
50	9.065	8.890	-0.175	19.637	6.967	0.550
100	8.890	8.737	-0.153	19.484	6.814	0.538
200	8.737	8.535	-0.202	19.282	6.612	0.522
400	8.535	8.294	-0.241	19.041	6.371	0.503
800	8.294	7.859	-0.435	18.606	5.936	0.469
1600	7.859	7.416	-0.443	18.163	5.493	0.434
800	7.416	7.445	0.029	18.192	5.522	0.436
200	7.445	7.522	0.077	18.269	5.599	0.442
50	7.522	7.588	0.066	18.335	5.665	0.447

Table B-13.5: Water content after test

Saturated sample		**Natural sample**	
Mass tin (g)	235.69	Mass tin (g)	234.55
Mass tin + wet specimen + ring (g)	483.53	Mass tin + wet specimen + ring (g)	468.93
Mass tin + dry specimen + ring (g)	461.42	Mass tin + dry specimen + ring (g)	455.33
Water content after test (%)	9.79	Water content after test (%)	6.16

Saturated sample:

$H_s = M_s/A/G_s\rho_w$ (mm) with

M_s = Mass dry specimen = 142.33g

$A = \pi D^2/4 = \pi(71.37)^2/4 = 4000mm^2$

$\rho_w = 10^{-3}$ g/mm^3
$G_s = 2.71$

Thus, H_s = 13.13mm

Natural sample:

$H_s = M_s/A/G_s\rho_w$ (mm) with

M_s = Mass dry specimen = 137.38g

$A = \pi D^2/4 = \pi(71.37)^2/4 = 4000mm^2$

$\rho_w = 10^{-3}$ g/mm^3
$G_s = 2.71$

Thus, H_s = 12.67mm

B-14: Jamestown pit 3

Table B-14.1: Natural water content

Mass tin (g)	179.24
Mass tin + wet soil (g)	416.92
Mass tin + dry soil (g)	369.42
Water content (%)	25.0

Table B-14.2: Ring properties

Diameter (mm)	71.37
Mass (g)	83.40
Height (mm)	20

Table B-14.3: Consolidation test results for saturated sample

Pressure	Reading (mm)		ΔH	H	$H-H_s$	e
(kN/m^2)	start	end	(mm)	(mm)	(mm)	$(H-H_s)/H_s$
12.5	-	9.001	-	20.000	8.160	0.689
25	9.001	8.942	-0.059	19.941	8.101	0.684
50	8.942	8.795	-0.147	19.794	7.954	0.672
100	8.795	8.539	-0.256	19.538	7.698	0.650
200	8.539	8.234	-0.305	19.233	7.393	0.624
400	8.234	7.823	-0.411	18.822	6.982	0.590
800	7.823	7.339	-0.484	18.338	6.498	0.549
1600	7.339	6.730	-0.609	17.729	5.889	0.497
800	6.730	6.801	0.071	17.800	5.960	0.503
200	6.801	6.952	0.151	17.951	6.111	0.516
50	6.952	7.110	0.158	18.109	6.269	0.529

Table B-14.4: Consolidation test results for natural sample

Pressure	Reading (mm)		ΔH	H	$H-H_s$	e
(kN/m^2)	start	end	(mm)	(mm)	(mm)	$(H-H_s)/H_s$
12.5	-	9.470	-	20.000	8.560	0.748
25	9.470	9.362	-0.108	19.892	8.452	0.739
50	9.362	9.149	-0.213	19.679	8.239	0.720
100	9.149	8.942	-0.207	19.472	8.032	0.702
200	8.942	8.633	-0.309	19.163	7.723	0.675
400	8.633	8.347	-0.286	18.877	7.437	0.650
800	8.347	7.859	-0.488	18.389	6.949	0.607
1600	7.859	7.394	-0.465	17.924	6.484	0.567
800	7.394	7.396	0.002	17.926	6.486	0.567
200	7.396	7.468	0.072	17.998	6.558	0.573
50	7.468	7.526	0.058	18.056	6.616	0.578

Table B-14.5: Water content after test

Saturated sample		**Natural sample**	
Mass tin (g)	235.58	Mass tin (g)	234.58
Mass tin + wet specimen + ring (g)	478.42	Mass tin + wet specimen + ring (g)	460.28
Mass tin + dry specimen + ring (g)	447.36	Mass tin + dry specimen + ring (g)	441.96
Water content after test (%)	14.67	Water content after test (%)	8.83

Saturated sample:

$H_s = M_s/A/G_s\rho_w$ (mm) with

M_s = Mass dry specimen = 128.38g

$A = \pi D^2/4 = \pi(71.37)^2/4 = 4000mm^2$

$\rho_w = 10^{-3}$ g/mm^3
$G_s = 2.71$

Thus, H_s = 11.84mm

Natural sample:

$H_s = M_s/A/G_s\rho_w$ (mm) with

M_s = Mass dry specimen = 123.98g

$A = \pi D^2/4 = \pi(71.37)^2/4 = 4000mm^2$

$\rho_w = 10^{-3}$ g/mm^3
$G_s = 2.71$

Thus, H_s = 11.44mm

Appendix C

Shear strength testing

C-1: Shear resistance versus shear displacement graphs

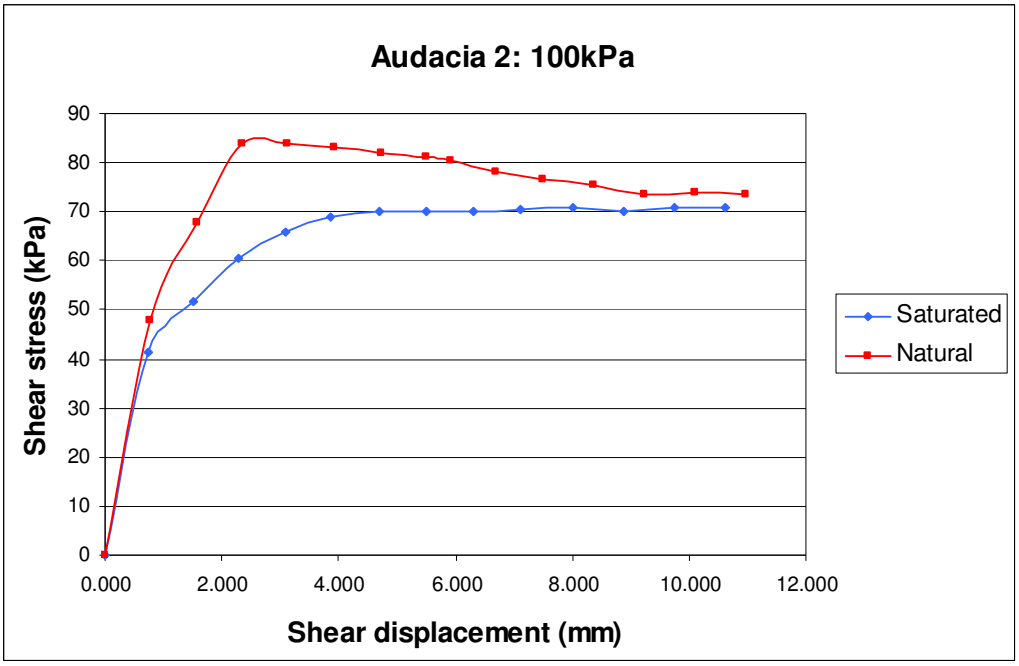

Figure C-1.1: Shear stress versus shear displacement of Audcia pit 2

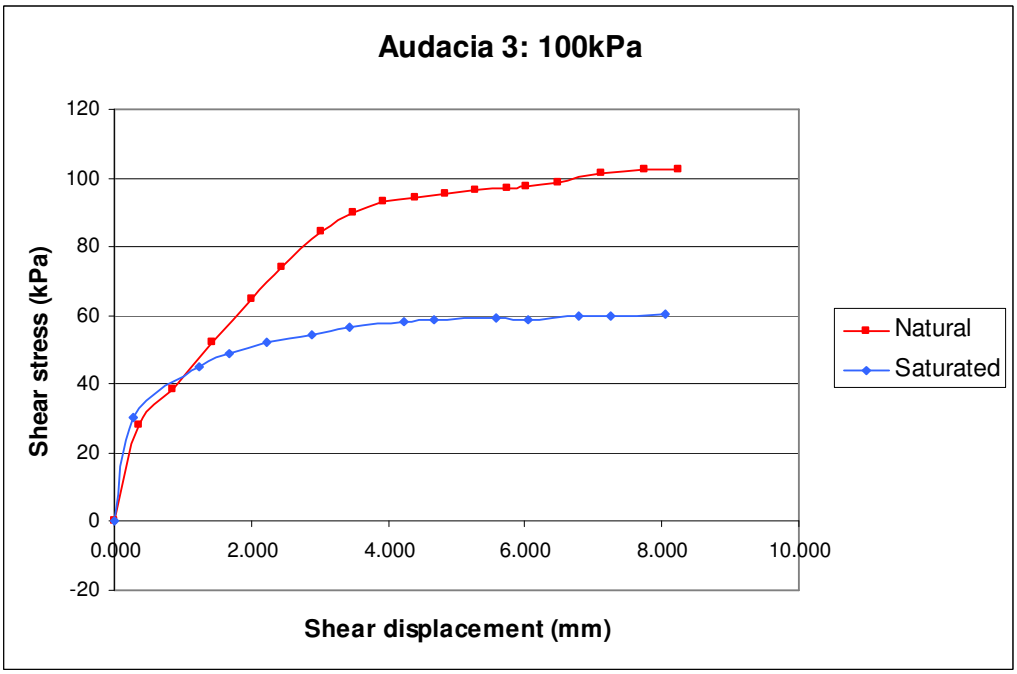

Figure C-1.2: Shear stress versus shear displacement of Audcia pit 3

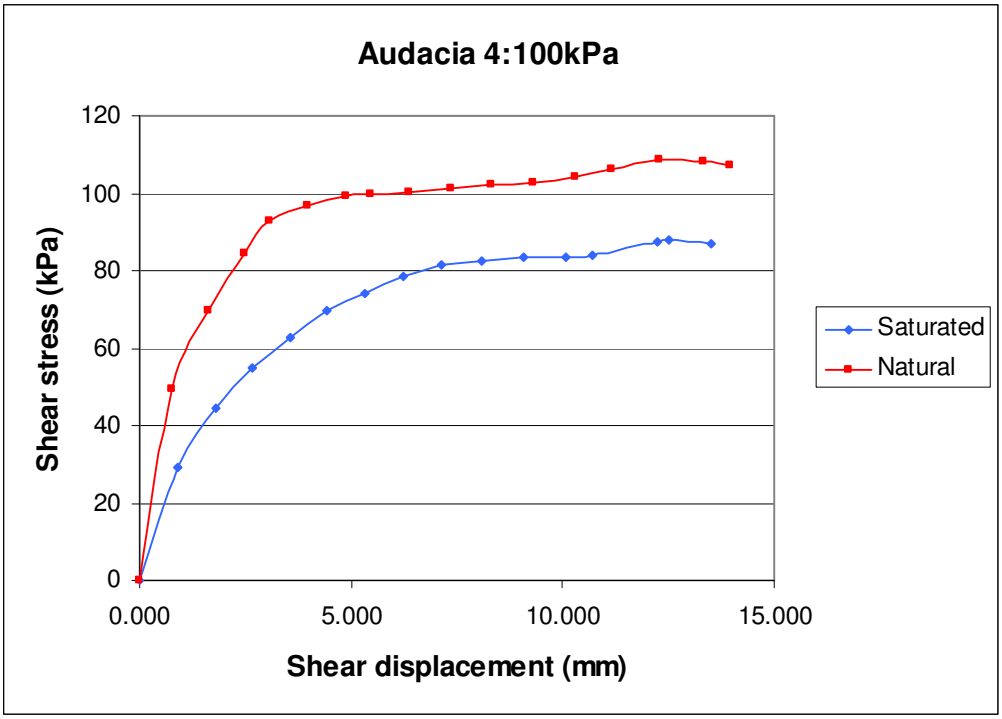

Figure C-1.3: Shear stress versus shear displacement of Audcia pit 4

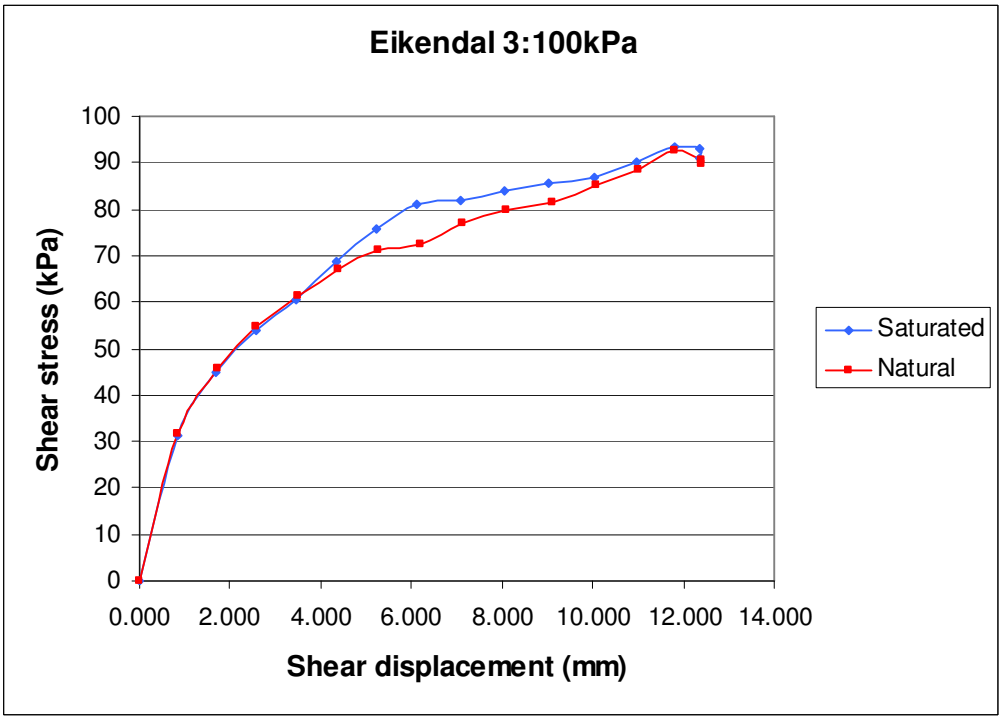

Figure C-1.4: Shear stress versus shear displacement of Eikendal pit 3

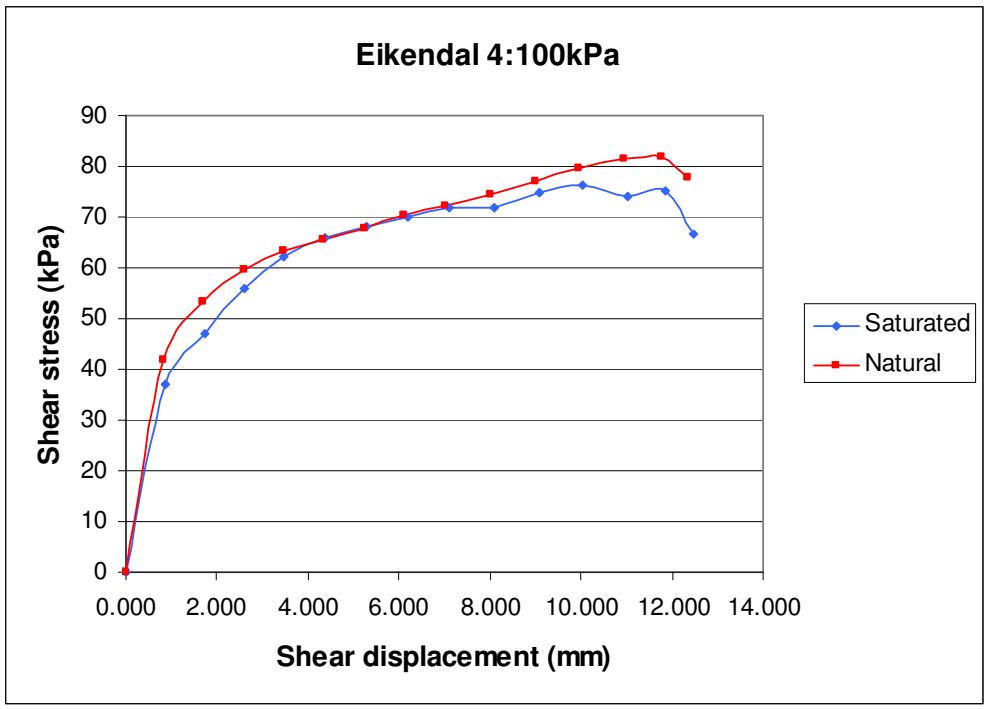

Figure C-1.5: Shear stress versus shear displacement of Eikendal pit 4

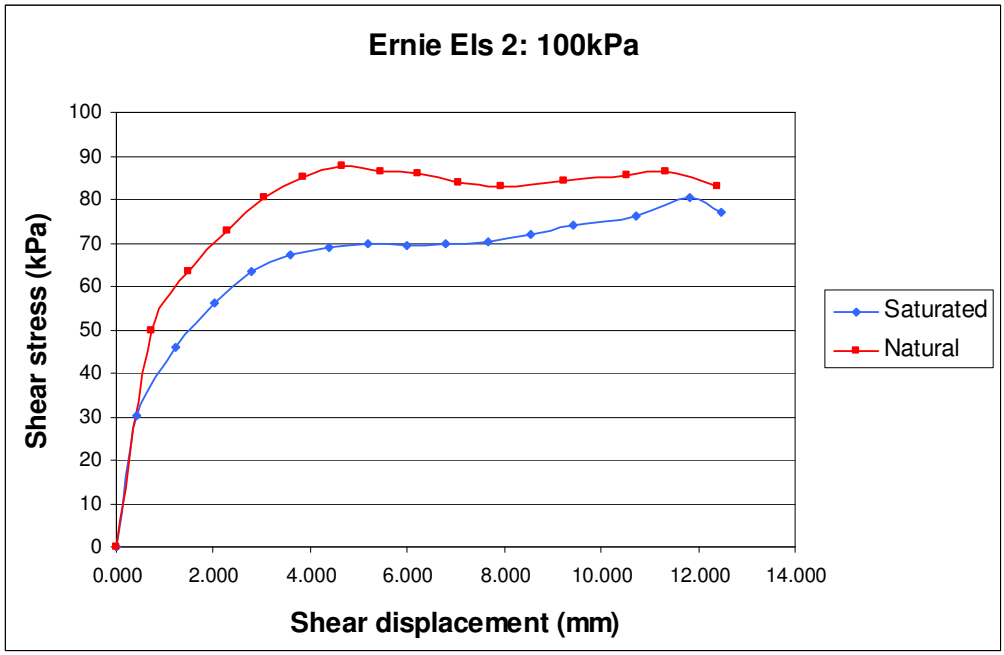

Figure C-1.6: Shear stress versus shear displacement of Ernie Els pit 2

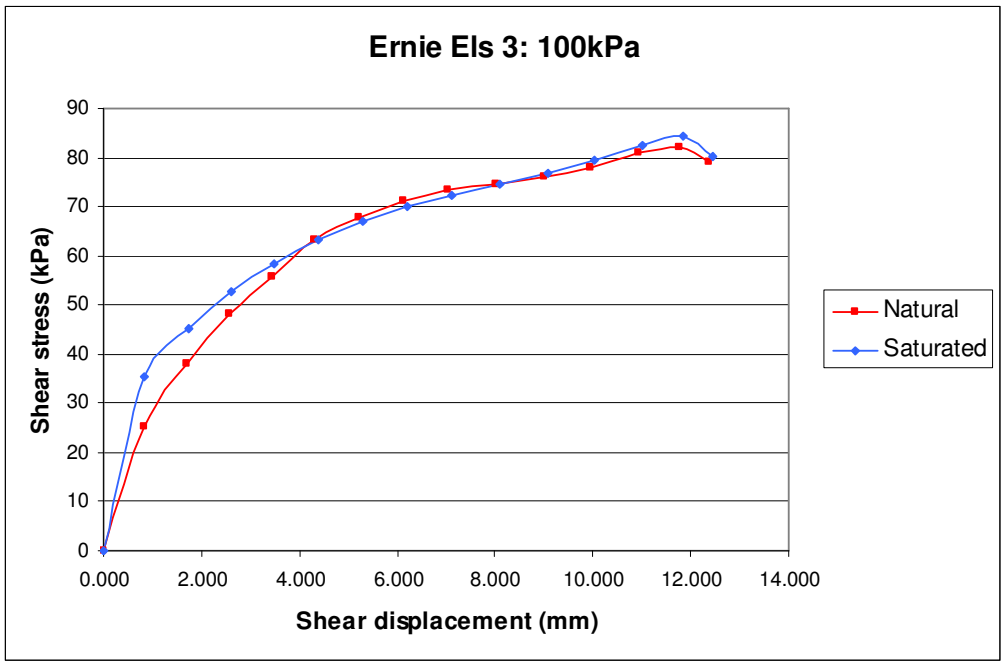

Figure C-1.7: Shear stress versus shear displacement of Ernie Els pit 3

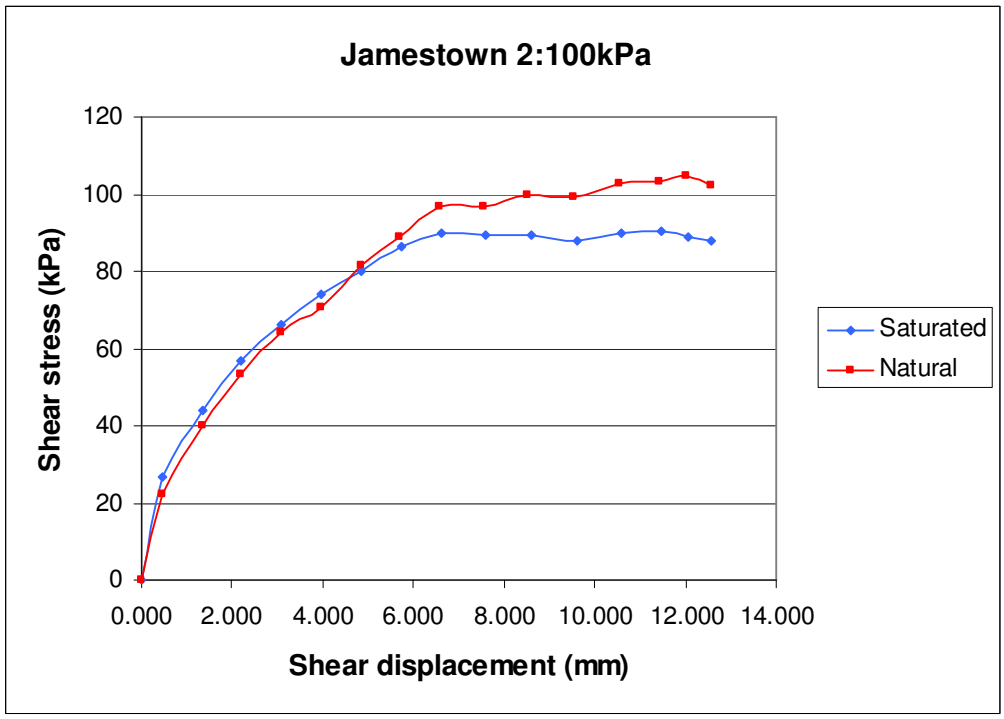

Figure C-1.8: Shear stress versus shear displacement of Jamestown pit 2

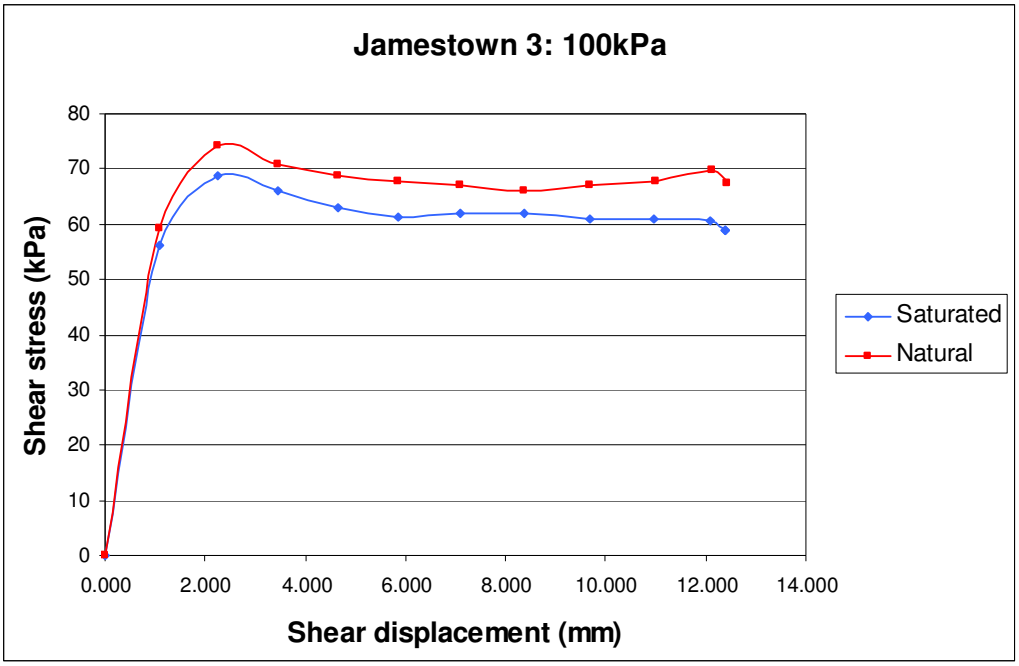

Figure C-1.9: Shear stress versus shear displacement of Jamestown pit 3

C-2: Vertical deformation versus shear displacement graphs

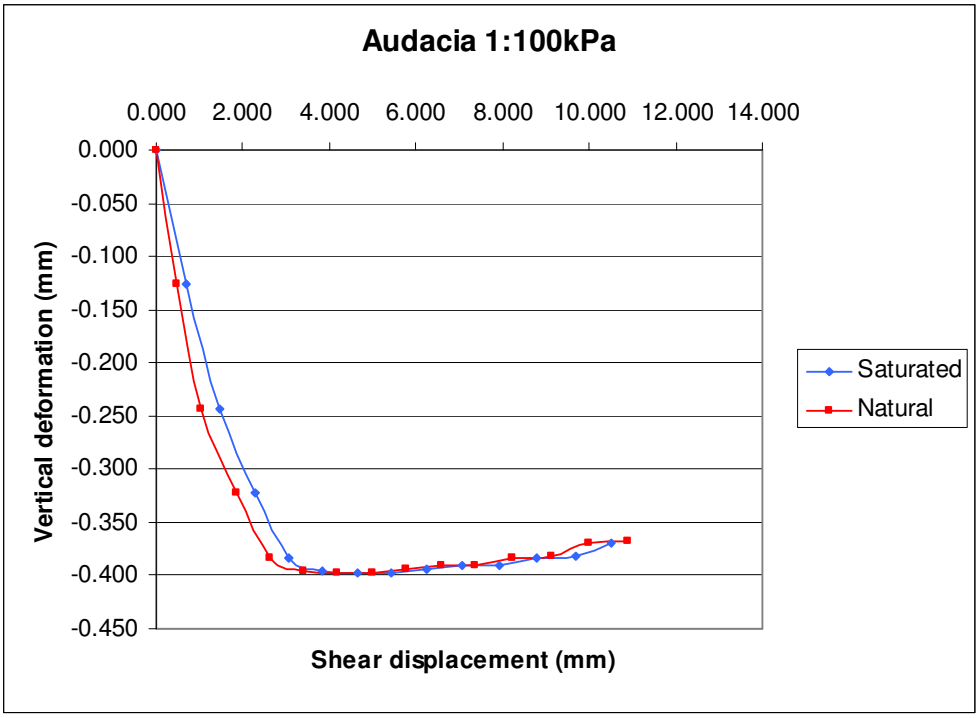

Figure C-2.1: Vertical deformation versus shear displacement of Audacia pit 1

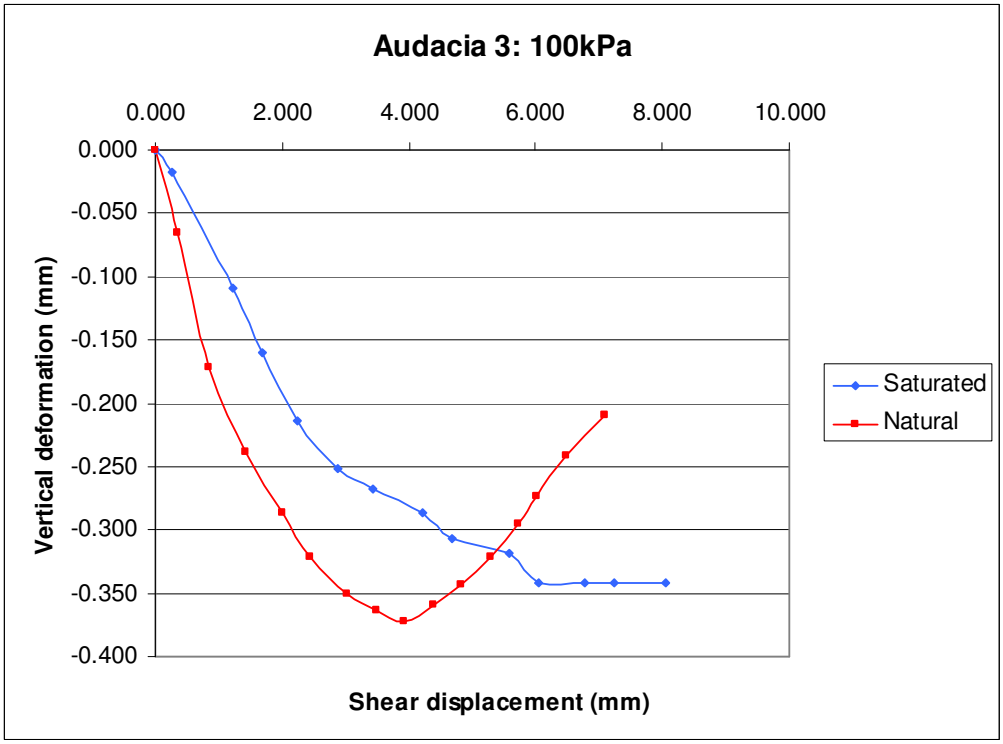

Figure C-2.2: Vertical deformation versus shear displacement of Audacia pit 3

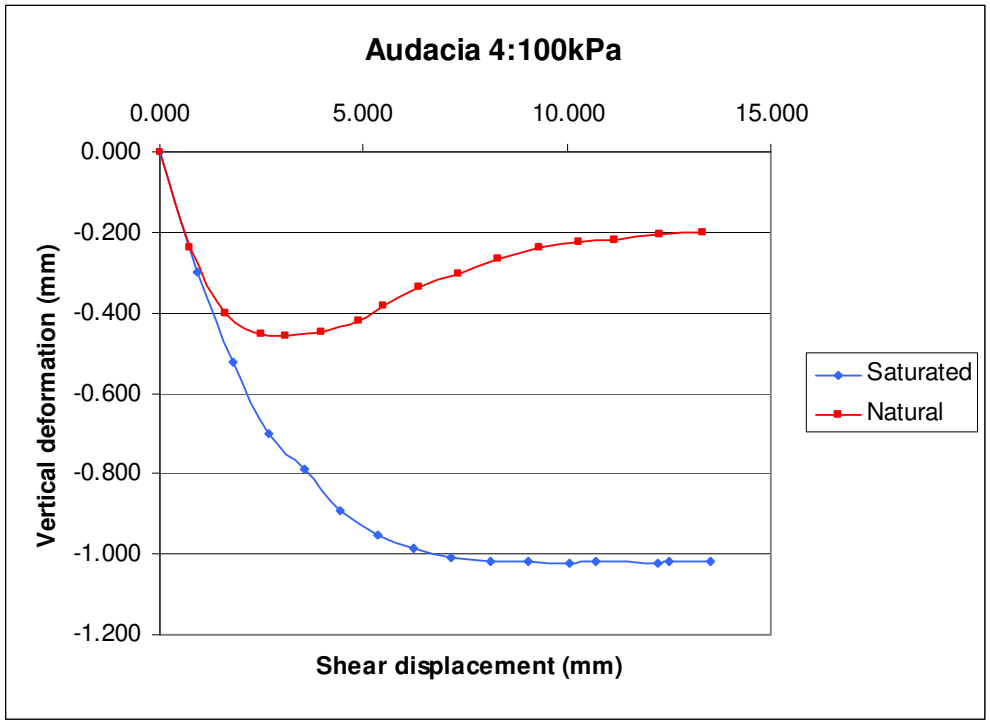

Figure C-2.3: Vertical deformation versus shear displacement of Audacia pit 4

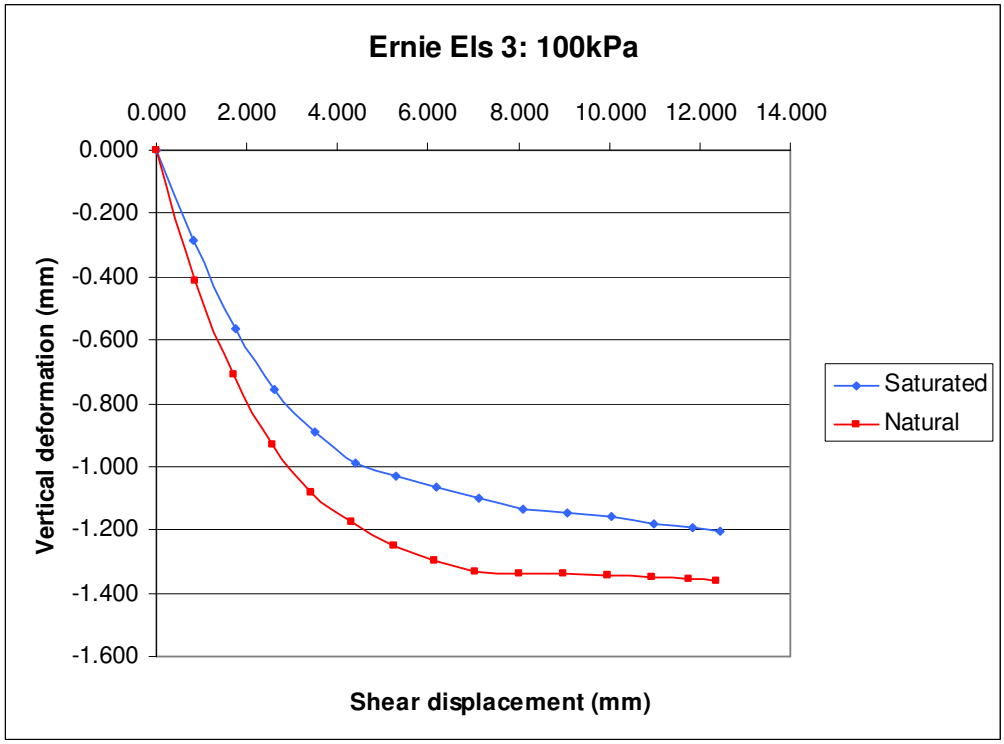

Figure C-2.4: Vertical deformation versus shear displacement of Ernie Els pit 3

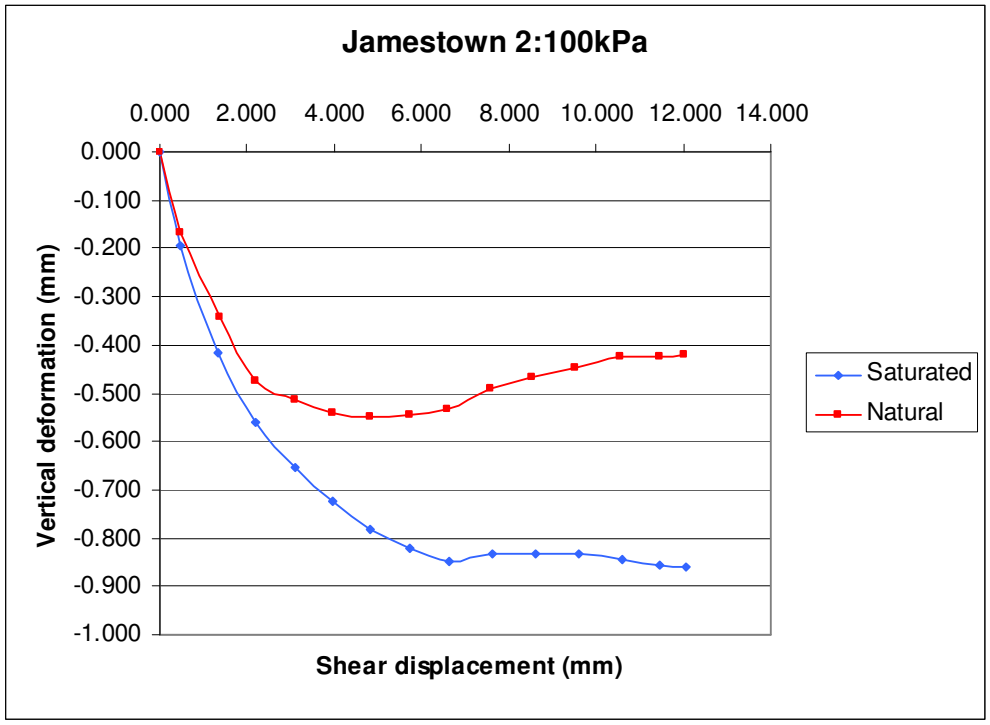

Figure C-2.5:Vertical deformation versus shear displacement of Jamestown pit 2

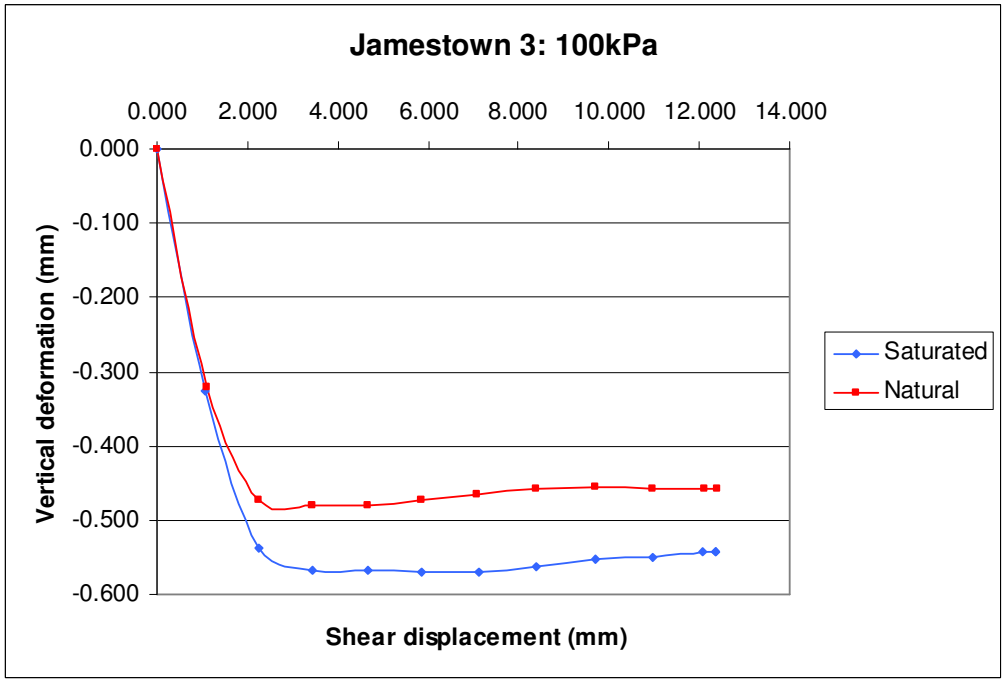

Figure C-2.6:Vertical deformation versus shear displacement of Jamestown pit 3